

**Montana Water Center
Annual Technical Report
FY 2012**

Introduction

The Montana University System Water Center (MWC), located at Montana State University in Bozeman, was established by the Water Resources Research Act of 1964. Each year, the Center's Director at Montana State University works with the Associate Directors from the University of Montana - Missoula and Montana Tech of the University of Montana . Butte, to coordinate statewide water research and information transfer activities. This is all in keeping with the Center's mission to investigate and resolve Montana's water problems by sponsoring research, fostering education of future water professionals and providing outreach to water professionals, water users and communities.

To help guide its water research and information transfer programs and to help develop research priorities and assess research proposals the Montana Water Center depends on advice from members of its advisory council.

During the 2012 research year, the Montana Water Research Advisory Council members were:

Duncan Patten, MWC Director; John LaFave, MWC Associate Director, Montana Tech of the University of Montana, Montana Bureau of Mines; William Woessner, MWC Associate Director ,University of Montana; John Kilpatrick, Director - Montana Water Science Center, U.S. Geological Survey; Bonnie Lovelace, Water Protection Bureau Chief Montana Department of Environmental Quality; Tom Pick, Natural Resource and Conservation Service (now retired); Jeff Tiberi, Montana Association of Conservation Districts, Executive Director; Kathleen Williams, Montana Legislature (Water Specialist); and Laura Ziemer, Trout Unlimited.

Research Program Introduction

Through its USGS funding, the Montana Water Center partially funded three new water research projects in 2012 and completed funding for two other projects for faculty at three of Montana's state university campuses. Those projects funded in 2010 for two years submitted final reports in spring 2012 and were included in the 2011 Annual Report. The Montana Water Center requires that each faculty research project directly involve students in the field and/or with data analysis and presentations.

This USGS 104b funding also provided research fellowships to nine students involved with water resource studies.

Here is a brief statement of the researchers' and students' work, with the three faculty research projects initiated in 2012 listed first.

Dr. Geoffrey Poole of Montana State University initiated work titled "Assessing Hydrologic, Hyporheic, and Surface Water Temperature Responses to Stream Restoration." He received \$14,000 for this study.

Dr. Andrew Wilcox of the University of Montana initiated work titled "Thresholds in fluvial systems: Flood-induced channel change on Montana rivers." He received \$13,883 for this study.

Dr. Laurie Marczak of the University of Montana initiated work titled "Nutrient dynamics and ecosystem function in coupled aquatic-terrestrial ecosystems during a mountain pine beetle infestation of whitebark pine." She received \$13,785 for this study.

Interim reports from these researchers are presented later in this annual report.

Student Fellowships funded in 2012 were:

Jared Bean of University of Montana received a \$1,000 award to support his study "Evaluating hydrogeomorphic controls on bull trout spawning habitat in mountain streams, Northwestern Montana".

Erika Calaiacomo of University of Montana State University received a \$1,000 award to support her study "Pool Response to Fine Sediment Loading from Dam Removal, White Salmon River, Washington".

Katie Davis of Montana State University received a \$750 award to support her study "An Investigation of Natural Treatment Systems in Cold Climates."

Fred Kellner of the University of Montana received a \$1,000 award to support his study "Quantifying the Sensitivity of Spring Snowmelt Timing to the Diurnal Snowmelt Cycle".

Michael LeMoine of University of Montana State University received a \$2,000 award to support his study "Invisible impacts of changing stream conditions: nongame fish assemblage response to changing stream temperatures".

Eric Richins of the University of Montana received a \$750 award to support his study "Food web effects of stream invasion by *Potamopyrgus antipodarum* and interactions with eutrophication."

Anthony Thompson of University of Montana received a \$500 award to support his study "Columbia River Treaty renegotiation process: collaborative in word or deed?"

Research Program Introduction

Karl Wetlaufer of Montana State University received a \$1,000 award to support his study "The Effect of Physiographic Parameters on the Spatial Distribution of Snow Water Equivalent: an Analysis of the Representativeness of the Lone Mountain SNOTEL Site."

Brett Woelber of University of Montana received a \$750 award to support his study "Soil temperature and moisture controls on stream recharge from snowmelt events, Lost Horse Canyon, Bitterroot Mountains, MT."

Final reports from these students are presented later in this research report.

During 2012 two MUS faculty researchers were selected for grants that the Montana Water Center administers under the USGS 104(b) research program, one from the University of Montana and one from Montana Tech of the University of Montana. Budget limitations at the time of this report reduced this support to only one faculty. In addition, four students were awarded fellowships to help support them as they pursue water-related research and education. These grants and fellowships will be funded with 2013 USGS 104(b) funds. The faculty grants are (if full funds are available):

Dr. Katie Hailer and Steve Parker of Montana Tech of the University of Montana received an award of \$13,835 to study whether sediments in the warm springs ponds operable unit act as a sink for organic wastewater compounds.

Dr. Maurice Valett of the University of Montana will receive an award of \$13,800 (if funds are available) to study nutrient limitation, algal abundance, and metabolism along the Upper Clark Fork River, MT.

The student fellowships to be awarded with 2012 USGS 104(b) funds went to one undergraduate and three graduate students. The funding indicated below is based on full 104b funding. Funding may be reduced depending on final budget.

Heidi Clark, a master's student at Montana State University Department of Land Resources and Environmental Studies received a fellowship of \$2000 to assist in her study "Rephotography as a tool to Understand the Effects of Resource Use on Rivers of the Greater Yellowstone Region".

David Dockery, a graduate student in Ecology at Montana State University received a fellowship of \$2,000 for his study "Maintaining Migratory Pathways of Imperiled Large River and Small Stream Prairie Fishes in the Face of Climate Change".

Thomas Matthews, an Master's student in Earth Sciences at Montana State University received a fellowship of \$2000 for his study "Understanding Trends in Snow Accumulation, Water Availability and Climate Changes Using Snow Telemetry Observations in the Missouri River Headwaters".

Robert Livesay, an undergraduate at University of Montana received a fellowship of \$1,000 for his study "Investigating Upstream Channel Response to Dam Removal, Black Foot River MT".

Methods for estimating wetland evapotranspiration through groundwater flow modeling of diurnal groundwater fluctuations

Basic Information

Title:	Methods for estimating wetland evapotranspiration through groundwater flow modeling of diurnal groundwater fluctuations
Project Number:	2011MT239B
Start Date:	3/1/2011
End Date:	2/28/2013
Funding Source:	104B
Congressional District:	At-large
Research Category:	Climate and Hydrologic Processes
Focus Category:	Wetlands, Models, Methods
Descriptors:	None
Principal Investigators:	Kevin Chandler

Publication

1. None

Methods for estimating wetland evapotranspiration through groundwater flow modeling of diurnal groundwater fluctuations

Gartside Prairie Fen, Crane Montana

May 6, 2013

Kevin Chandler (PI) and Jon Reiten, Montana Bureau of Mines and Geology, Billings Montana

MSU-Water Center Seed Grant: G207-11-W3491



Table of Contents

Introduction.....	4
Hydrogeological Setting.....	4
Methods.....	6
<i>Field Work</i>	<i>6</i>
<i>Laboratory Work.....</i>	<i>9</i>
<i>The Tarp Test</i>	<i>9</i>
<i>Aquifer Tests</i>	<i>12</i>
Field Work Results	13
<i>Well Installation Results</i>	<i>13</i>
<i>Water-level Results</i>	<i>14</i>
<i>Field Water-chemistry Results</i>	<i>16</i>
<i>Tarp Test Results.....</i>	<i>17</i>
<i>Aquifer Test and Laboratory Test Results.....</i>	<i>18</i>
Modeling the Diurnal Water-level Fluctuations at Gartside	19
Conceptual Model	20
Computer Code	21
Stratigraphy Modeling	21
Steady State Model Development and Calibration.....	22
<i>Model Grid.....</i>	<i>22</i>
<i>Hydraulic Parameters.....</i>	<i>23</i>
<i>Boundary Conditions</i>	<i>24</i>
<i>Sources and Sinks</i>	<i>24</i>
<i>Steady-state Model Calibration</i>	<i>24</i>
Transient Model Development and Calibration	26
Simple Model Development	26
<i>MODFLOW Grid.....</i>	<i>26</i>
<i>Model Layer Properties</i>	<i>27</i>
<i>Model Boundary Conditions</i>	<i>28</i>
<i>Steady-state Model.....</i>	<i>28</i>

<i>Transient Model and Calibration</i>	29
Modeling Results	31
<i>Complex Model Results</i>	31
<i>TT model results</i>	32
Discussion	35
<i>Discussion of Field Work</i>	35
<i>Discussion of Numerical Modeling Results</i>	37
<i>Discussion of Numerical Modeling Results</i>	37
<i>Recommendations</i>	40
References	41
Appendix A: Well Data	42
<i>Well locations and specifications</i>	42
<i>Well Logs</i>	43
Appendix B: Sieve Analyses	49
<i>Sieve Analyses Data Tables</i>	49
<i>Sieve Analyses Charts</i>	51
Appendix C: Water Level Charts	55
<i>2011 Season</i>	55
<i>2011 Paired Well Water-level Comparisons</i>	63
<i>2012 Season</i>	64
Appendix D: Ash Content Analyses	68

List of Figures

Figure 1: Site location map for the Gartside study area.....	5
Figure 2: Cross-section along the Crane Creek drainage up-gradient of Gartside Reservoir.	6
Figure 3: Locations of the Gartside monitoring wells and surface condition changes.	7
Figure 4: Hand auger drilling Gart 3.....	8
Figure 5: Image of Gart 4 Casing.....	10
Figure 6: Water-level fluctuations recorded hourly at Gart 17 and 18	11
Figure 7: Tarps installed around Gart 18	11

Figure 8: The water-level response in the shallow water zone at Gart 7	12
Figure 9: Leakage from Gart 9.....	14
Figure 10: Water-level fluctuations measured at Gartside wells	15
Figure 11: Water level changes recorded in Gart 2.....	16
Figure 12: The water-level fluctuations in Gart 18.....	17
Figure 13: Diurnal water-level fluctuations at Gart 17 and 18	18
Figure 14: Potentiometric surface for September 10th, 2011.	21
Figure 15: The upper image is a borehole cross-section created in GMS.....	22
Figure 16: The MODFLOW grid with 5 feet square cells	23
Figure 17: Diurnal water-level fluctuations in July of 2011 at selected Gartside wells.	25
Figure 18: Telescoping MODFLOW grid	27
Figure 19: The hydraulic properties were varied using polygons in layer 2 of the TT model.....	28
Figure 20: TT model responses to changes in HK of layer 1.....	29
Figure 21: TT model responses to changes in the SY assigned to layer 1.....	30
Figure 22: TT model head responses to ET rate changes.	30
Figure 23: The computed heads from simulation Gart2-22-13Cal3	31
Figure 24: Calibration markers in GMS	32
Figure 25: ET polygon used in GMS	33
Figure 26: The diurnal water-level fluctuations at Gart 18.....	34
Figure 27: The TT34 edge cells respond more like the actual system.....	34
Figure 28: The installation of Gart 11 on 7/5/2011 shows vegetation the damage to.....	35
Figure 29: Well installation and development at Gart 4	36
Figure 30: Hydrographs of Gart 17 and 18.....	39
Figure 31: Diurnal water-level fluctuations at Gart 17 and 18 and surface temperature fluctuations.	39

List of Tables

Table 1: Field Water-chemistry Results.....	16
Table 2: Aquifer Material Properties from Aquifer Tests and Sieve Analyses	19
Table 3: Material Properties Assigned to the Complex Model.....	24
Table 4: TT model hydraulic properties	27
Table 5: Well Construction Information	42

Introduction

The prairie fen at Gartside Reservoir forms where the waters of the Crane Creek drainage enter the Yellowstone River valley alluvial plain in Section 16, T21N, R58E (Figure 1). Flowing surface water in the Crane Creek drainage upstream from the wetland is only seen during runoff periods in high precipitation years such as the spring of 2011. The wetland area near Gartside Reservoir is a natural discharge point for groundwater from the West Crane aquifer of the Lower Yellowstone Buried Channel (LYBC), (Reiten, personal communication). The groundwater discharge produces a flourishing wetland ecosystem very different from the dry grasslands of the surrounding hills. It covers approximately 30 acres with diverse vegetation and surface conditions. The fen portion of this wetland is characterized by a saturated peat bog which feels like a ‘water bed’ underfoot.

Gartside Reservoir dam near Crane Montana was constructed in 1962 to impound the waters draining from the Crane Creek watershed. Problems created by the high water table up-gradient of the reservoir prompted a study by HKM Associates for Montana Fish, Wildlife, and Parks (FWP) between 1985 and 1991. A simple groundwater flow model was constructed to determine the likelihood of water impounded at the reservoir could raise the water table under up-gradient agricultural land and cause marshy conditions making it unsuitable for farming. Monitoring wells (1988) and a drainage system (February 1991) were installed in the farmland and near the reservoir. Kirk Waren of Montana Department of Natural Resources and Conservation (DNRC) reported on the model and the potential impacts to the agricultural land in October of 1993. The model suggested that the high water table condition on the land up-gradient from Gartside Reservoir was “aggravated” by the reservoir water level. The monitoring wells installed by HKM provided valuable information about the stratigraphy of, and water-level change in this shallow aquifer.

This project’s goal was to develop field work and numerical modeling methods to improve ET estimates for wetland ecosystems. Information gained from the field study was used to construct a numerical groundwater flow model capable of simulating diurnal water-level fluctuations resulting from evapotranspiration (ET) at Gartside. Field work during 2011-2012 provided the background data necessary for model development.

Hydrogeological Setting

The marshlands at Gartside are supplied by groundwater which appears to be forced to the land surface by sedimentary bedrock layers of the Fort Union formation (Vuke, Wilde, & Smith, 2003). The development of a fen requires a steady supply of groundwater for long time periods (Amon, Thompson, Carpenter, & Miner, 2010). The fen’s existence for many years is supported by decomposed peat layers found at depths greater than 14 feet below land surface. Additionally, dense clay layers containing mollusk shells interbedded with the peat deposits point to times when the marshland was covered by water.

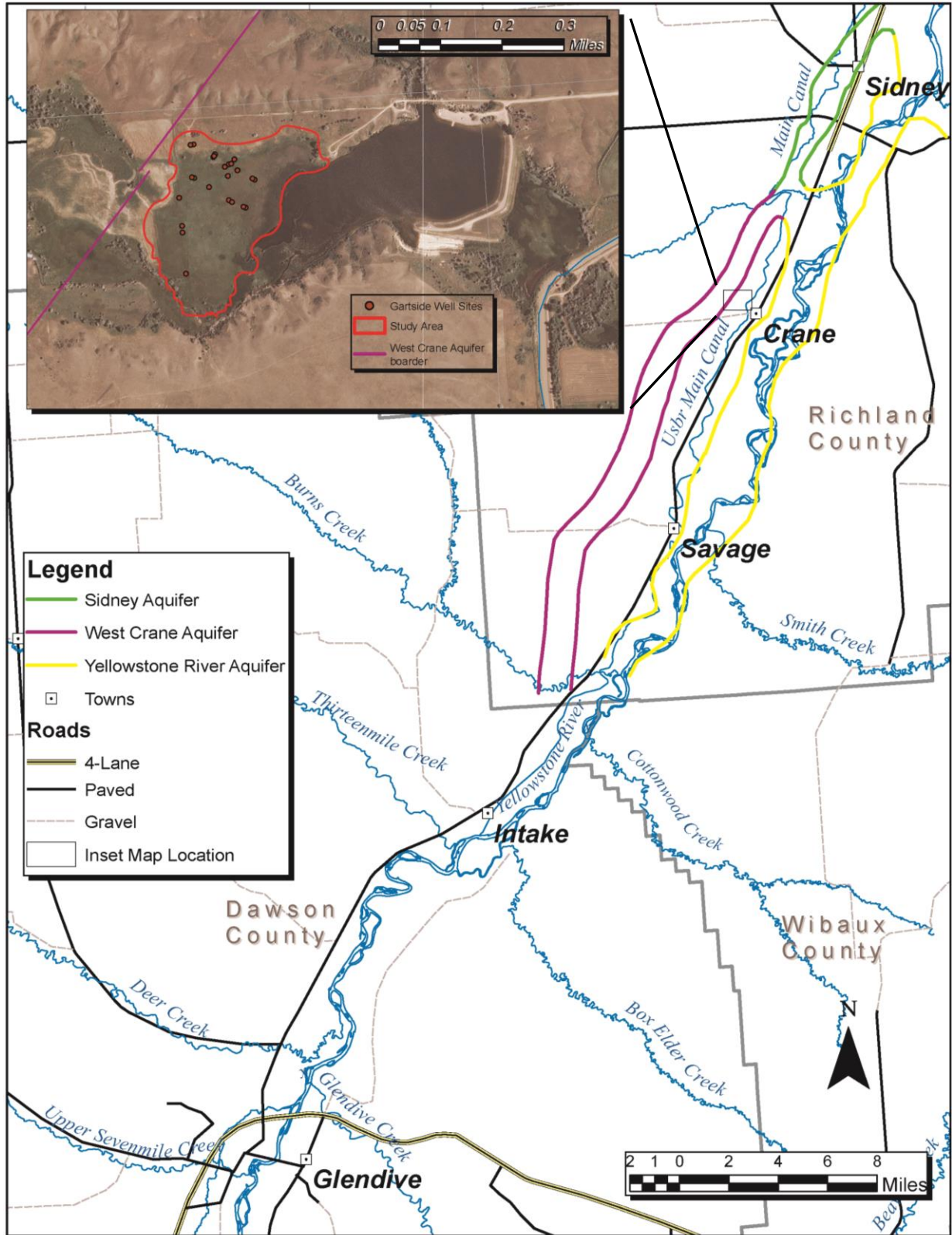


Figure 1: Site location map for the Gartside study area.

The surface conditions and plant communities of the wetlands change as one walks from the highest elevation wells, Gart 2 and Gart 3, (Figure 3) southeastward towards the reservoir. Standing water is first encountered on the surface indicated by the dotted blue line near wells Gart 8, Gart 17, and Gart 18. There is another noticeable change in surface conditions at the location indicated by the dashed line near Gart 9, Gart 5, and Gart 10 where the surface vegetation appears to float on the saturated peat. Walking across this floating sedge and *sphagnum* matt generates surface waves that propagate for several feet. The land surface feels firm underfoot again near the reservoir where the vegetation changes to cattails seen in figure 3 as dark green. Visible changes in the vegetation seem to reflect variations in the subsurface conditions.

Most of the monitoring wells installed in the Crane Creek drainage near Gartside are completed in silty sand and gravel aquifer materials between 15 and 20 feet below the land surface. Only one of the FWP monitoring wells, MW 7 was drilled deep enough to penetrate the Fort Union bedrock in the Crane Creek drainage up-gradient of the reservoir, but bedrock outcrops on both sides of the drainage at Gartside Dam. A cross-section drawing representing the conceptual subsurface geology for 0.5 miles along Crane Creek up-gradient of Gartside Reservoir is shown in Figure 2. The up-stream bedrock contact elevation of 1944 ft (AMSL) was estimated from wells with GWIC ID's 253448 and 234036. The location of the edge of the Buried Channel aquifer up-stream from Gartside Reservoir is uncertain, but head elevations and water chemistries from the monitoring wells show a connection to the larger aquifer.

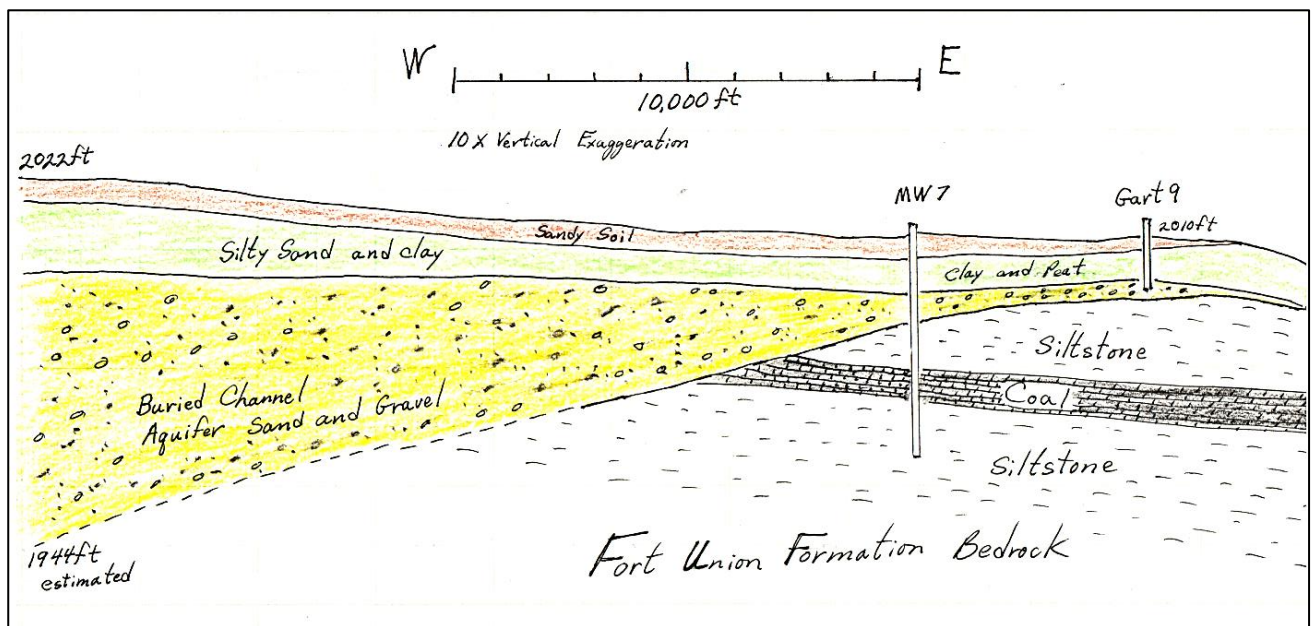


Figure 2: Cross-section along the Crane Creek drainage up-gradient of Gartside Reservoir.

Methods

Field Work

Field work at Gartside started April 29th, 2011 with a site visit. The rancher leasing this parcel of state land was visited, showed interest in the project and provided valuable information concerning the best way to access the study site. The first monitoring well, Gart 1 was installed by driving a short section of

2-inch PVC pipe repetitively into the saturated silty sand and clay, and pulling it to remove material from the hole. A six foot section of 2 inch PVC pipe was perforated with handsaw slots for one foot on the bottom end and installed approximately five feet into the hole. After the water levels in the well stabilized, an In-Situ Level Troll® 300 programmed to record water levels and water temperature hourly was installed. The well transects locations were selected to best monitor the conditions at sites representing the varied vegetation types found in the wetland.

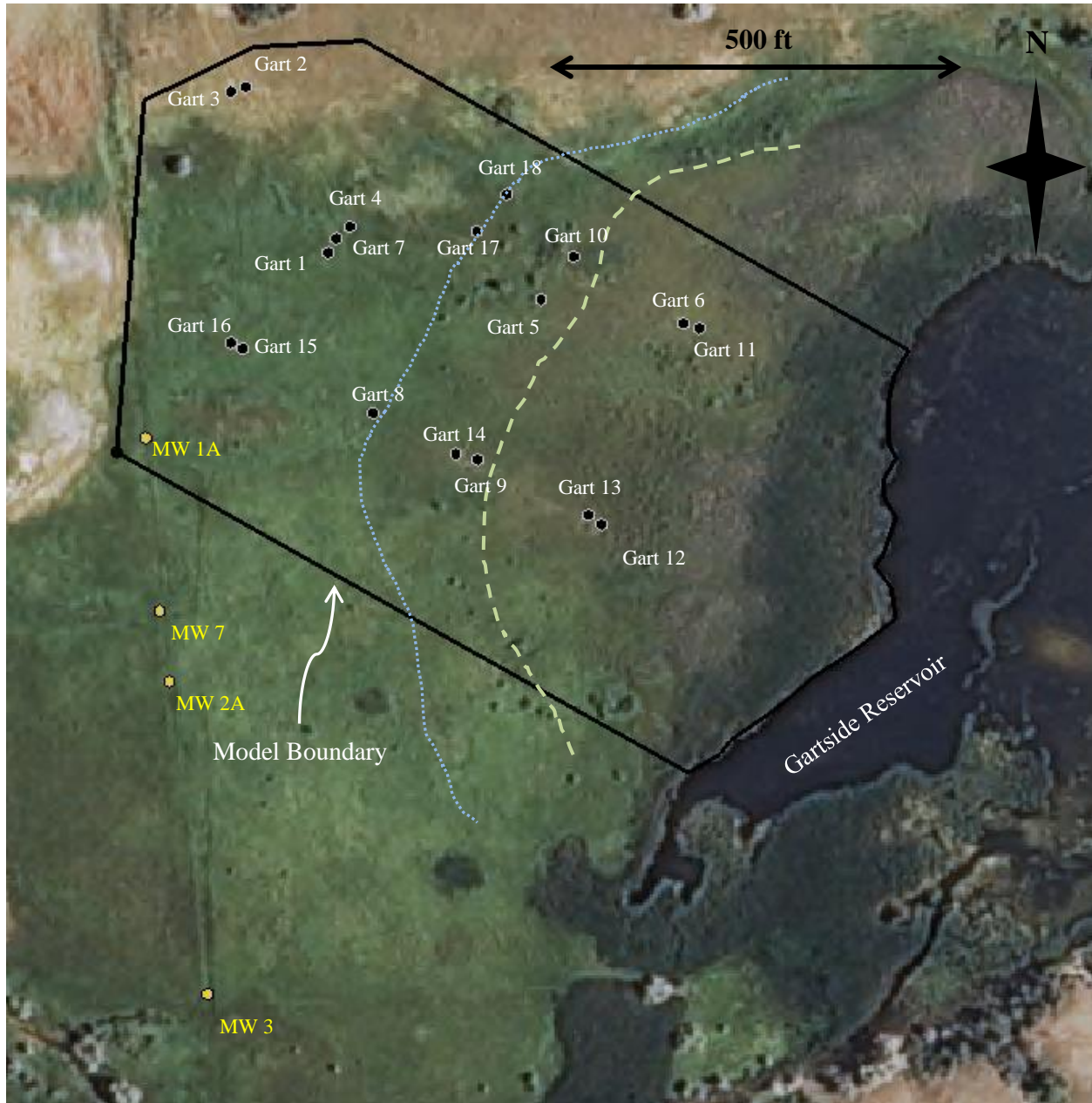


Figure 3: Locations of the Gartside monitoring wells and surface condition changes.

Installation of multiple wells in transects started during a site visit May 31st through June 2nd 2011. Eight wells, Gart 2 to Gart 9 were installed to depths between 4.5 and 20 feet below land surface using a 4.0 inch diameter hand auger (figure 4). Lithologic logs were recorded for each borehole and sediment

samples collected for sieve analyses. All wells were cased with 2.0-inch diameter PVC casing and screened with 2.0-inch diameter 0.020 inch factory slotted PVC well screen (figure 5). The annular space between the screen and the borehole wall was backfilled with 10/20 silica well sand. Bentonite chips were placed opposite blank casing above the sand to the ground surface. A 12-volt sampling pump was used to develop the wells and produce samples for initial field water-chemistry measurements. In-Situ Rugged Troll[®] 100 data loggers were installed in the new wells programmed to record level and temperature hourly. A Baro Troll[®] 300 was hung in Gart 2 above the water level to record the barometric pressure changes at Gartside for the duration of the study.

Seven additional wells were installed early in July 2011 to expand the areal monitoring well coverage and to explore earlier observations that there were at least two water bearing units in the shallow aquifer system. Well pairs, deep and shallow, were installed in most of the locations to measure the vertical hydraulic gradient. Figure 3 shows the locations of the wells relative to Gartside Reservoir. The locations of all wells were recorded using a hand held GPS unit and their relative elevations measured using a site level. All 16 wells were pumped for field chemistry measurements and data loggers programmed to record hourly water levels and temperatures were installed. Most of the data loggers were removed from the wells on November 16, 2011 and the wells with water levels above ground surface were winterized. Several data loggers were left at depths below frost to record winter water levels and temperatures.



Figure 4: Hand auger drilling Gart 3. MSU-B student Erika Peters drills the borehole for Gart 3 next to Gart 2.

Gartside was revisited in March of 2012, but many of the wells were still frozen. In late April 2012 data loggers were re-deployed in six wells and wells damaged by the winter were repaired. Most well completions showed evidence of “frost jacking” and some well-head altitudes had increased by four or more inches. Also during this site visit two new wells (Gart 17 and Gart 18) were installed in areas of similar surface condition and vegetation. The wells were screened in the upper water bearing zone with hope that the diurnal water-level fluctuations would reflect the site likeness. The materials encountered in the two new boreholes were very similar with Gart 18 completed in material slightly more fine grained.

Data loggers were installed in the new wells and programmed to record hourly water level and temperature readings.

Laboratory Work

Sieve analyses were conducted on samples of aquifer materials collected during installation of the wells. The samples were dried and lightly crushed to break up clods, but not rocks. Sieve sizes 25, 35, 45, 60, 120, 170, and 230 were selected and used with an automated shaker. The samples were shaken with a Gilson SS-15 8-inch sieve shaker for 10 to 17 minutes depending on the type of material. The sandier materials sorted in less time. Then the material remaining in each sieve weighed with an Ohaus ® digital top-loading balance.

Grain sizes were charted so that the coefficient of uniformity could be calculated and the Hazen (1911) method used to calculate hydraulic conductivity values (Fetter, 2001). Ash content analyses were conducted on samples containing peat to help determine the classification of peat, and to narrow the range of reported hydraulic conductivities (Verry, Boelter, Päivänen, Nichols, Malterer, & Gafni, 2011). Cuttings from the boreholes that contained shells in the clay or peat were studied using a stereo microscope to identify the small mollusk shells found in the clay and peat samples.

The Tarp Test

The “tarp test” was an attempt to restrict or eliminate ET from an area around one well and compare the diurnal water-level response to a water-level fluctuations in a control well. Water-level fluctuations in Gart 17 and 18 were compared and found to have nearly identical responses for more than two months before the “tarp test”(Figure 6). The periods of continuous high ET days show as water-level declines with uniform diurnal water-level fluctuations. Precipitation events show as sharp water-level recovery spikes. A period of days forecast to have warm sunny weather was selected to insure consistent diurnal water-level fluctuations for the test. On September 2nd, 2012 the pre-test data were downloaded from the data loggers installed in Gart 17 and 18. The loggers were then re-programmed to record data every ten minutes starting at 13:00, and installed to the same depth in the wells. Four poly tarps were used to cover the vegetation around Gart 18 with double thickness coverage 15 feet by 22.75 ft (341 ft²). The poly tarps were installed with the reflective silver side up and blue side down to prevent vegetation damage from overheating. The corners of the tarps were staked down using tent stakes and twine (Figure 7). The area around Gart 18 remained covered for a 24 hour period. Post-test water-level data were recorded in both wells at hourly sampling rates.



Figure 5: Image of Gart 4 Casing. MSU-B student Erika Peters holds the well casing before installation in Gart 4, one of the deeper wells (screen section at the bottom 3 feet).

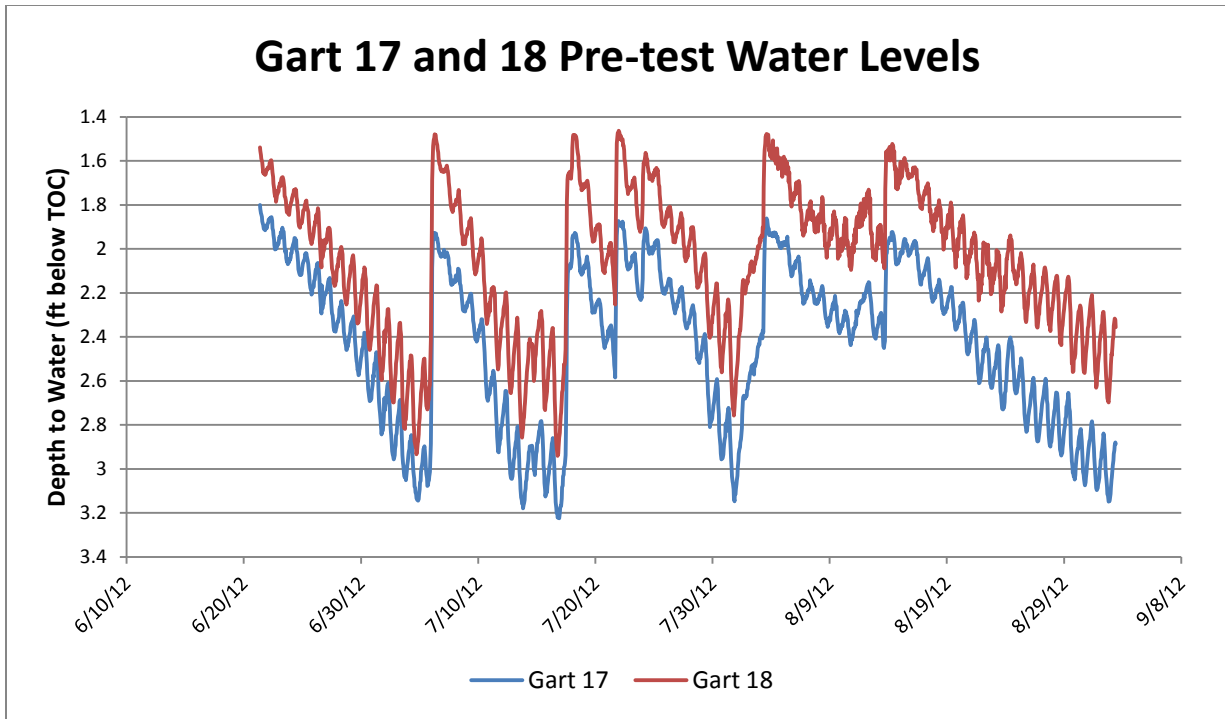


Figure 6: Water-level fluctuations recorded hourly at Gart 17 and 18 before the “tarp test” in the summer of 2012.



Figure 7: Tarps installed around Gart 18 for the “tarp test” and Gart 17 control well in the distance, 9/2/2012.

Aquifer Tests

After the tarps were installed for the “tarp test” at Gart 18, short-duration aquifer tests were conducted at wells Gart 4, 7, and 8. Data loggers were set to record water levels every minute and installed as deep as possible in each well for the tests. A Masterflex[®] model 7518-02 peristaltic pump mounted on a cordless drill was used to pump the shallower wells Gart 7 and 8. Gart 4 was pumped with a Proactive[®] Super Twister 12-volt sampling pump. The wells then were pumped as long as possible at low rates and then allowed to recover (Figure 8). The pump used in Gart 4 was pulled quickly when it started to suck air to prevent back-flushing of the in-line water when the pump was stopped. The wells all pumped dry in less than 10 minutes since it was difficult to maintain pumping rates low enough to extend the drawdown time.

An aquifer test using the wells penetrating the lower more productive sand and gravel unit was planned for the late fall of 2012, but was cancelled due to weather. A 12-volt sampling pump was used to pump both of the productive wells, Gart 12 and 9 for water quality testing. The pumping rates were greater than five gallons per minute with little drawdown in either well. A properly installed test well in the lower productive zone may be able to maintain 20 to 50 gpm pumping rates. This estimate is based on the observed combined seepage from both Gart 9 and 12, which has produced approximately 10gpm for months without causing detectable water-level decline in the study area (Figure 10).

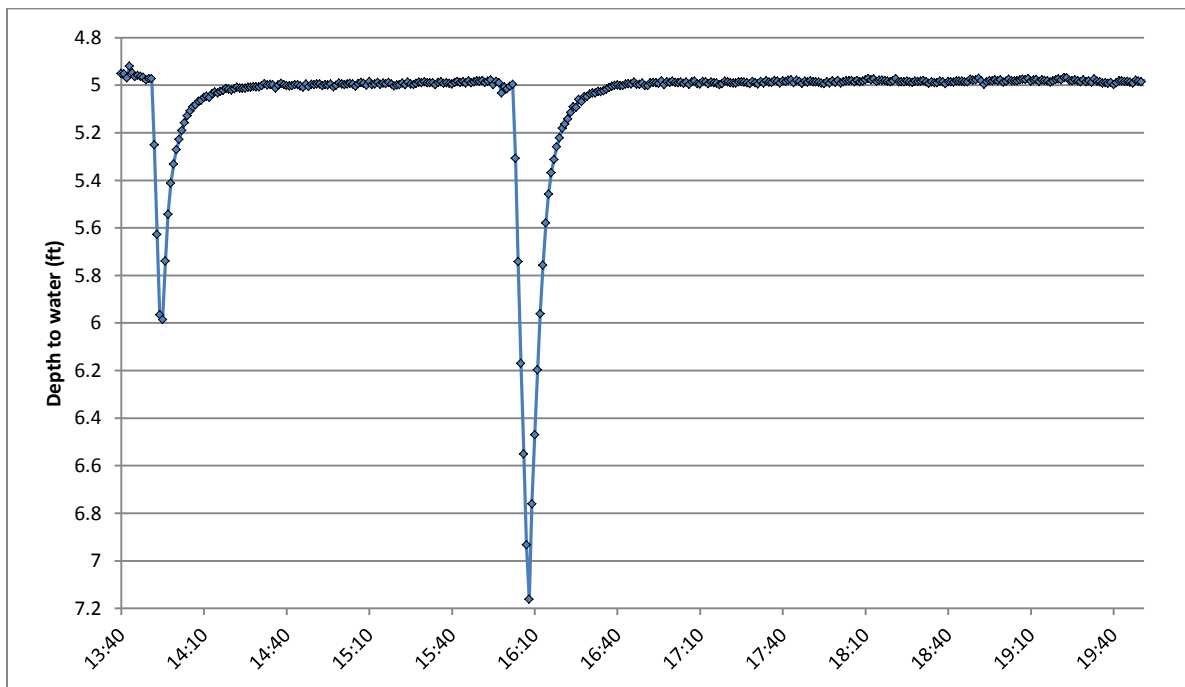


Figure 8: The water-level response in the shallow water zone at Gart 7 during the short-duration aquifer tests show the drawdown and recovery from pumping at 0.125 gpm with a peristaltic pump, data collected at 1.0 minute intervals.

Field Work Results

Well Installation Results

All of the wells except Gart 1 were installed with a hand auger. This method, although slow and labor intensive, provided detailed information about the shallow stratigraphy. Cuttings were easily collected for examination and grain size analyses. Many of the boreholes remained open through the saturated fine grained upper layers, but began to cave when the silty sand, or the sand and gravel of the lower water bearing unit was encountered. Gart 4 remained open for close to twenty feet below the surface. When drilling through the fine grained upper materials, it was often difficult to determine the points where water was encountered. A 12-volt sampling pump was used to dewater some of the boreholes for visual inspection before the casing was installed. We were surprised to see water flowing out of distinct points in the dense clay layers of Gart 4 and 7. These points seemed to be preferential flow paths in the otherwise very tight clay. The green/gray clay cuttings contained rusty-red deposits in the upper layers graduating to white tubular deposits with depth. The white deposits were determined to be carbonates using an acid test. These flow paths may be remnant root ways or animal burrows, but they greatly increase the water flow through this clay which would otherwise be an aquitard and appear to be locations for precipitation if minerals from the mineral rich ground water.

Drilling was difficult in the peat bog section of the fen. This was most notable at Gart 6 and 11 where the saturated peat and clay layers below the root zone caved around the auger making removal difficult at best. Pulling up on the auger stem directed pressure downward around the borehole which helped to collapse the material around the auger. This problem was overcome during the installation of Gart 12 by installing a section of 4 inch thin-walled PVC drain pipe as temporary external casing through the loose saturated peat and clay layers. The casing was simply pushed downward and advanced using the 3-inch auger to remove material from inside and below the casing. With this method, we were able to drill down to the lower water bearing unit without fighting the collapsing upper layers of peat and clay. We were able to pull the temporary casing when we were ready to install the 2-inch monitoring well casing.

In the installation of Gart 9 and 12, the coarse sand and gravel of the lower water bearing unit was encountered. The boreholes quickly filled with water, and began flowing at five to ten gallons per minute in both cases. The formation sand and gravel collapsed quickly around the lower end of the screened section of the 2-inch well casing, and 10/20 silica sand was used to fill the rest of the annular space around the screen. Initially the bentonite chips used to fill the annular space to the surface sealed the 2-inch casing and prevented upward water flow in the annular space. The initial heads in the wells were approximately two feet above the fen surface. In both cases the bentonite seal failed, and water flows continually to the surface at approximately five gallons per minute. It appears the vegetation which forms a floating mat on top the saturated peat and clay was damaged by the trampling during well installation. Once the mat is damaged, it fails to hold pressure from above or below. More bentonite chips, and sod cuttings were installed around well casing, but the new seal failed before the next field visit. Precipitant iron oxides color the leak areas rusty red, similar to the areas where the agricultural drains discharge up-gradient from Gartside (Figure 8).



Figure 9: Leakage from Gart 9 April 25th, 2012 (left) and outflow from a drain (right) near Gartside show iron oxidation.

Most of the wells the shallow wells in the Gartside wetland area show evidence of “frost jacking” after the surface thaws in the spring. Rust lines on the casing of Gart 9 (Figure 9) show approximately 4 inch change in well stick-up from one season of this process. Most of the FWP monitoring wells have been “jacked” for enough seasons that the well stick-ups are six feet above the surface making water-level measurements difficult. This process also changes the position of the well screen in the formation.

Water-level Results

As the Gartside wells were installed in the summer of 2011, all wells were instrumented with data loggers programmed to record hourly water temperature and level. Wells completed in the upper fine-grained silty-sand, silty-clay, and peat showed lower heads than deeper wells nearby (Appendix C, Paired Water-level Comparisons). This was most evident at the well pairs, Gart 9 and 14, Gart 12 and 13, and Gart 15 and 16. The shallow wells at the Gartside study area also were more likely to show larger diurnal water-level fluctuations resulting from evapotranspiration (figure 10).

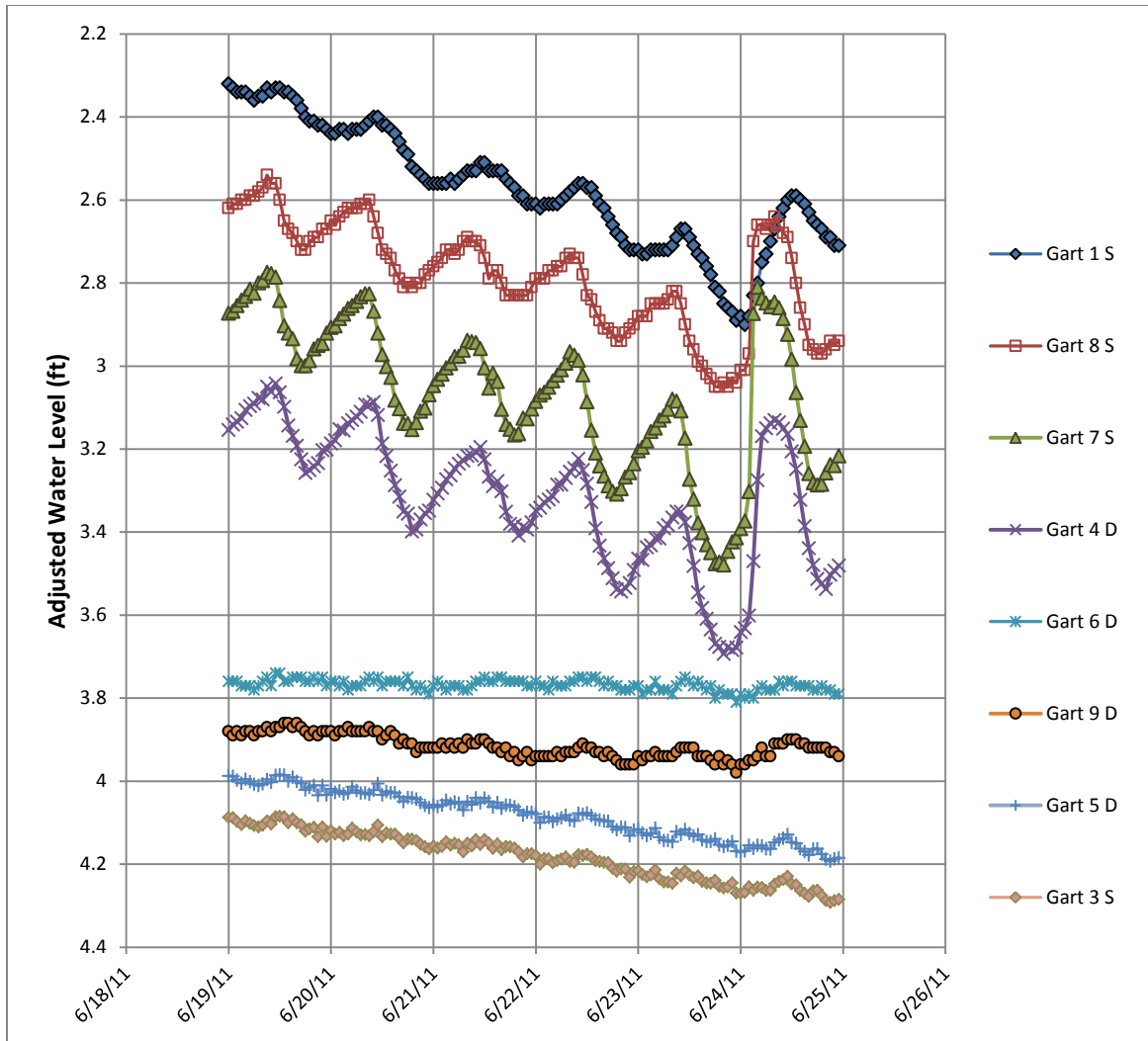


Figure 10: Water-level fluctuations measured at Gartside wells in June of 2011. The actual water levels below the top of the well casing have been adjusted to show all the traces on one chart, where the focus is on the amount of change, not the exact water level. The single letter in the well name indicates the completion depth, S for shallow, D for deep.

Gart 4 and Gart 6 are exceptions to this trend since Gart 4 is the deepest well in the study area, and Gart 6 is relatively shallow. Even though Gart 4 is almost 20 feet deep, the silty-sands near the bottom are likely connected to shallow waters which are impacted by ET. On the other hand, the saturated peats at Gart 6 seem to be able to supply more water to the surface than the plants can uptake, conditions that minimize diurnal water-level fluctuations.

Water levels were recorded in several wells all year around for about two years. These wells show the typical seasonal trends with declines in the summer months due to active ET use of the groundwater by phreatophytes. Recovery of the water levels in the fall starts early in September as ET decreases with the cooling temperatures and leaf senescence (Figure 11). Charts of the water level changes at other Gartside wells can be found in Appendix C.

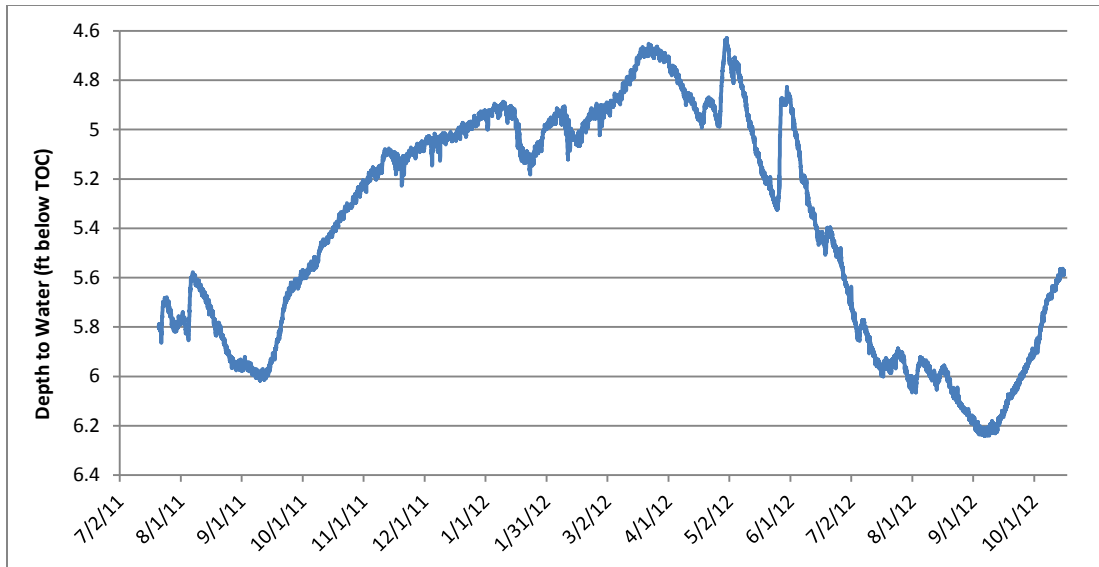


Figure 11: Water level changes recorded in Gart 2, a well with water levels deep enough to prevent winter freeze.

Field Water-chemistry Results

The water chemistry was measured in waters produced from the shallow wells at Gartside in July of 2011. All of the shallow waters sampled showed nearly neutral pH, even waters from wells completed in the saturated peat layers (Gart 11). The water temperatures in July were 7-10 °C in the deeper wells, and 11-15 °C in the shallow wells. The specific conductance of waters from Gart 2 and 3(mean= 1182µS/cm) were significantly higher than the waters from all the other wells (mean = 848 µS/cm) (Table 1). Gart 2 and 3 are located on the north edge of the wetlands in an area where the vegetation yellows in the summer. This observation supports the idea that some groundwater enters the wetland flow system from bedrock and terrace high grounds north of the Crane Creek alluvium, but not in great enough quantities to produce noticeable water chemistry gradients in the wells on the north side of the study area.

Table 1: Field Water-chemistry Results

Well Name	Date/Time	PH	Temp (°C)	Specific Conductance (µS/cm)
Gart 2	7/21/11 20:50	7.16	8.78	1146
Gart 3	7/21/11 20:30	7.14	11.13	1218
Gart 4	7/21/11 6:45	7.01	8.78	862
Gart 5	7/20/11 20:37	7.26	8.33	856
Gart 6	7/20/11 18:02	7.29	13.1	806
Gart 7	7/21/11 7:00	7.14	13.92	860
Gart 8	7/21/11 7:20	7.1	14.69	969
Gart 9	7/20/11 17:40	7.06	7.74	831
Gart 11	7/20/11 18:37	7.08	8.76	842
Gart 12	7/20/11 17:00	6.98	7.63	851
Gart 13	7/20/11 17:10	7.04	12.05	829
Gart 14	7/20/11 17:45	7.26	12.38	836
Gart 15	7/21/11 7:40	7.06	9.58	799
Gart 16	7/21/11 8:00	7.23	13.32	839

Tarp Test Results

The tarps were installed around Gart 18 at 12:20 on 9/2/2012, and the water levels responded to the reduction in ET over the next 24 hours as can be seen on the actual curve for Gart 18 (Figure 12). The vegetation showed little sign of being covered when the tarps were removed at 13:22 on September 3rd. The diurnal water-level fluctuation at the control well Gart 17 maintained a consistent diurnal pattern before, during, and after the test. Figure 12 shows the diurnal water-level fluctuations at Gart 17 and Gart 18 including the three days before the test and includes the test period on the fourth day. The dashed line shows the water-level fluctuations predicted for Gart 18 if no tarps were installed. The values assigned to this curve were based on the pre-test water-level fluctuations observed at Gart 17 and 18. The days before the test show very similar water-level fluctuations at Gart 17 and 18 with those at Gart 18 being slightly larger. After the test, the data loggers were reset to record hourly water levels at both wells. The post-test data show a return to similar curves at both wells, but a change in the seasonal trend which commonly occurs early in September (Figure 13).

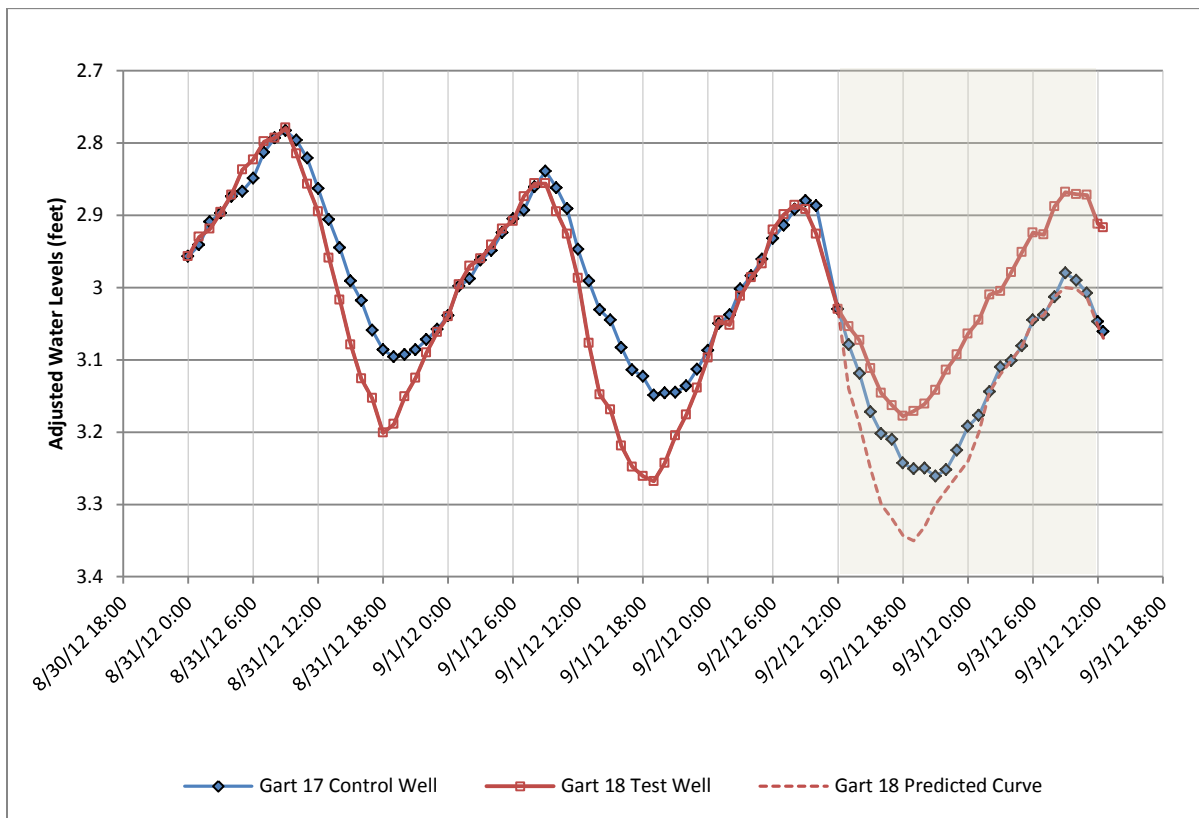


Figure 12: The water-level fluctuations in Gart 18 change in response to installation of 341 ft² of tarps around the well whereas the water-level fluctuations at Gart 17, the control well remain consistent. The actual water levels were adjusted to the same starting point on 8/31/2012 for comparison purposes. The shaded area shows the time when the tarp was installed.

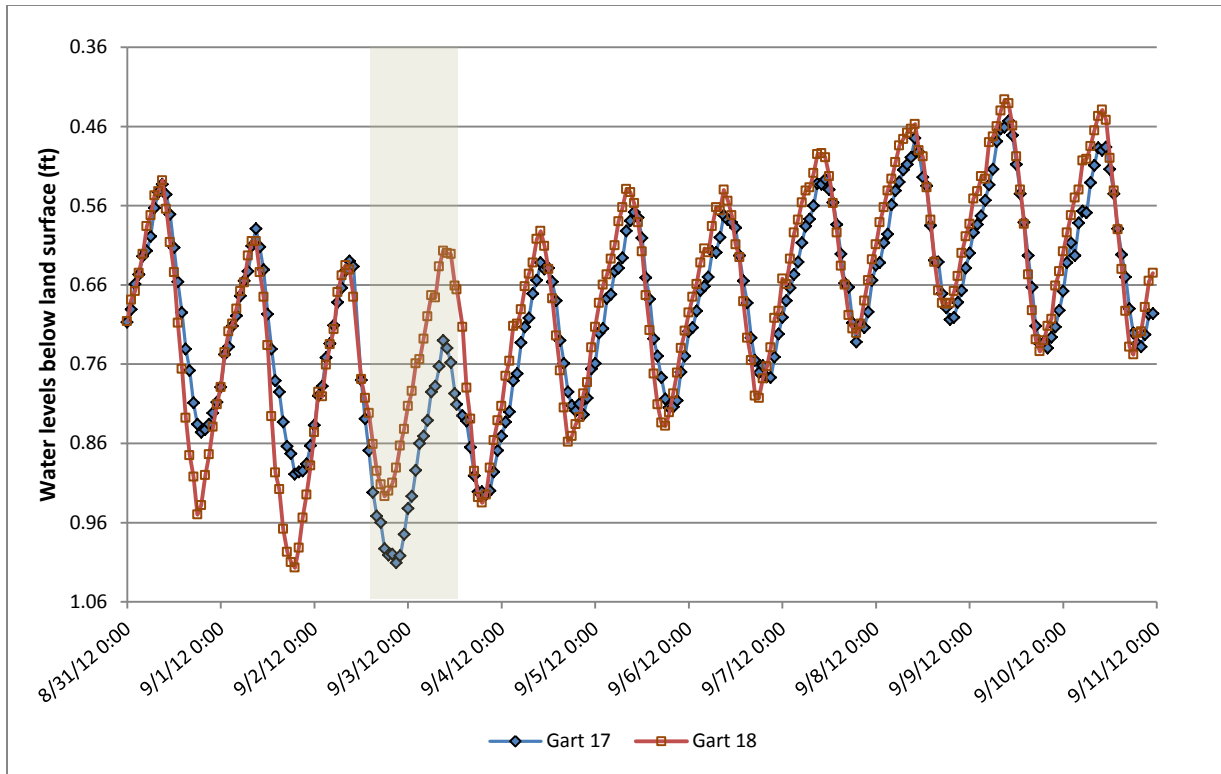


Figure 13: Diurnal water-level fluctuations at Gart 17 and 18 before, during, and after the “tarp Test”. The shaded area shows the time period when the tarp was installed at Gart 18.

Aquifer Test and Laboratory Test Results

The water level data collected during the short-duration aquifer tests were entered into Excel spreadsheets and charted. The analyses of these tests focused on the recovery periods since the pumping drawdown was likely only draining casing and wellbore storage. It was also noted that the pumping rates changed as the wells drained. The recovery period was viewed as the aquifer’s response to the pumping, and the pumping rates were averaged over the drawdown period for use in the analyses. Semi-log plots of residual drawdown versus time were plotted and slopes of the straight line sections were used to calculate the transmissivity T (Table 2).

Cuttings from the hand auger drilling were collected for select boreholes. From the collected material, samples from the aquifer zones were selected for sieve analyses. Samples that were predominately clay were not included since the d_{10} sizes would fall far below 0.1 mm lower size limit for the Hazen Method (Hazen 1911) (Fetter, 2001). The percent of the sample remaining in each sieve was plotted against the sieve opening size (Appendix B) for selection of the d_{60} and d_{10} sediment sizes (d_{60} size where 60% of the sample passes and d_{10} size where 10% of the sample passes). The uniformity coefficient was calculated using:

$$C_u = d_{60}/d_{10}$$

Uniformity coefficients less than 4 are considered well sorted, and greater than 6 are poorly sorted (Fetter, 2001). The Hazen Method (Hazen 1911) used the d_{10} size for calculation of the hydraulic conductivity using:

$$K = C(d_{10})^2$$

The coefficient C ranges from 40 to 150 depending on the material (Fetter, 2001). For most of the Gartside samples 40 was the C value use for the calculations. The exception was Gart 9 sand and gravel, where the 80 was selected as the low end of the coarse sand, poorly sorted category (Fetter, 2001). Results of the sieve analyses and uniformity calculations are displayed in Table 2.

Hydraulic conductivities of peat have been shown to vary greatly with depth and compaction (Quinton, Hayashi, Carey, & Myers, 2007). From the visual analysis, the peat from the upper peat zones would be classified as a fibrous peat, with a large porosity, and lower ash content. The lower layer peats encountered in Gart 4 approximately 14 feet below the surface, were more decomposed, compacted and had high ash content (Appendix D).

Cuttings from different well-bore levels were inspected using a stereo microscope in the laboratory. The bivalve mollusks observed in peat and clay layers were determined to be of the genus *Pisidium*, a type of pill clam present in aquatic environments the last 10-12,000 years. Their presence indicates the area was a lake or stream environment with a stable bed conditions (Cvancara, 1983). Snail shells of genus *Helisoma* and *Stagnicola* were also found, and their presence indicates similar environments.

Table 2: Aquifer Material Properties from Aquifer Tests and Sieve Analyses

Aquifer Test Results: Recovery Period			
Well	Water Producing Materials	T (ft ² /day)	K (ft/day)
Gart 4	Silty clay, Silty sand, Peat	4	0.8
Gart 7	Silty Sand	28	11
Gart 8	Clay and silty sand with roots	23	8
Hazen Method (1911) Hydraulic Conductivity and Uniformity Coefficients			
Well	Water Producing Materials/Depth	Uniformity Coefficient	K (ft/day)
Gart 4	Silty Sand, 18.5 to 18.8 ft	4.76, partially sorted	2
Gart 9	Fine Silty Sand 5.8-8.2 ft	3, well sorted	8
Gart 9	Sand and Gravel 8.2-9.4	4.14, partially sorted	50
Gart 10	Dark Silty Sand, 5.65-7.67 ft	1.75, well sorted	16
Gart 11	Peat, 3.87 to 3.92	4.15, partially sorted	3
Gart 15	Coarse Brown Sand	2.9, well sorted	8

Modeling the Diurnal Water-level Fluctuations at Gartside

The observational and water-level data from the field work conducted at Gartside were used to develop MODFLOW based numerical flow models. The goal of the modeling was to determine the model applied ET rates necessary to replicate the observed diurnal water-level fluctuations, and through this process develop methods to improve ET estimates for wetland environments. Two different modeling approaches

were tested in attempt to replicate the observed diurnal water-level fluctuations. The first model developed contains detailed stratigraphy modeling and a grid structure necessary to represent the actual complex system as closely as possible. This process included attempts to match the observed water-level fluctuations at the paired observation points throughout the model domain. A second more simplistic model was developed to replicate the water-level fluctuations at Gart 17 and 18 for the period of the “tarp test” and will be referred to as the TT model. The TT model simulates the hydrologic conditions in the center of the study area using a two layer model, and does not attempt to match the observed heads at all points in the monitoring well network.

Conceptual Model

The West Crane aquifer of the LYBC appears to supply a relatively constant supply of groundwater to the fen near Gartside Reservoir and eventually to the reservoir. The groundwater intersects the land surface where the Crane Creek alluvium thins and outcrops of the Tongue River member of the Fort Union formation are visible in the low hills. Crane creek has eroded the Tongue River member forming a low point in the sedimentary layers which bound the buried channel aquifer, and thus creates a natural discharge point. Ground-water levels in the alluvium up-gradient of the reservoir are considerably higher than the reservoir surface and the hydraulic gradient steepens rapidly towards the east at a point beginning 300-400 feet of the reservoir’s western edge (figure 14). This condition could only exist if the highly permeable sands and gravels of the lower water bearing layers pinch out into less permeable material close to the reservoir. The low permeability material acts as a dam forcing the ground water upwards to the fen surface. From there the water is evaporated, transpired or slowly flows towards the reservoir overland through the dense vegetation.

Wells Gart 9, and 12 (Figure 14) were completed in highly permeable sand and gravel and are artesian wells with heads several feet above the land surface; the heads are almost seven feet higher than observed reservoir levels. This strong upward gradient keeps the shallow soils and peat bogs of the fen saturated even during the late summer. There also appears to be a small groundwater flux into the model area from the north side of the Crane Creek canyon. Water samples from Gart 2 and Gart 3 in the northwest corner of the model area have a distinctly different chemistry compared to the water from wells completed within the fen. Water levels in Gart 2 (deep) and Gart 3 (shallow) are nearly identical and don’t show the strong upward gradient observed at other well pairs.

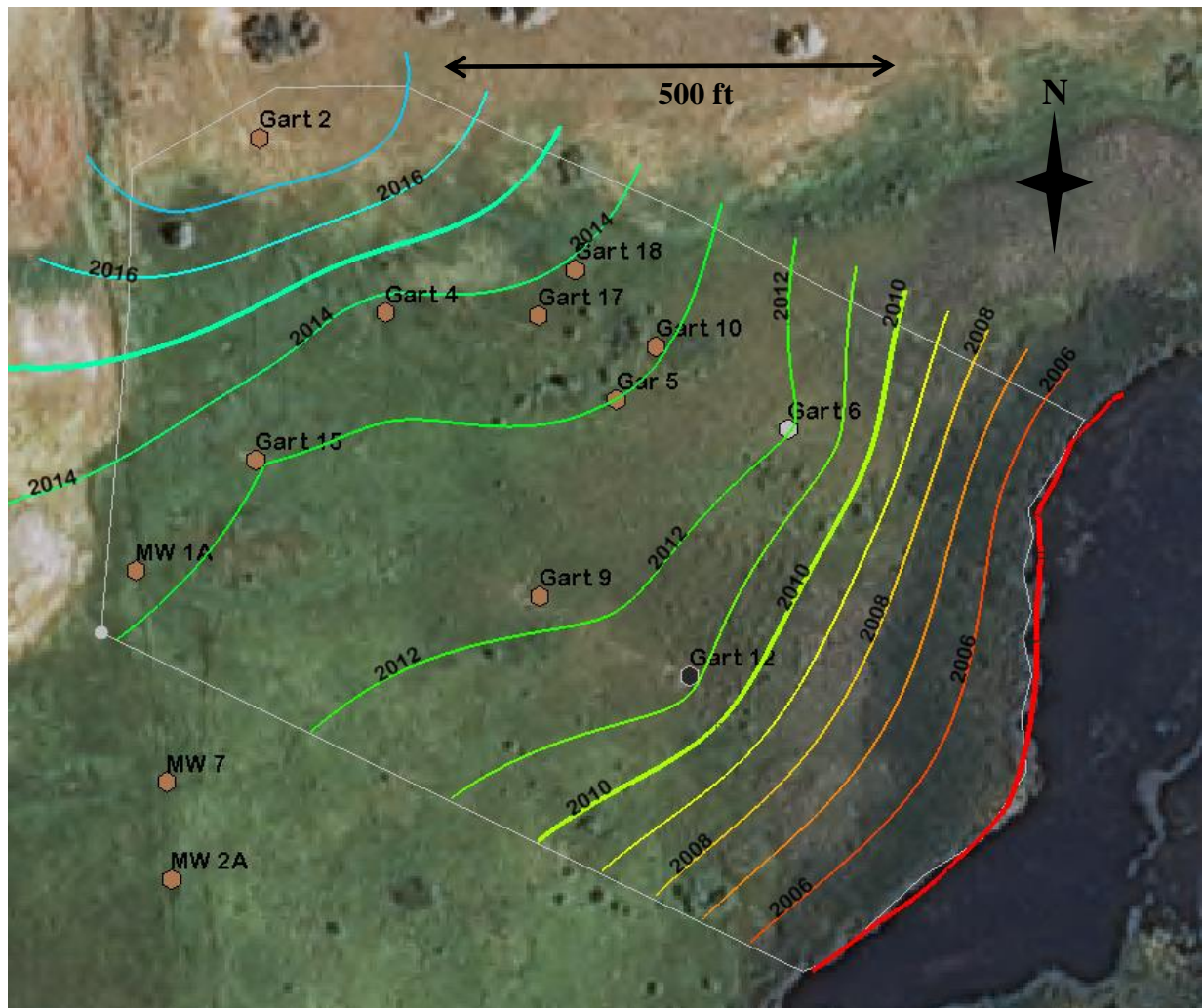


Figure 14: Potentiometric surface for September 10th, 2011. Not all wells are shown in this view for clarity purposes.

Computer Code

The numerical modeling of the Gartside Fen evapotranspiration was accomplished using the graphical user interface Groundwater Modeling System (GMS) 8.3.7 (Aquaveo, LLC.) to program MODFLOW 2000 (Harbaugh, 2000) numerical model simulations. The Hydrologic Unit Flow (HUF) package in GMS was used to apply the material properties to the borehole stratigraphy for aquifer characterization.

Stratigraphy Modeling

The stratigraphy of the Gartside Fen was modeled in GMS using the ‘boreholes to cross-sections to solids’ method. Borehole materials and contact elevations were entered directly into the GMS using the well log information for assigning the subsurface material elevations, and using Google Earth to pick surface locations and elevations. The locations of the wells show as light spots in the dark green fen on the August 11, 2011 aerial image in Google Earth. The locations of Gart 17 and Gart 18, which were installed in July of 2012, were approximated. The August 2011 imagery was also downloaded from Montana Natural Resource Information System (NRIS) and used as a base image in GMS and to likewise

locate the boreholes. Dummy boreholes were constructed to define the stratigraphy at the reservoir edge since no shallow wells could be installed there during summer months. The GMS function to automatically assign model horizons to the borehole stratigraphy by comparing boreholes failed. Therefore the contacts and horizons were manually defined.

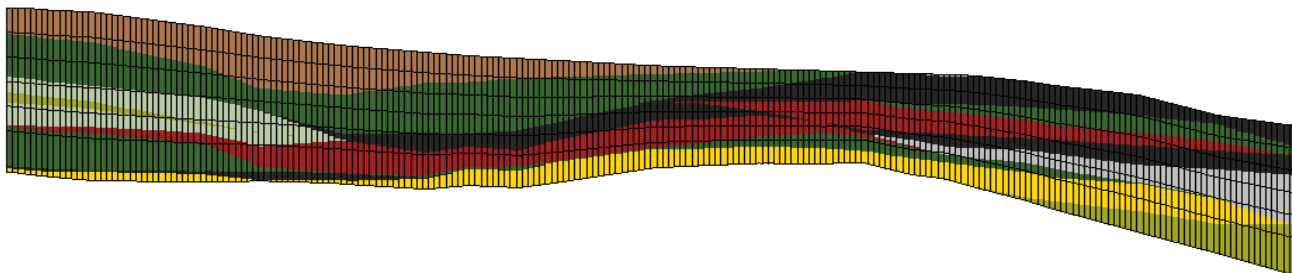
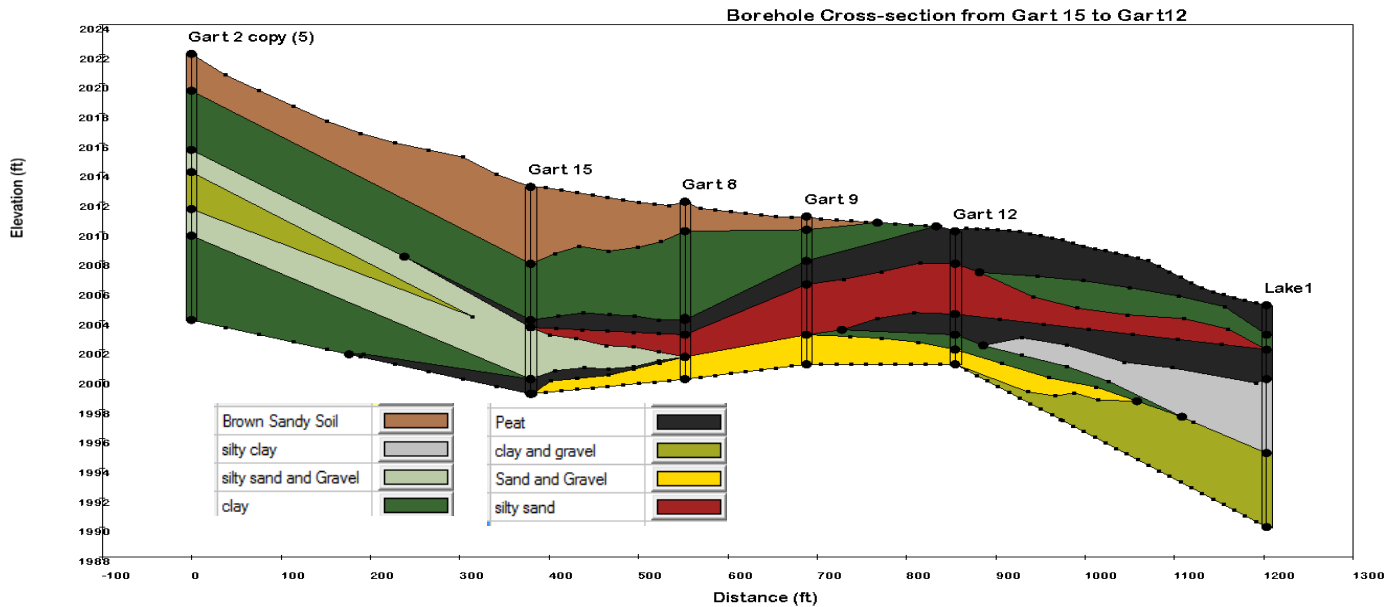


Figure 15: The upper image is a borehole cross-section created in GMS and the lower image is the stratigraphy along row 85, which is approximately a transect from Gart 15 to Gart 8, Gart 9, and Gart 12 (10X vertical exaggeration) after interpolation to MODFLOW layers using krigging as the interpolation method.

Borehole cross-sections were also manually constructed and used to guide the interpolation of borehole horizons to material solids using the “nearest neighbor” method. Borehole cross-sections generated in GMS show the complex subsurface in the fen area (Figure 15)

Steady State Model Development and Calibration

Model Grid

A MODFLOW grid was developed in GMS to represent six layers of 5.0-ft x 5.0-ft cells covering a 1,100 ft by 640 ft area. The grid was rotated 26 degrees south of east to align the cells with the mapped groundwater flow direction (figure 16). The lowest layer, layer 6, was set at 25 percent of the model thickness, and the remaining 75 percent was split evenly into the top five layers. The design attempts to

keep the highly conductive sand and gravel materials at the base of the flow system within layer 6. Once the grid and layers were developed, a ‘boundary’ coverage was created to select 131,895 active cells.

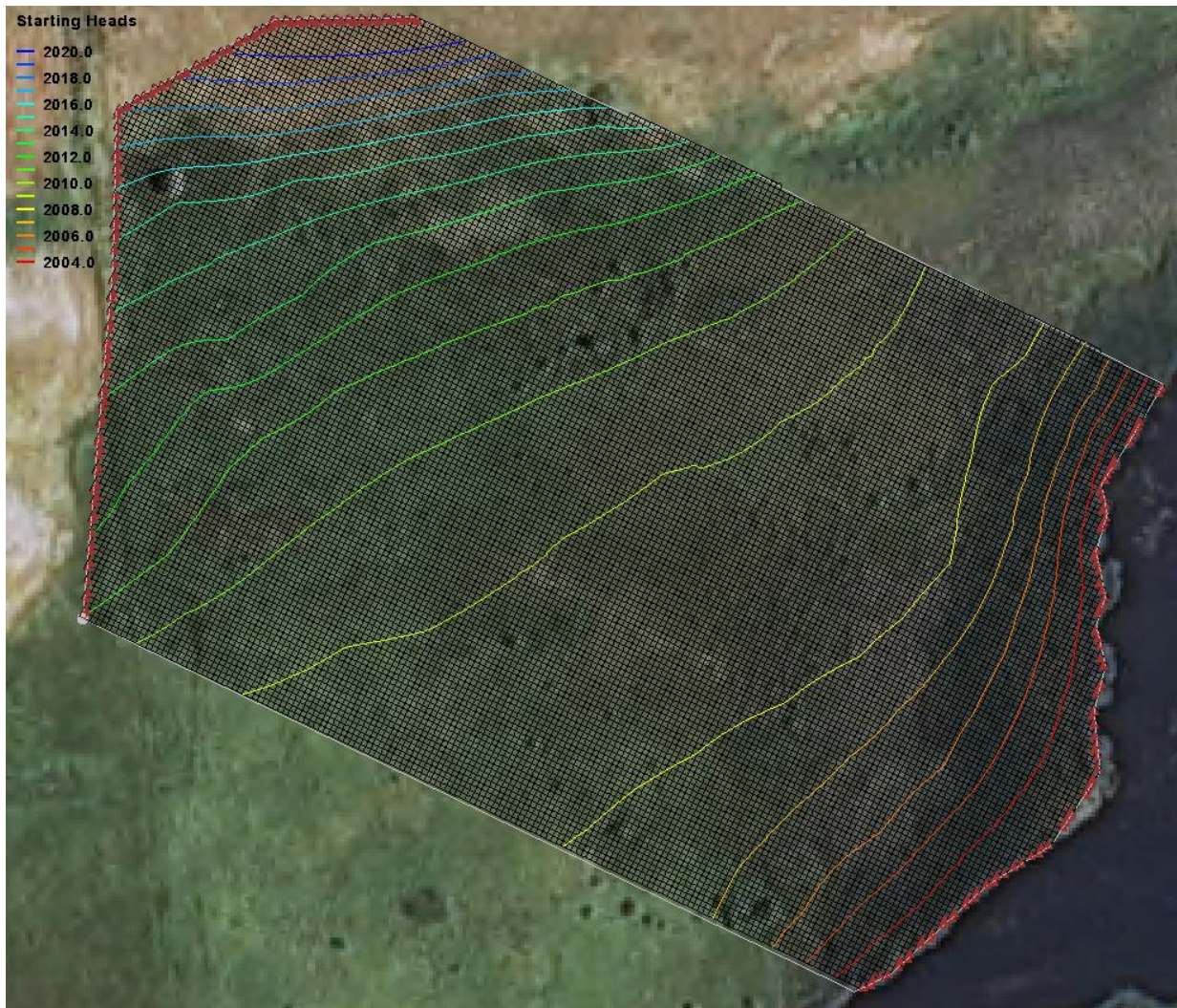


Figure 16: The MODFLOW grid with 5 feet square cells contours of the starting heads and locations of the GHB cells are shown in this image.

Hydraulic Parameters

After grid establishment, ‘material solids’ were converted to hydrogeologic units (HGU’s) assigned to MODFLOW Layers. The HGU’s were used to assign aquifer properties associated with each subsurface material to the MODFLOW grid cell in which they are found. Grid cells containing multiple materials are assigned aquifer properties calculated from the contained HGU’s. This method was selected because the layers of subsurface materials are discontinuous. Table 2 lists the subsurface materials and their assigned aquifer properties. The material property values were initially set using a range of values found in the literature, and using the values determined during the short-duration aquifer tests and sieve analyses (Table 3).

Table 3: Material Properties Assigned to the Complex Model

Material	HK (ft/day)	VK (ft/day)	Sy
clay	0.001	0.0003	0.01
Silty clay	0.01	0.003	0.1
Peat	0.01	0.003	0.15
Silty Sand and Gravel	1	0.2	0.05
Brown Sandy Soil	2	0.5	0.1
Sandy Clay and gravel	5	1	0.1
Silty Sand	10	4	0.1
Sand and Gravel	100	30	0.15

Boundary Conditions

The boundary conditions include head-dependent flow, specified flow, and no-flow. The model's lower surface is assumed to be a no-flow boundary due to the large range in hydraulic conductivities between the transmissive sand and gravel at the model's base the relatively impermeable siltstone and claystone layers of the Fort Union Formation below. Water-level measurements in, MW 7, completed in the bedrock show that heads in the bedrock units are lower than those of the wells completed within the fen indicating that the alluvium may be supplying some water to the underlying bedrock units. The north and south model boundaries were assumed to be along flow lines and thus to be no-flow boundaries. The east boundary at the reservoir was set as a head dependent flow boundary; the west boundary was defined to be a head dependent flow boundary and account for underflow into the model. The surface of the model was set as a specified flow boundary to represent evapotranspiration. For steady-state model, ET-specified flow was set at 0.019 ft/day, in the range of values of ET published for similar sites (Sloan, 1972).

Sources and Sinks

The sources and sinks for the steady-state model include the head-dependent flow and specified flow boundaries. The west side head-dependent flow boundaries were modeled using the General Head Boundary (GHB) package in MODFLOW. The head values were specified by setting the node elevations at the ends of General Head arcs in GMS. The arcs were assigned a conductance with a starting value similar to the hydraulic conductivity of the material intersected by the arc. The west boundary was split by layer assignment to simulate the greater heads in the lowest layer, the clean sand and gravel. The boundary at the reservoir was also split and assigned different conductance values, but the heads were assigned to equal the observed reservoir level (2005 ft) for all layers.

Specified flow polygons were assigned to layers one and two of the model to simulate ET water flow out of the model. The initial flow was set to be approximately 4.0 ft/year or 0.019 ft/day over the 7 month active ET period.

Steady-state Model Calibration

The steady-state model was calibrated to water levels observed on September 10, 2011 at the 16 Gartside wells. The data were used to create an observation coverage in GMS to observe head changes at the

modeled monitoring well locations that result from the calibration efforts. Calibration simulations continued until modeled heads at most of the calibration points were within the calibration interval, +/- 1.0 ft of the observed water levels. Run-to-run conductance values of the general head boundaries (GHB) were modified first to bring modeled water levels close to the calibration targets. Then hydraulic conductivities of the aquifer materials were varied within reasonable limits to improve the calibration. PEST automated parameter estimation in GMS was then used to adjust calibration differences by automatically varying the GHB conductance and horizontal hydraulic conductivities and comparing each model run to the calibration targets. The final automated PEST values offered only minor adjustments to the initial manual calibration. The specified flow cell values were increased and decreased by a factor of 10 during the calibration process to evaluate the how sensitive the model was to changes in ET rates.

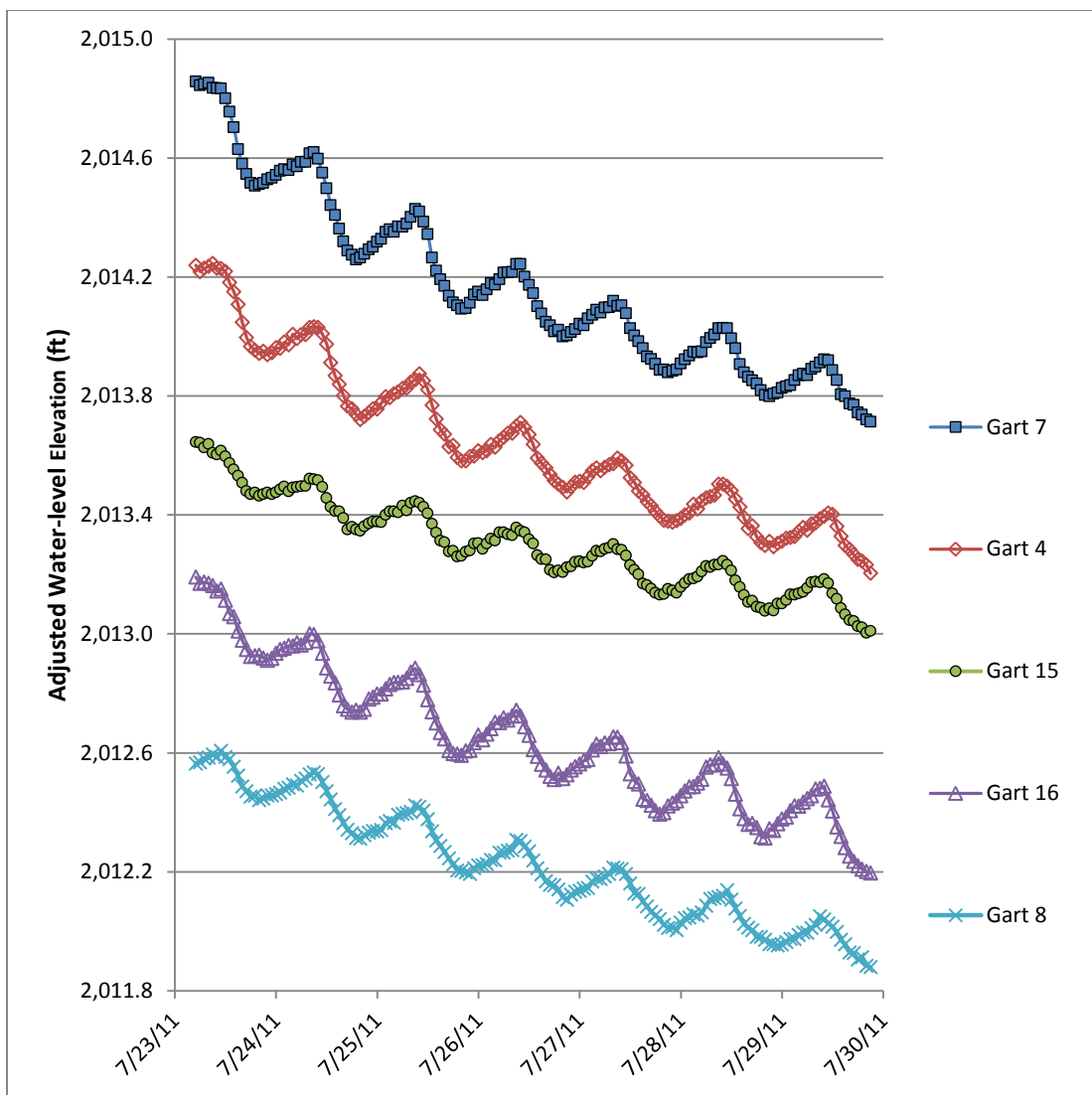


Figure 17: Diurnal water-level fluctuations in July of 2011 at selected Gartside wells.

Transient Model Development and Calibration

The best steady-state model simulation was used as the starting point for the transient model development. July 26-29, 2011 was selected from the Gartside water-level data as a period during which multiple wells showed consistent diurnal water-level fluctuations (Figure 17). During this time period data coverage was also good with data loggers in 15 of 16 wells collecting hourly water-level and temperature measurements. At Gart 9, the data logger was accidentally left on the surface, and so was unable to record water-level data. Fortunately it did record the land-surface temperatures in the grass near Gart 9 which provided valuable information about the timing of the diurnal temperature changes. The transient model was set with 95 stress periods, each period with one time step. The hourly water-level data for the July 26-29 period were entered into the observation well coverage as calibration targets for the transient model.

Simple Model Development

A second more simplistic groundwater flow model was constructed to simulate localized water-level fluctuations at wells Gart 17 and Gart 18. The goal of this model was to quickly evaluate different combinations of aquifer properties, hydraulic gradients, and ET rates which could produce the diurnal water-level fluctuations observed at Gart 17 and Gart 18 in the late summer of 2012. These two wells were selected since they were installed in nearly identical sites with respect to their position in the flow system, surface vegetation type, and depth of completion. The hydrographs for the two wells show nearly identical water-level fluctuations. Gart 18 was the well site used for the “Tarp Test” explained in the methods section. The simple model was used to model the changes in water-level fluctuations observed during the test and will be referred to as the TT model for “tarp test”.

The simple TT model had a runtime of approximately 12 seconds per simulation as compared to the 35 minute simulation time for the complex model. With the faster runtimes of the simple model, many different combinations of the variables controlling the diurnal water-level fluctuations and the sensitivity of the model to each variable could be evaluated.

MODFLOW Grid

The rectangular grid was set to represent an area 1000 feet long and 600 feet wide with surface elevations and grade similar to that at the Gartside wetland. The cells of the grid were sized to be 10 feet by 10 feet square with grid refinement down to two feet square cells at the points representing Gart 17 and Gart 18 (Figure 18). In the TT model the Layer Properties Flow (LPF) package in GMS was used to represent the system as two continuous layers. Layer 1 of the model simulating the fine grained layers of silty clay, silty sand and peat which are found in the top 6 to 20 feet of the wetland. Layer 2 represents the highly conductive sand and gravel aquifer which supplies ample water to the system and establishes the strong upward gradient. The deeper monitoring wells installed at Gartside were screened in the productive lower sand and gravel aquifer and show heads up to two feet higher than the wells completed in the upper fine-grained layers.

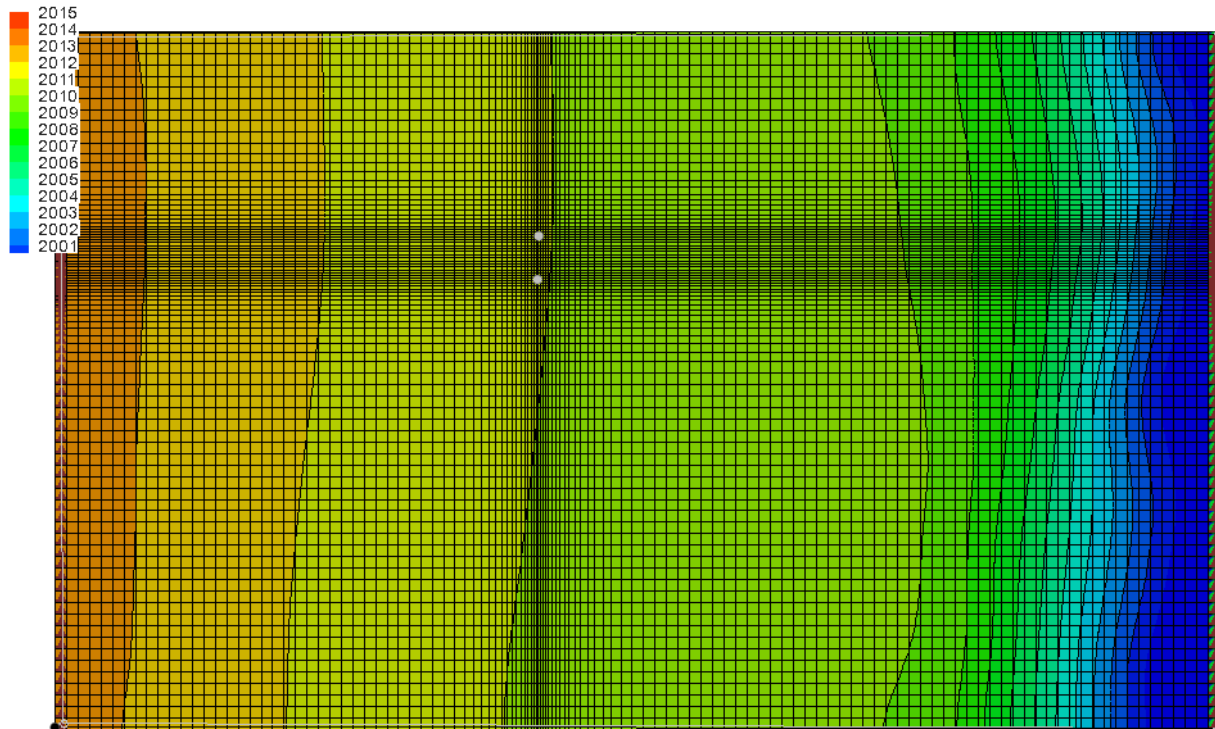


Figure 18: Telescoping MODFLOW grid used with the “tarp test” model showing the two points used to refine the grid.

Model Layer Properties

The hydraulic properties of each layer were specified using polygons in the map module of GMS which allows areal variations for each layer. The properties of layer one were applied equally to all cells in that layer. Layer two was divided into two polygons, one large polygon representing the highly conductive aquifer material, and a smaller polygon on the down-gradient end assigned lower hydraulic conductivity to establish the steep hydraulic gradient observed near the reservoir (Figure 19). The values of the hydraulic properties assigned to each layer are shown in Table 4.

Table 4: TT model hydraulic properties

Layer Hydraulic Properties	HK	VK	Sy
Layer 1 (total Layer)	0.13	0.04	0.015
Layer 2 (large polygon)	100	30	0.15
Layer 2 (Small polygon)	1	0.3	0.01

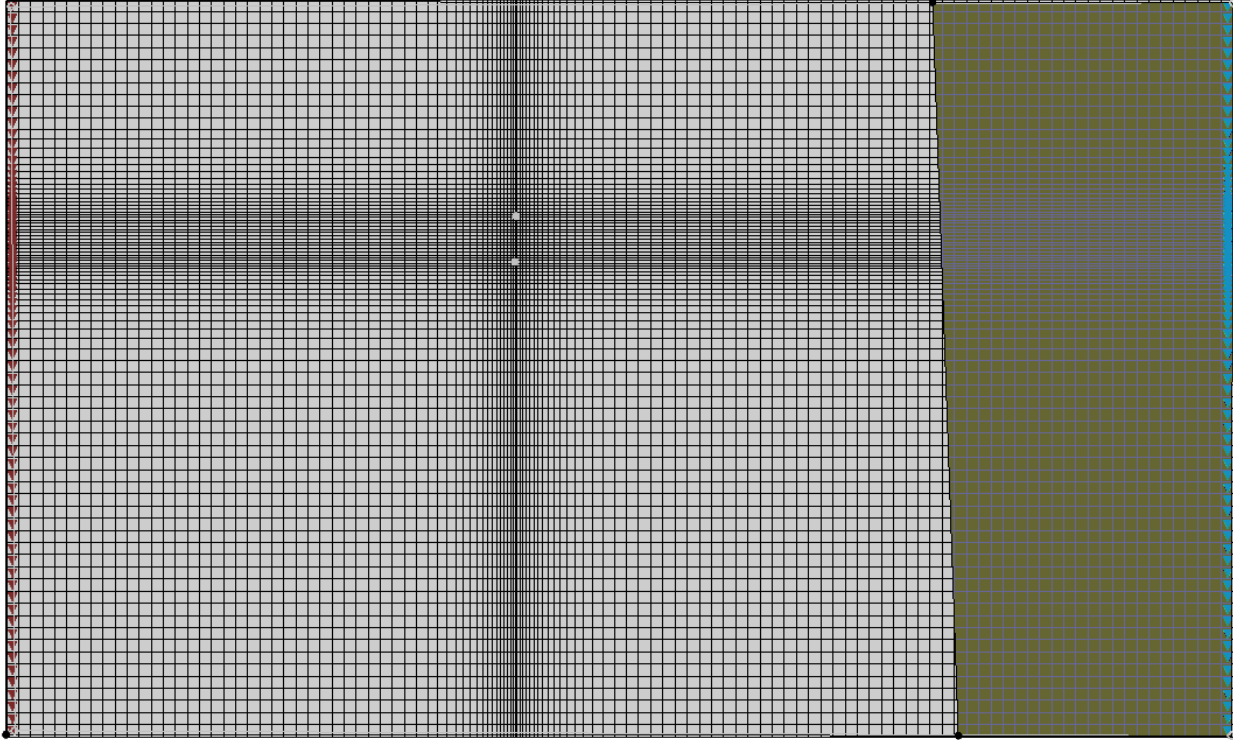


Figure 19: The hydraulic properties were varied using polygons in layer 2 of the TT model.

Model Boundary Conditions

Head-dependent flow boundaries were assigned to the up-gradient and down-gradient ends of the TT model using the general head boundary (GHB) package in GMS. Arcs in each layer were specified as GHB arcs and assigned a conductance value similar to the horizontal hydraulic conductivity of the layer. Head elevations were assigned to nodes at the ends of the arcs. The head and conductance values assigned to the arc on the up-gradient end of layer 2 were higher than the values assigned to the corresponding GHB arc in layer 1. This was done to maintain the upward gradient as observed in the study area. The sides of the model were no-flow boundaries since they were established along flow lines. The bottom of the model was a no-flow boundary to represent the contact of the aquifer material with the Fort Union bedrock.

Steady-state Model

Several steady-state model simulations were run to visually evaluate the boundary conditions assigned to the TT model. The steady-state model maintained heads close to or above the top of layer one with upward gradients from the lower layer, similar to the actual flow system. The goal of the TT model was to evaluate the conditions needed to produce the observed diurnal water-level fluctuations at one point in the wetland and not to match a static set of head measurements. Therefore, the model was not calibrated to a specific set of head measurements, but was evaluated on the model's ability to replicate the flow system observed at Gartside.

Transient Model and Calibration

The steady-state model was then programmed to simulate the four days from August 31st to September 3rd, 2012 with 95 hourly stress periods. Each stress period was set to have only one time step to keep the simulation time as short as possible. The two wells set in the model as points for grid refinement were placed at the approximate position in the system as Gart 17 and Gart 18 are in the wetland. These points in the model were monitored for changes in the model output with each trial simulation, and the output model head data compared to the actual diurnal head changes at Gart 18.

Series of transient simulations were run and the time series heads (model output) at the point representing Gart 18 were graphed in Excel for comparison to the observed values. The hydraulic conductivity (HK and VK), the specific yield (Sy), and the ET rates were systematically varied to generate a series of model response curves. Charts of these simulations (Figures 20-22) were used to select combinations of the layer properties (HK-VK, Sy, and ET rate) in the curve matching calibration process whereby the TT model generated head fluctuations were matched to the observed diurnal water-level fluctuations at Gart 18.

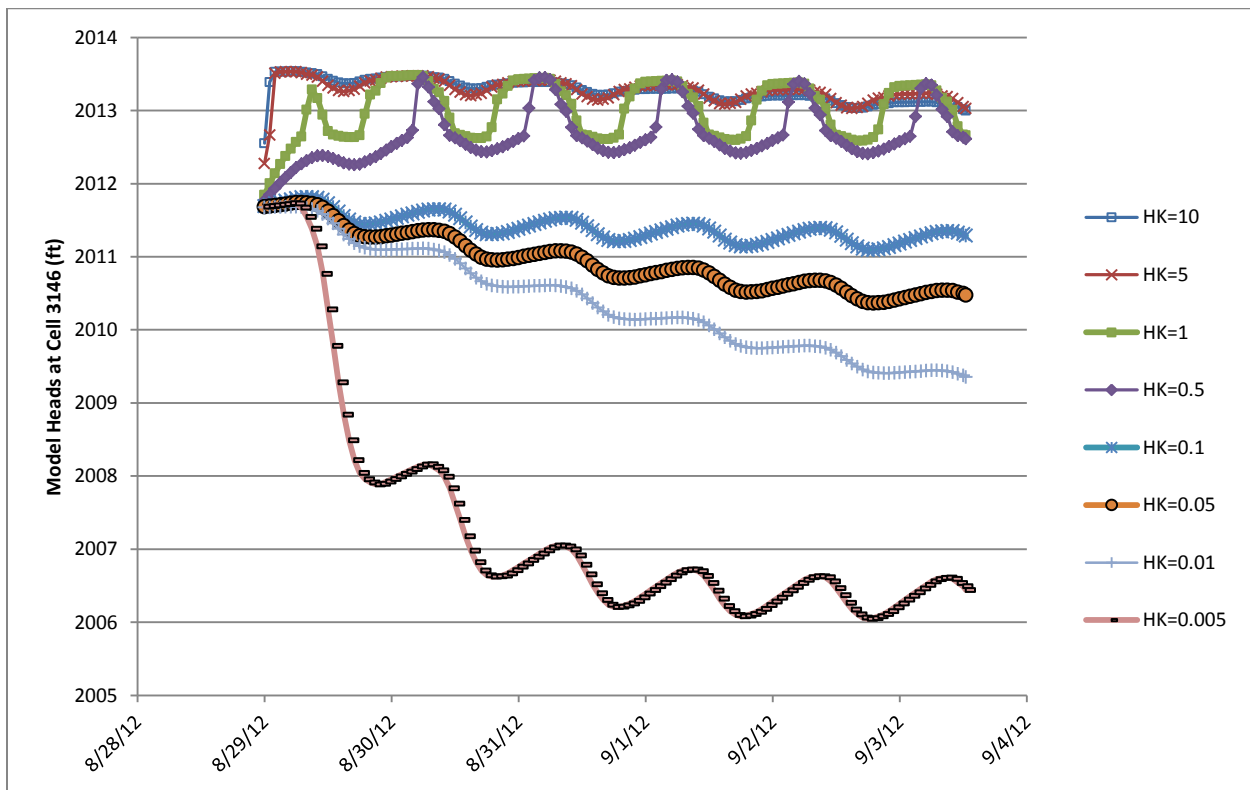


Figure 20: TT model responses to changes in HK of layer 1.

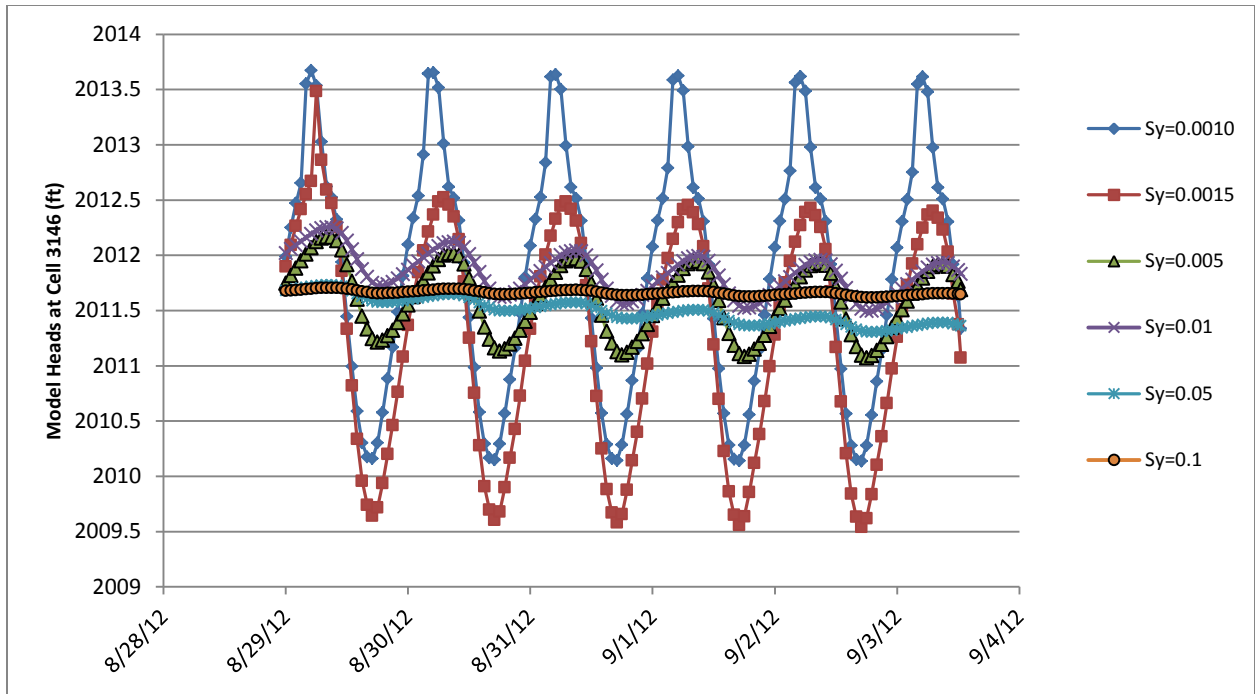


Figure 21: TT model responses to changes in the SY assigned to layer 1.

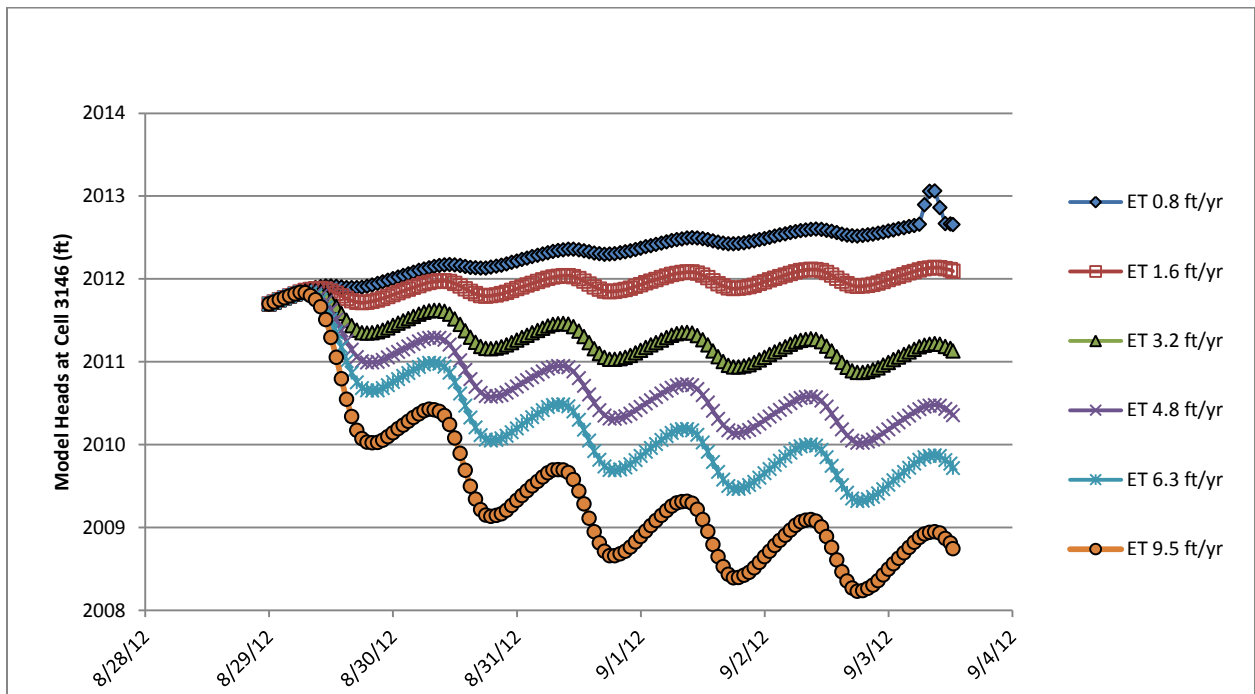


Figure 22: TT model head responses to ET rate changes.

Modeling Results

Complex Model Results

Even with more than 20 wells, the stratigraphy modeling for the complex model was difficult. There were considerable changes in the subsurface materials, even when only moving short distances between boreholes. The process of defining hydrologic units was simplified by grouping of materials into like categories based on texture and position. The interpolations from borehole cross-sections to solids and then to hydrologic units were complicated by having wells of varying depths, but the program generated reasonable results. There is a large uncertainty when it comes to predicting how connected the higher conductive layers are and if there are preferential flow paths, or buried stream channels in the deposits. Old stream channels are visible in some of the aerial imagery of Gartside Reservoir, revealing the pre-dam topography.

The steady-state version of the complex model produced head results close to the calibration targets with the calibration interval set at ± 1.0 feet (Figure 23). The calibration targets in GMS show the relationship between the observed head and the computed head at a given observation point. If the computed head falls within the calibration interval, in this case ± 1.0 feet, then the target is colored green and indicates if the computed value is above or below the observed value. Yellow coloration indicates the computed head falls within two times the calibration interval. Computed values outside that range are indicated if the calibration target is red. The calibration target for Gart 8 indicates poor calibration with a computed value 2.32 ft above the observed value (figure 24). The calibration targets for the well pairs show that the model was able to simulate the head differences between shallow and deep water bearing units.

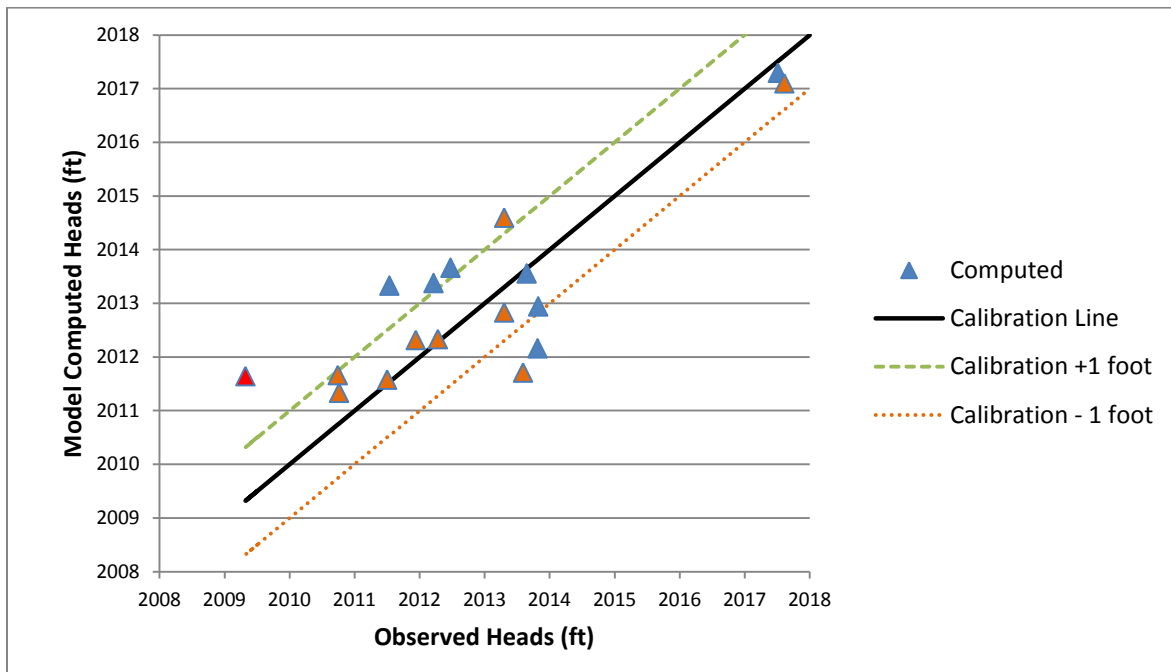


Figure 23: The computed heads from simulation Gart2-22-13Ca3 are shown here with a calibration line of the observed values and the calibration interval used. The orange triangles represent the shallow wells. The red triangle shows the computed value for Gart 8 which fell in the poor calibration range.

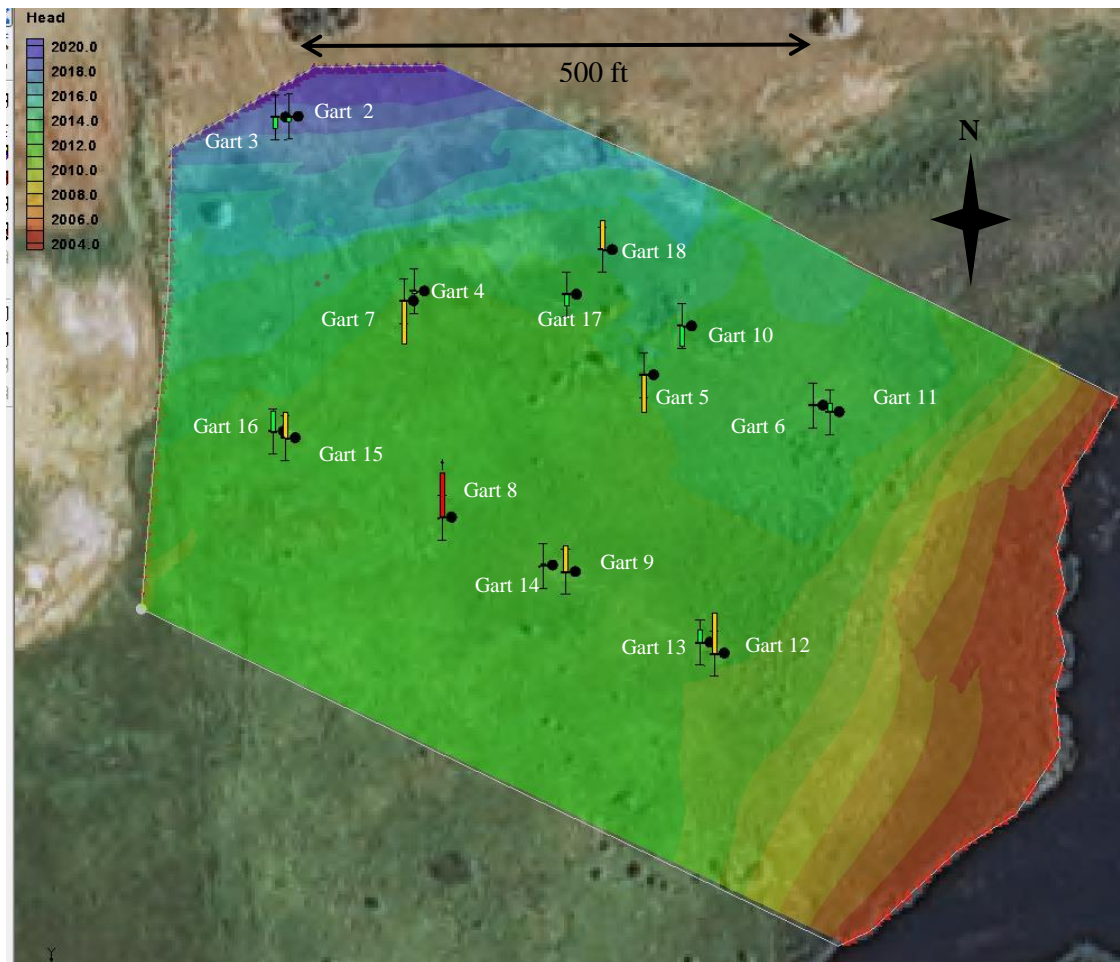


Figure 24: Calibration markers in GMS show good agreement between model heads and observed data at almost all calibration points (steady-state model simulation Gart2-22-13 Cal 3).

Automated parameter estimation (PEST) in GMS was used in attempt to improve the model calibration by adjusting the material properties assigned to different stratigraphic units in the model. Results from the PEST simulations showed only slight variations from the values assigned during manual calibration.

TT model results

The TT model steady-state simulations were only used to test the boundary conditions necessary for simulating the generalized flow system at Gart 17 and Gart 18. The TT model runtimes were approximately 8 seconds or nearly 300 times faster than the complex model. The upper water-bearing zone was modeled as a single layer assigned composite hydraulic properties determined during the calibration process. Curve matching calibration was guided by the charts shown as Figures 20-22. Variations in the HK assigned to layer 1 of the model caused changes in the slope of the multi-day trend, and some changes to the daily fluctuation curve shape (Figure 20). Variations in the Sy mainly changed the amplitude of the diurnal fluctuation, with large fluctuations resulting from low Sy values (Figure 21). Variations in ET rates mainly produced changes in the multi-day trend, but also produced

changes in the diurnal water-level curve amplitude (Figure 22). The HK, Sy, and ET values assigned to layer 1 were systematically varied to match the model curve to the “predicted” curve for Gart 18 (Figure 12). This curve includes three days of observed pre-test data, and one day of predicted data during the tarp test.

Once a good fit had been achieved, the model was modified to reflect the changes in ET caused by the tarps being installed around Gart 18 during the “tarp test”. This was accomplished by setting the ET rate on the fourth day to zero in the model area representing the tarp covered area of the Gartside wetland. A small polygon created in the ET coverage was assigned the modified ET rate (Figure 25). The model area defined by the polygon reduced the ET in 64 grid cells representing 351 ft², whereas the actual tarp coverage was 341 ft². All cells intersected by the polygon were assigned the reduced ET rate during the fourth day of the simulation. Simulations with and without the “tarp” polygon ET restriction were run, and the model heads compared to the observed and predicted heads at Gart 18 during the actual “tarp test”.

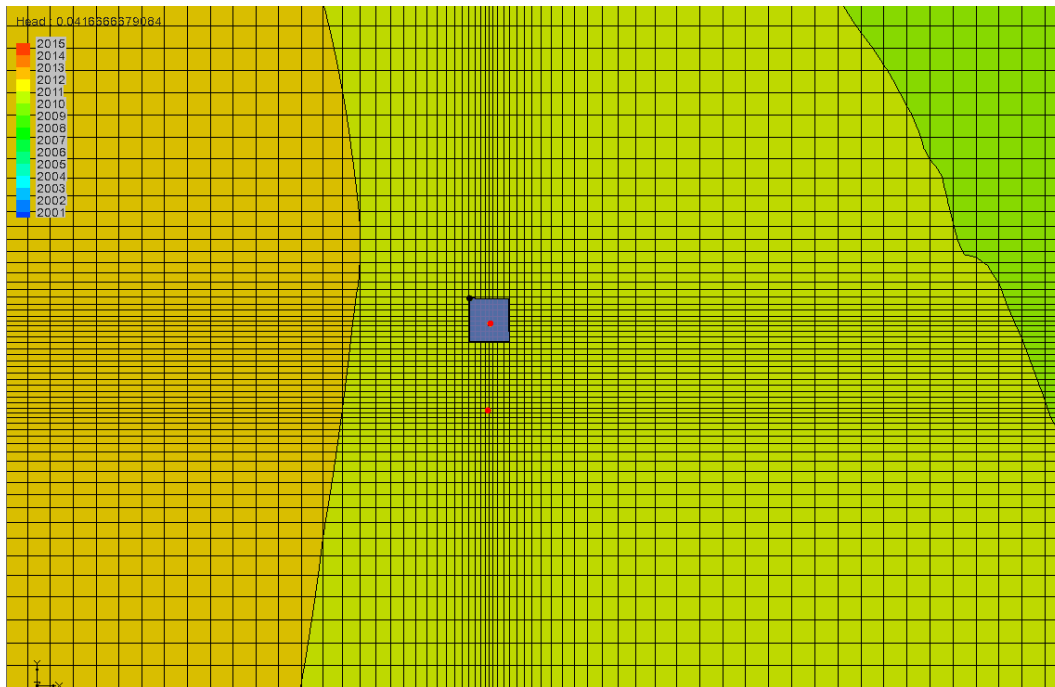


Figure 25: ET polygon used in GMS to represent the area covered in the “tarp test” at Gart 18.

The TT model simulations were able to match the observed and predicted diurnal water-level fluctuations at Gart 18 closely. The diurnal head fluctuations of the model simulation were output for the cell representing Gart 18 and compared to the actual and predicted water-level fluctuations. The model run TT30 without the “tarp” polygon compares favorably to the curve predicted for Gart 18 in the absence of the “tarp test”. Model run TT35 with the “tarp” polygon ET restriction responded similar to Gart 18 during the “tarp test”. The model responded more quickly to the ET restriction than the actual system (Figure 26). The model generated head fluctuations in the “tarp” polygon area vary from cell to cell, with the cells near the edge showing the best match to Gart 18 (Figure 27).

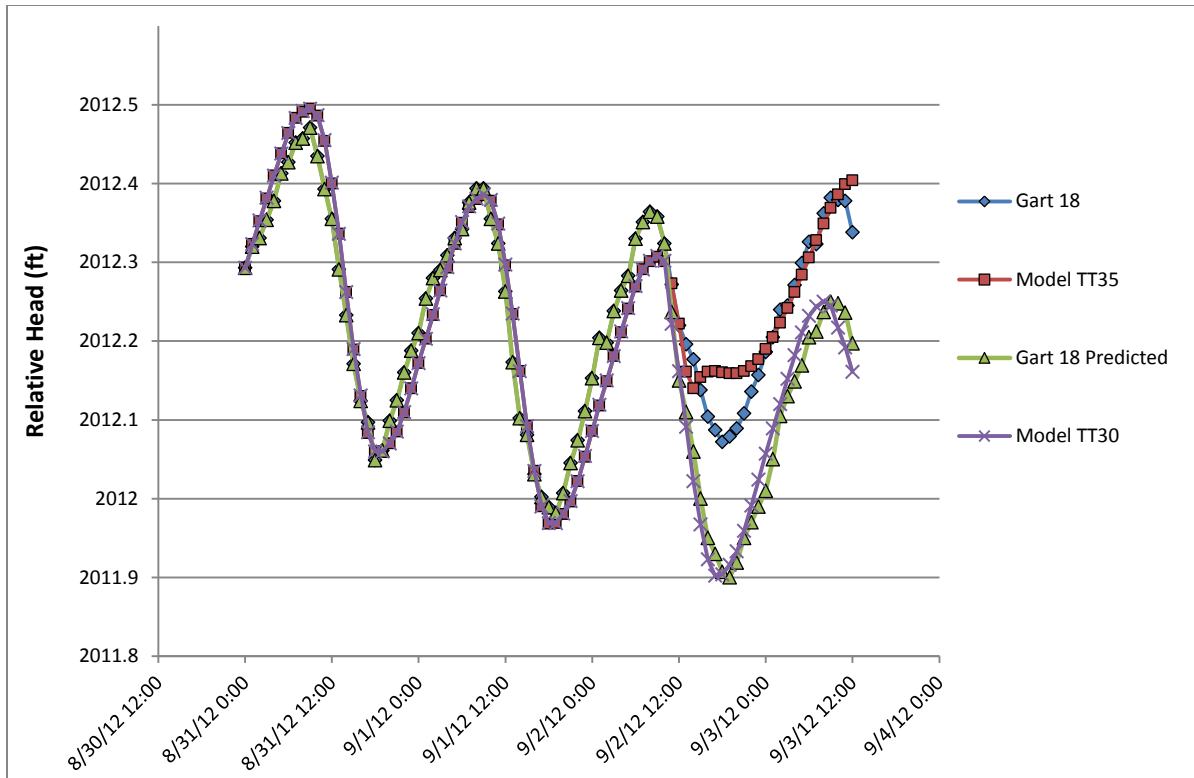


Figure 26: The diurnal water-level fluctuations at Gart 18 and the fluctuations predicted at Gart 18 without the “tarp test” are closely matched by TT35, a model with a “tarp” polygon, and model TT30 without an ET restriction.

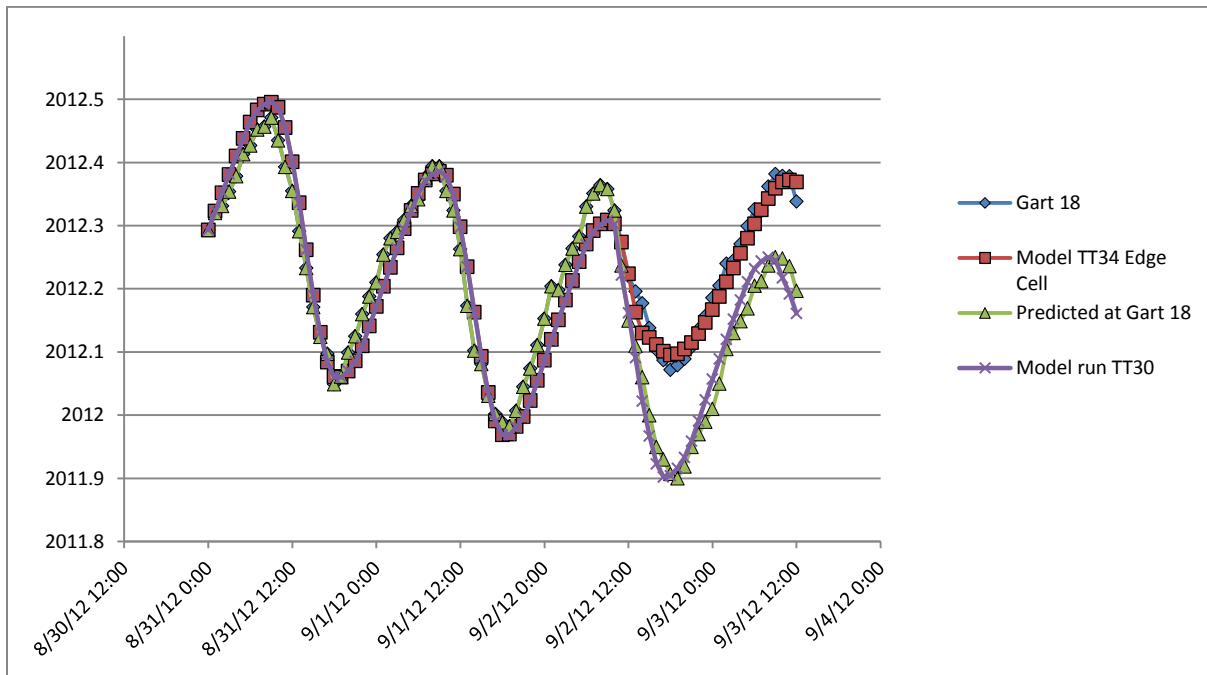


Figure 27: The TT34 edge cells respond more like the actual system when ET was restricted in the model.

The flow budgets from the TT model simulations show approximately 40,420 ft³ of water was removed from the model by the ET package over the 5.52 day simulation period giving a daily rate of 0.012 ft/day over the 600,000 ft² of the model area. This rate calculates to be approximately 2.6 ft/year assuming seven months of active ET per year. The White method (1932) was used to calculate the ET rate from the diurnal water-level fluctuations at Gart 17 and 18 using the fluctuations from the three days before the “tarp test. This method produced ET estimates for Gart 17 of 1.8 ft/year, and for Gart 18 of 2.2 ft/year based on seven month ET period per year.

Discussion

Discussion of Field Work

Since the goal of this project was to develop field and modeling methods for estimating ET rates through the modeling of diurnal water-level fluctuations, there were discoveries in both areas. The monitoring well network provided valuable information about the hydrogeologic system. It confirmed the idea that the wetland is supplied by a relatively constant supply of mineral-rich groundwater. The hand-auger drilling method provided detailed stratigraphic information which unveiled the true complexity of the system, never imaginable with only a surface view. The layers of fine clay and peat point to periods of alternating water levels. A pebble discovered in the middle of five feet of dense clay suggests ice rafting of the stone.

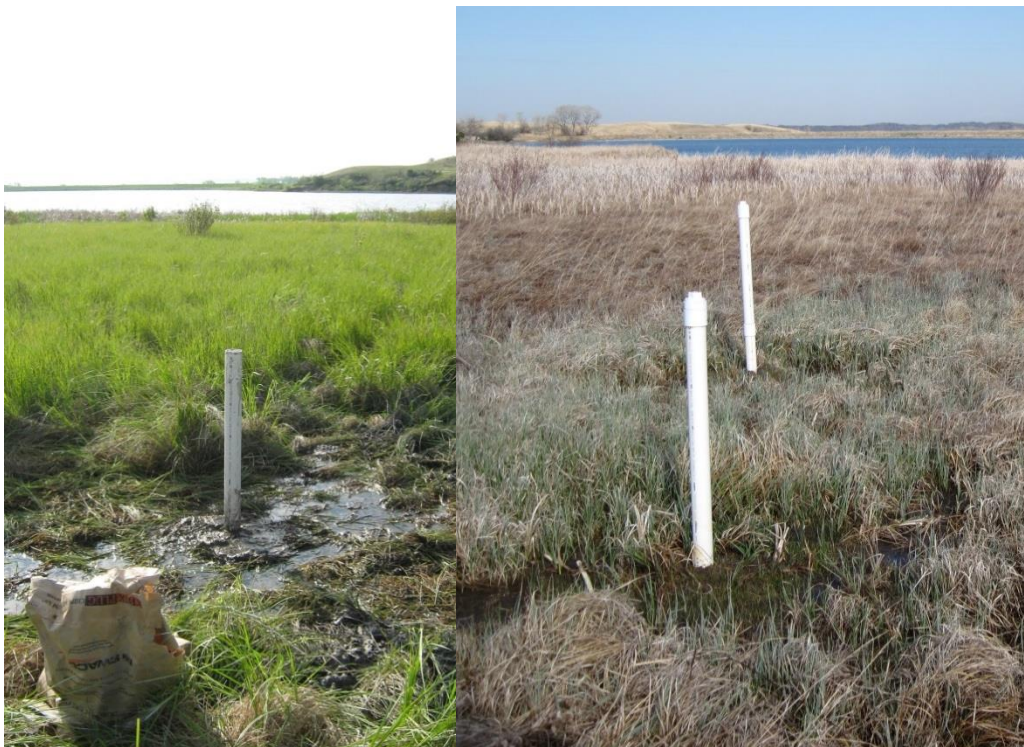


Figure 28: The installation of Gart 11 on 7/5/2011 shows vegetation the damage to the sedge/Sphagnum mat during well installation (left). The same site 4/25/12 shows Gart 6 (near) and Gart 11 (distant) with the vegetation recovery. Notice the lack of sedges near the well, but the Sphagnum has filled in.



Figure 29: Well installation and development at Gart 4 (left) and Gart 7 6/2/2011. The bottom image shows the site looking south on 8/7/2012 with nearly full recovery of the vegetation, Gart 4 in foreground.

The fen portion of the study area required the development of new methods for well installation. The floating sedge/Sphagnum mat while interesting to walk on, made well installation and monitoring a challenge. The use of external thin walled PVC temporary casing to prevent caving on the auger was a major advancement in our well installation methods. All of the bentonite, silica sand, and casing had to be packed to each well site. This required multiple trips across the floating sedge mat which created trails in the vegetation. The trampling of the vegetation at the well site and on these trails created weak spots in the floating mat (Figure 28). Once this was discovered, different routes to the wells were taken on each site visit if possible. One could minimize the damage to the sites by installing the wells when the surface is frozen, or by using plywood as a temporary work platform when installing the wells. The vegetation was also disturbed around the wells where the surface was solid, but the vegetation seemed to recover quickly, and paths between wells were hardly visible with the new season in 2012 (figure 29).

The finding of “preferential flow paths” in otherwise dense clay was quite interesting and helps explain how water can move through this very fine grained material and supply ground water to the wetland. The origin or the mechanism is not understood at this point, but in the case of the light green-gray clay with

white carbonate deposits, the deposits seem to act as tubes through the clay. In the green clay layer with rusty-red flecks, the rusty areas are most likely flow paths colored by iron oxidation. Chemical analyses of the ground water at different depths in the fen may provide better understanding of flow system. The short-duration aquifer tests, and aquifer material property results from numerical model calibration both assign hydraulic conductivity values to the upper water-bearing zone higher than would be predicted for the mostly clay aquifer material. The “preferential flow paths” in the clay may be the reason for these results.

The idea for the tarp test came from searching for a way to determine the actual area around a well that was responsible for the diurnal water-level fluctuations observed in the well. Gart 17 and 18 were installed with the hope of finding two wells that responded similarly each day to the natural drivers of ET, and we were successful with Gart 18 showing only a slightly larger diurnal water-level fluctuation (Figure 12). The well logs for the two wells show more fine-grained material encountered in Gart 18, which would lower the overall specific yield, or the effective specific yield which is the water available for ET. With less water available, the ET causes a larger water-level fluctuation. The success of this initial test raises questions like, what would be the response to; larger tarps, tarps that block light more effectively, longer test periods, different shaped covered areas, or how do covered areas affect the water levels in nearby wells?

Discussion of Numerical Modeling Results

The detailed stratigraphy documented during the monitoring well installation was used in the development of the complex model. Even with 18 wells in a relatively small area, the complex model showed the data were insufficient to model the fen at a high detail level. No wells were installed at the reservoir edge due to the difficult conditions there, so the water level in the water bearing units was assumed to be the level of the reservoir. Although the water level at this boundary may not change the levels in the center of the study area near Gart 17 and 18, they are important to the flow through the overall system.

The installation of paired monitoring wells, a deep and a shallow, provided valuable information about the upward hydraulic gradients, and provided target values for calibration of the models. The complex steady-state model showed reasonable calibration at most of the well pairs, showing that the model did represent a part of the flow system.

Discussion of Numerical Modeling Results

The detailed stratigraphy documented during the monitoring well installation was used in the development of the complex model. Even with 18 wells in a relatively small area, the complex model showed the data were insufficient to model the fen at a high detail level. No wells were installed at the reservoir edge due to the difficult conditions there, so the water level in the water bearing units was assumed to be the level of the reservoir. Although the water level at this boundary may not change the levels in the center of the study area near Gart 17 and 18, they are important to the flow through the overall system.

The installation of paired monitoring wells, a deep and a shallow, provided valuable information about the upward hydraulic gradients, and provided target values for calibration of the models. The complex steady-state model showed reasonable calibration at most of the well pairs, showing that the model did represent a part of the flow system.

The biggest short-coming of the complex model was the long simulation runtimes. At approximately 35 minutes per simulation, it was difficult to test the many different combinations of variables controlling the ground water flow calculations for each cell. Only several transient models were run before deciding to simplify the model. The complex model did provide reasonable starting layer properties for the simple TT model.

The simplified TT model showed that the diurnal water-level fluctuations could be matched by the numerical model using reasonable hydraulic property values, and that the model did well to simulate the forced changes in ET as demonstrated with the “tarp test”. The model showed temporal deviations from the actual system, but with better calibration, these discrepancies may be reduced. The fact the edge cells under the “no ET” polygon in the model matched the “tarp test” water levels at Gart 18 provides evidence that the tarp installed at Gart 18 may have not stopped, but only restricted ET. The TT35 simulation with the “no ET” polygon showed about 3.0 ft³ less water loss to ET than the TT30 simulation when the model flow budgets were compared. When this volume is spread over the 351ft² area of the polygon, and the test time was one day, the ET reduction rate calculates to be 0.0085 ft/day or a rate of 1.8 ft/year.

It is unlikely that the solutions produced by the best calibrated TT model are unique. It is more likely that a range of HK-VK, Sy, and ET values would generate similar results. The fact that the model can reasonably match the observed water-level fluctuations before and during the tarp test, likely narrows the range of acceptable values. If the model matched a more extensive “tarp test”, perhaps larger area, or longer duration, then the model solution may be more valid.

When looking at the 2012 hydrograph for Gart 17 and 18, the periods of water level decline with strong diurnal fluctuations were punctuated by sharp water-level recovery periods during precipitation events, mostly in June and July (Figure 30). The ET rate applied to model representing four days in September would be close to a maximum ET rate for the system at that location. The model could be used to match other sections of the water-level record for Gart 18 by varying the diurnal ET rates, and through the curve matching process determine a better average ET rate for the season.

The water-level data for Gart 17 and 18 show a change from a declining trend to an inclining trend with the inflection point near the time of the “tarp test”. This change in water-level trends must have resulted from small changes in the climatic conditions since no precipitation events were recorded during this period. The water level-fluctuations recorded in Gart 17 and 18 plotted with the surface temperature recorded by the data logger for Gart 9, which was mistakenly left on the land surface in the grass, shows that the low surface temperatures each day decreased significantly at the inflection point in the seasonal trends (Figure 31). The daily low temperatures recorded between 3:00 and 5:00 AM show a 5-6°C decline after a couple cool days around September 3rd. The temperature curve in Figure 31 shows little change in the daily maximum temperatures, but the recorded high temperatures may only be reflecting the logger’s exposure to solar radiation, whereas the recorded low temperature reflects the actual surface temperature at night.

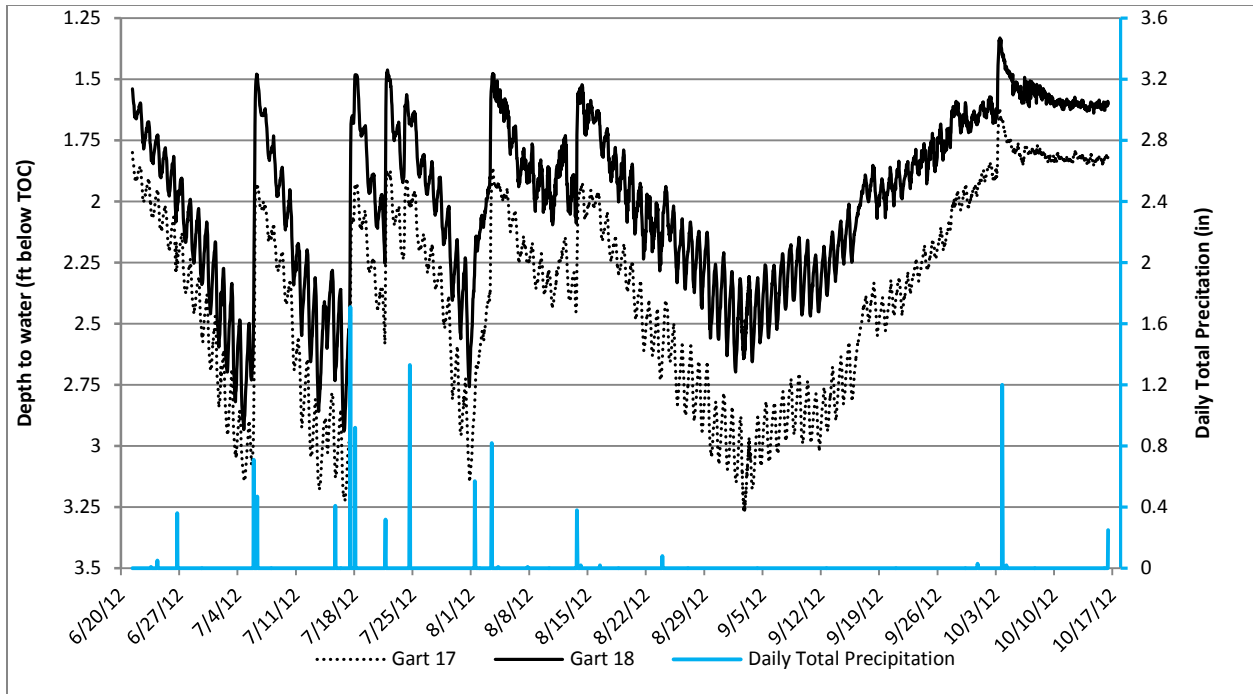


Figure 30: Hydrographs of Gart 17 and 18 show periods of water-level declines punctuated by rapid recovery during precipitation events.

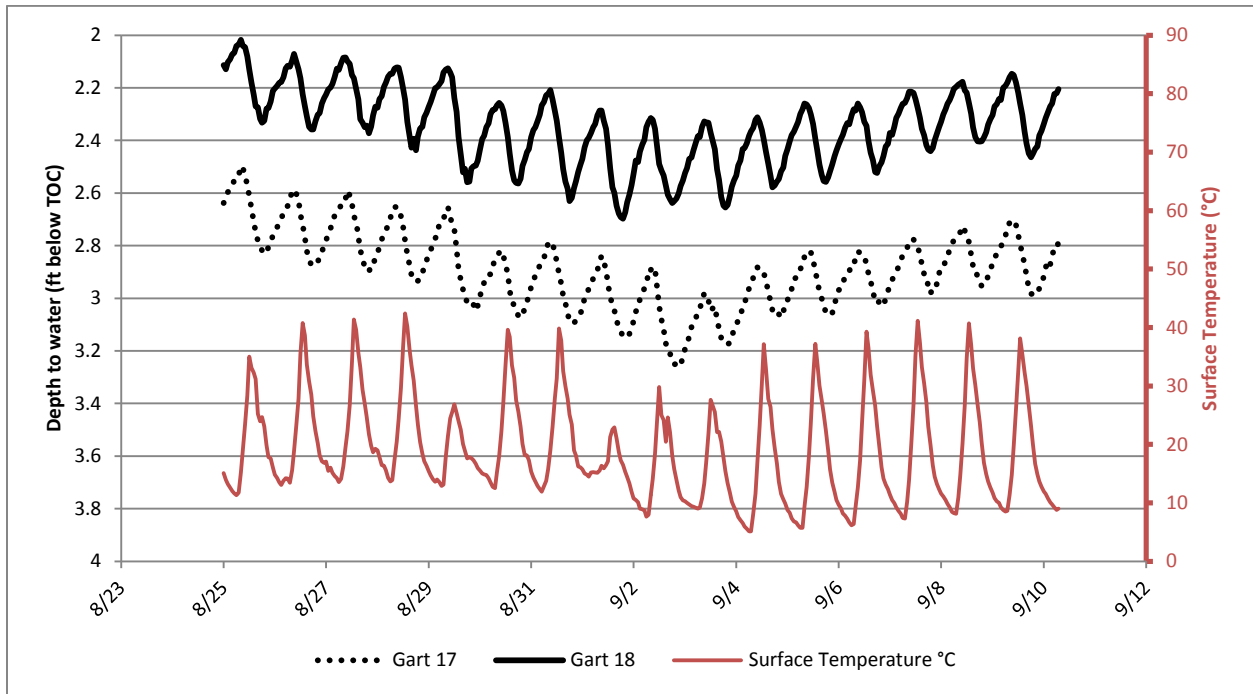


Figure 31: Diurnal water-level fluctuations at Gart 17 and 18 and surface temperature fluctuations.

Recommendations

The success of the simple model showed that a complex flow system can be simulated conceptually by grouping similar materials into single hydrologic unit with “averaged” hydraulic properties. A small number of wells installed in a wetland using methods capable of sampling the subsurface materials would most likely provide sufficient stratigraphic information for simple model development. The hand-auger methods using temporary thin walled PVC casing in caving materials, and precautions to minimize vegetation damage are highly recommended. Driven well points could be added quickly to provide more water-level information for potentiometric surface development, and to confirm water-level trends. Devices to record air temperatures at different levels in the vegetation may provide more insight into the drivers of seasonal water-level changes.

Calibration of any numerical flow model is always the most difficult part of the process. Ground-water fluxes and water-level information are often measured to construct a flow budget for a system, leaving ET as the primary “unknown” in the equation. Flows into and out of wetlands can be very difficult to determine making the “flow budget” approach to determining wetland ET impractical. Models calibrated to water-levels alone have non-unique solutions, but if a model can be calibrated to water-level changes both natural and forced by temporary reduction in ET using methods such as the “tarp test”, the range of viable solutions produced by the model may be narrowed to provide realistic site-specific ET estimates. More testing at Gartside fen and other wetland sites is needed to confirm the validity of this approach.

References

- Amon, J. P., Thompson, C. A., Carpenter, Q. J., & Miner, J. (2010, January 22). *TEMPERATE ZONE FENS OF THE GLACIATED MIDWESTERN USA*. Retrieved 9 20, 2012, from <http://www.tarleton.edu/Faculty/cthompson/SWSposter.htm>
- Cvancara, A. M. (1983). *Aquatic Mollusks of North Dakota*. Report of Investigation No.78, North Dakota Geological Survey, Fargo.
- Fetter, C. W. (2001). *Applied Hydrogeology*. Upper Saddle River, New Jersey: Prentice-Hall, Inc.
- Hill, M. C. (2006, November–December). The Practical Use of Simplicity in Developing. *Ground Water*, Vol. 44(No. 6), 775–781.
- Liu, S., Graham, W. D., & Jacobs, J. M. (2005). Daily potential evapotranspiration and diurnal climate forcings: influence on the numerical modelling of soil waterdynamics and evapotranspiration. *Journal of Hydrology*, 39–52.
- Podniesinski, G. S., & Leopold, D. J. (1998, September). PLANT COMMUNITY DEVELOPMENT AND PEAT STRATIGRAPHY IN FORESTED FENS IN RESPONSE TO GROUND-WATER FLOW SYSTEMS. *Wetlands*, Vol. 18(No. 3), 409-430.
- Quinton, W. L., Hayashi, M., Carey, S. K., & Myers, T. (2007). Peat Hydraulic Conductivity in Cold Regions. *64th EASTERN SNOW CONFERENCE*, (pp. 253-266). St. John's, Newfoundland, Canada .
- Sloan, C. E. (1972). *Ground-Water Hydrology of Prairie Potholes in North Dakota*. GEOLOGICAL SURVEY PROFESSIONAL PAPER 585-C, The Department of the Interior.
- Verry, E. S., Boelter, D. H., Päivänen, J., Nichols, D. S., Malterer, T., & Gafni, A. (2011). Physical Properties of Organic Soils. In *Peatland Biogeochemistry and Watershed Hydrology* (pp. 135-176). Taylor and Francis Group, LLC.
- Vuke, S. M., Wilde, E. M., & Smith, L. N. (2003). *GEOLOGIC AND STRUCTURE CONTOUR MAP OF THE SIDNEY 30'x 60' QUADRANGLE EASTERN MONTANA AND AD*. Butte, Montana: Montana Bureau of Mines and Geology.
- Weight, W. D., & Sonderegger, J. L. (2001). *Manual of Applied Field hydrogeology*. New York: McGraw-Hill.
- Wong, L. S., Hashim, R., & Ali, F. H. (2009). A Review on Hydraulic Conductivity and Compressibility of Peat. *Journal of Applied Sciences*, 3207-3218.

Appendix A: Well Data

Well locations and specifications

Table 5: Well Construction Information

Well Name	Date Drilled	Latitude*	Longitude*	Surf. Elev. (ft AMSL)*	Stick-up (ft)	Screen (ft)	Total Depth (ft TOC)
Gart 1	4/29/2011	47.585779°	-104.281738°	2016	1.00	1.00	4.00
Gart 2	5/31/2011	47.586078°	-104.281987°	2022	1.35	3.00	16.33
Gart 3	5/31/2011	47.586047°	-104.282098°	2022	1.65	4.40	11.65
Gart 4	6/1/2011	47.585809°	-104.281528°	2016	2.25	5.00	21.00
Gart 5	6/1/2011	47.585259°	-104.280786°	2012	4.40	2.60	13.00
Gart 6	6/1/2011	47.585211°	-104.280054°	2012	2.70	2.00	10.30
Gart 7	6/1/2011	47.585827°	-104.281561°	2016	1.67	2.00	7.25
Gart 8	6/2/2011	47.584978°	-104.281748°	2013	2.50	3.00	6.86
Gart 9	6/2/2011	47.584802°	-104.281156°	2011	3.82	3.00	13.00
Gart 10	7/5/2011	47.585403°	-104.280529°	2012	2.62	3.00	10.75
Gart 11	7/5/2011	47.585156°	-104.279960°	2012	3.15	2.00	8.00
Gart 12	7/6/2011	47.584514°	-104.280336°	2010	3.90	2.00	12.00
Gart 13	7/6/2011	47.584538°	-104.280408°	2010	2.54	2.00	7.00
Gart 14	7/6/2011	47.584821°	-104.281249°	2011	3.52	2.90	8.00
Gart 15	7/7/2011	47.585180°	-104.282099°	2013	3.08	8.00	18.00
Gart 16	7/7/2011	47.585202°	-104.282184°	2013	2.13	4.00	8.28
Gart 17	4/26/2012	47.585446°	-104.280974°	2013	2.25	4.00	8.48
Gart 18	4/26/2012	47.585585°	-104.280802°	2013	1.80	4.00	7.54

* Determined from the 2011 Google Earth® Image where well sites were visible.

Well Logs

Depth From Surface (ft)			
Well Name	From	To	Material Description
Gart 2	0	1.7	brown sand with some water
	1.7	2.6	brown sand with some water but more clay
	2.6	3.6	light brownish gray clay with some sand
	3.6	5.3	same (60% clay)
	5.3	6.4	same but more sand
	6.4	7.3	silty sand less clay
	7.3	8.7	silty sand with few gravel pebbles of quartzite and larger sand grain
	8.7	9.2	more gravel (orange quartzite) large grained sand with more clay
	9.2	10	70% clay with gravel
	10	10.5	95% clay, gray with red streaks and some gravel
	10.5	11.3	sandier with more gravel
	11.3	11.7	silty gravel and sand
	11.7	12.3	silty gravel and sand
	12.3	13.1	bentonite with some clinker
	13.1	13.7	red and gray bentonite
13.7	14.3	silty bentonite	
14.3	14.7	clay with rusty red streaks	
Gart 3	0	2	brown silty sand
	2	3.4	silty sand, more silt
	3.4	9	silty sand coarsening downwards
	9	9.8	clay and gravel

Depth From Surface (ft)			
Well Name	From	To	Material Description
Gart 4	0	0.5	silty clay
	0.50	4.00	brown with roots
	4.00	4.80	green, red, gray clay
	4.80	7.80	gray bentonitic clay
	7.80	8.40	same but with some sand
	8.40	9.70	gray/green clay
	9.70	10.50	gray clay with rust color streaks, some snail shells
	10.50	11.20	Red, green and gray clay, more shells, bone fragments, roots and wood.
	11.20	12.40	Red and gray clay with bivalve shells, tubular plant fragments.
	12.40	12.70	dark gray clay with more plant material
	12.70	13.60	really dark gray and fine clay
	13.60	14.70	Light colored loose clay with 5-6 inches of peat and many small shells
	14.70	14.90	light gray dense clay with peat stringers
	14.90	15.80	dark gray clay, very dense with a little water
	15.80	16.30	same with shells
	16.30	17.10	same clay with some sand and some gravel
	17.10	18.50	little lighter gray clay
	18.50	18.80	light gray, looser with more water
18.80	19.10	light gray dense clay	
19.10	19.50	gravel and sand with gray clay	
Gart 5	0	1	loose clay and roots
	1.00	2.40	dark gray clay with some silt
	2.40	2.80	orange brown streaked gray clay with some shells
	2.80	3.70	dark gray silty clay
	3.70	4.30	silty clay with peat stringers(6-7 inches) at bottom back to tight clay with shells
	4.30	5.00	peat really loose
	5.00	5.60	peat loose
	5.60	5.90	fine grained sand but real tight
	5.90	6.20	dark grey silty clay
	6.20	6.60	1-2 inches of peat then really loose greyish sand
	6.60	7.50	dark sand, really loose with water coming up
	7.50	7.70	same sand with some caving
	7.70	8.60	1st half sand then silty clay and 1 inch at bottom of clay

Depth From Surface (ft)			
Well Name	From	To	Material Description
Gart 6	0	1	roots and top soil
	1.00	1.90	light brown to gray clay, lots of tiny shells no grit
	1.90	3.70	peat, some till last couple inches
	3.70	5.60	organic rich clay, half foot of silty/sandy clay
	5.60	7.60	silt/sandy clay, 4-5 inches of peat
Gart 7	0	1	silty clay
	1.00	4.00	brown, green, and red clay
	4.00	4.30	green and brown clay, silty
	4.30	5.20	silty sand (water flowing in borehole about 2.5 ft. down when pumped)
Gart 8	0	0.3	top soil
	0.30	0.80	grey and black fine clay
	0.80	1.90	light brown sand
	1.90	2.60	fine clay with white hard chunks
	2.60	3.50	really fine light grey clay
	3.50	3.90	light grey clay with white hard chunks
	3.90	4.30	same
Gart 9	0	0.3	top soil
	0.30	0.90	brown clay
	0.90	1.90	light greyish brown clay with shells
	1.90	2.40	dark grey lots of shells with reddish brown streaks
	2.40	3.10	6-8 inches of same, rest is green clay
	3.10	3.70	1 inch of coarse sand ,grey fine silty sand
	3.70	4.10	grey clay with peat stringers
	4.10	5.30	silty sand, grey
	5.30	5.80	grey silty sand, looser (water coming up really fast)
	5.80	8.20	grey coarse sand
8.20	9.40	loose sand and gravel some caving (water up to ground level)	

Depth From Surface (ft)			
Well Name	From	To	Material Description
Gart 10	0	0.09	Roots and Brown soil
	0.09	1.50	same
	1.50	2.26	Loose grey silty clay with shells and few red streaks and some water
	2.26	3.45	Real fine grained clay with shells
	3.45	4.12	same but with roots
	4.12	4.36	clay, peat last 4 inches
	4.36	4.85	Peat with clay stringers
	4.85	5.36	Darker Peat
	5.36	5.65	Tight black dark grey clay
	5.65	6.57	fine silty sand with water rising
	6.57	6.99	Loose dark sand in the aquifer, some caving
	6.99	7.67	dark and loose sand
Gart 11	0	2.08	Roots and tight clay
	2.08	3.25	same with 1 inch of peat at end
	3.25	4.65	Peat
Gart12	0	2.2	Tight peat, water at surface (Caving)
	2.20	3.35	Sand
	3.35	3.87	fine silty sand
	3.87	3.92	same, caving
	3.92	5.20	sand
	5.20	5.60	coarse sand; caving sand, silty fine sand clay
	5.60	5.80	silty fine sand
	5.80	6.40	peat with shells
	6.40	7.91	peat, grey silty clay
	7.91	7.49	CAVING , silty sand fine grained, caving sands and gravel
	7.49	8.37	coarse sand, mostly quartz, gravel
Gart 13	0	2	Brown peat into loose grey peat
	2.00	3.55	silty clay
	3.55	3.62	sand
	3.62	4.42	Clay like with little bit of grit

Depth From Surface (ft)			
Well Name	From	To	Material Description
Gart 14	0	2.2	Clay with shells
	2.20	2.90	clay
	2.90	3.00	grittier clay
	3.00	3.65	peat
	3.65	4.20	Brown peat
	4.20	4.70	fine silty sand
Gart 15	0	0.4	Brown silty sand
	0.40	1.40	light gray clay
	1.40	2.00	silty sand with some water
	2.00	2.24	brown medium grained sand
	2.24	3.25	2 inches of sand then silty clay
	3.25	3.60	some clay then silty sand
	3.60	4.00	coarser brown sand with some caving
	4.00	4.50	same brown sand
	4.50	4.80	same brown sand
	4.80	5.20	same brown sand
	5.20	7.20	fine dark gray clay, really tight
	7.20	7.70	dark gray tight clay really fine grained
	7.70	8.20	gray clay with rusty streaks and little shells
	8.20	8.50	same
	8.50	8.90	Water, same goo stick type
	8.90	9.60	Decomposed peat
	9.60	9.40	Caving sands and gravel
	9.40	10.30	2 inches of gravel in silty sand matrix
	10.30	10.80	silty sand with some of gravel, caving
	10.80	11.20	clay with shells
	11.20	11.11	Caving conditions with water
	11.11	12.00	Gray clay with red streaks and shells
12.00	12.40	clay	
12.40	12.06	Caving, some silty clay	
12.06	11.95	Same	
11.95	13.40	sandier looser clay	
13.40	12.70	Caving conditions	
12.70	13.75	Silty clay and peat with shells	
13.75	13.90	Same	

Depth From Surface (ft)			
Well Name	From	To	Material Description
Gart 16	0	2	Soil
	2.00	3.00	Fine silty sand with little bit of water
	3.00	3.60	grey silty clay with reddish streaks
	3.60	3.90	fine silty sand
	3.90	4.10	fine silty sand greenish grey
	4.10	4.45	same
	4.45	4.65	same but coarser
	4.65	4.95	same
	4.95	5.15	same but coarser silty sand
	5.15	5.65	clay
Gart 17	0	1.5	Silty Sand Light gray
	1.50	2.50	green clay with red streaks
	2.50	4.00	green-gray clay with white deposits
	4.00	4.50	Tight gray clay
	4.50	5.50	Loose sandy clay
	5.50	6.30	tight clay
	6.30	8.48	
Gart 18	0	1.5	Silty sand and brown clay
	1.50	3.00	dark gray clay with red flecks and some sand
	3.00	4.20	tight gray clay organic reeds white deposits
	4.20	6.30	very light clay at bottom

Appendix B: Sieve Analyses

Sieve Analyses Data Tables

GART 9, 8.2-9.4 ft	
TIME:	14 minutes
START WEIGHT	822.74
END WEIGHT	818.33
PERCENT RECOVERED	99.46
SIEVE#	WEIGHT IN GRAMS
25	317.44
35	76.12
45	51.60
60	153.91
120	142.17
170	25.18
230	16.04
PAN	35.87

GART 9, 5.8-8.2 ft	
TIME:	17 minutes
START WEIGHT	481.25
END WEIGHT	478.76
PERCENT RECOVERED	99.48
SIEVE#	WEIGHT IN GRAMS
25	5.72
35	40.77
45	32.28
60	133.00
120	205.77
170	10.59
230	25.10
PAN	25.53

GART 10, 7.0-7.67 ft	
TIME:	11 minutes
START WEIGHT	457.33
END WEIGHT	456.23
PERCENT RECOVERED	99.76
SIEVE#	WEIGHT IN GRAMS
25	2.93
35	16.66
45	13.93
60	84.18
120	283.42
170	38.35
230	9.22
PAN	7.54

GART 10, 5.65-6.57	
TIME:	14 minutes
START WEIGHT	505.03
END WEIGHT	501.72
PERCENT RECOVERED	99.34
SIEVE#	WEIGHT IN GRAMS
25	5.41
35	17.07
45	18.79
60	119.37
120	229.65
170	41.34
230	20.72
PAN	49.37

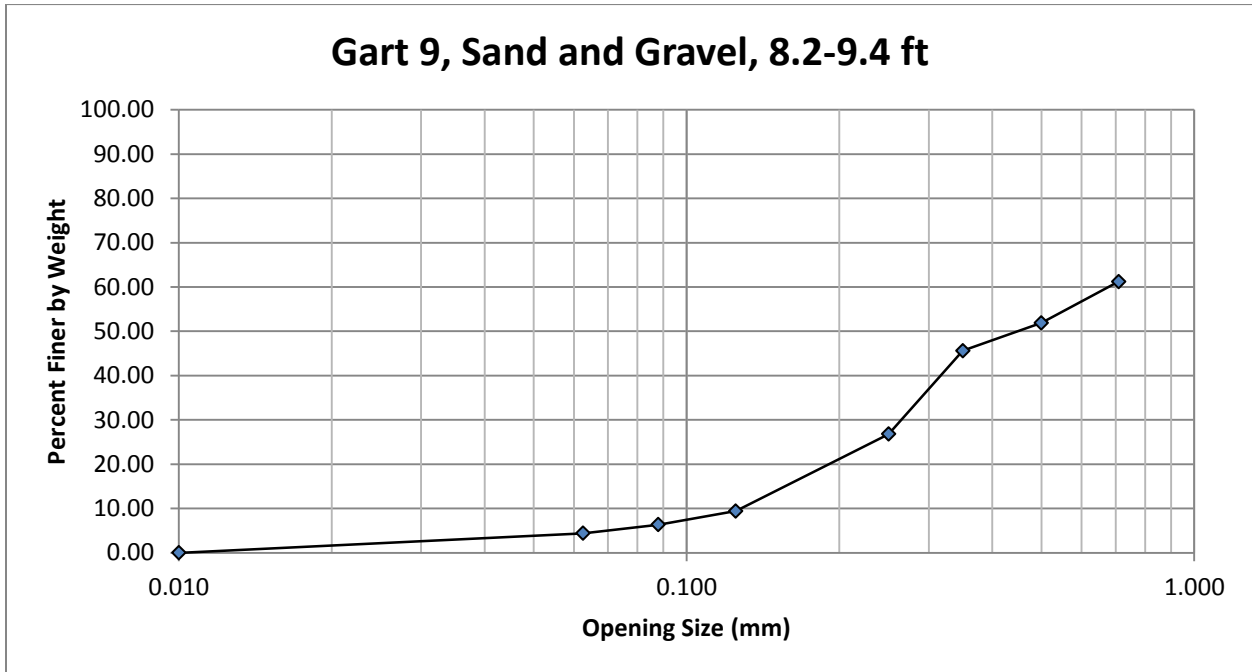
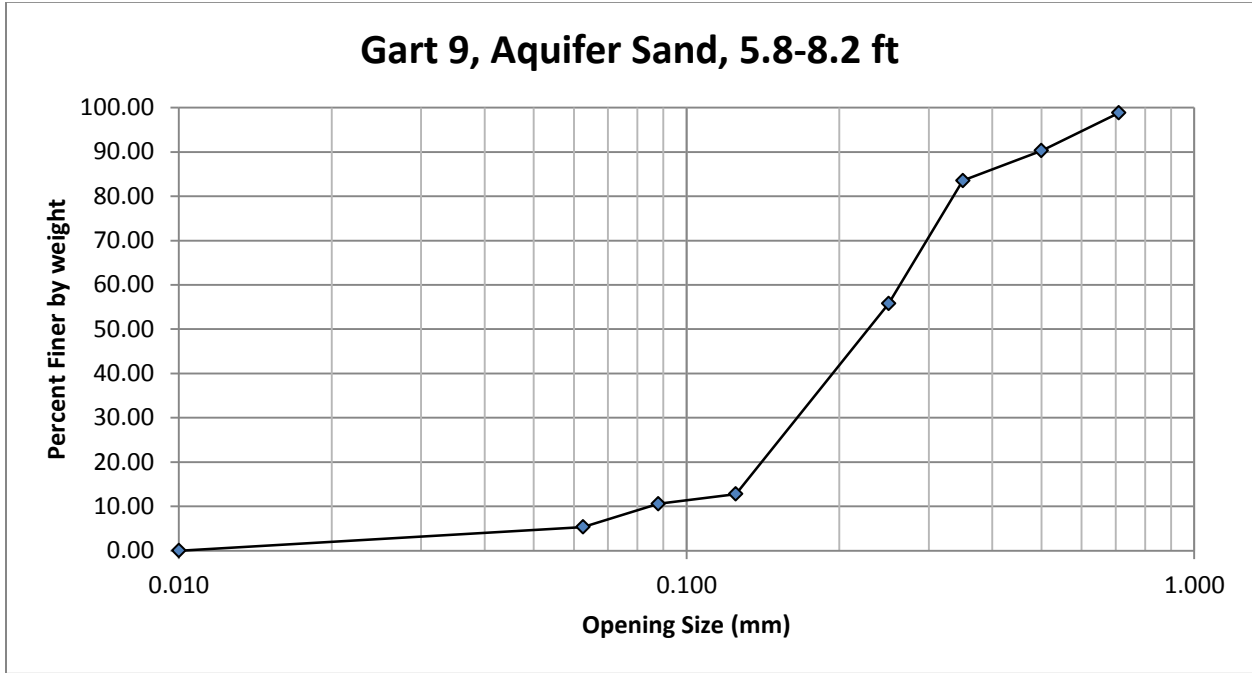
GART 4 18.5-18.8	
TIME:	13 minutes
START WEIGHT	625.71
END WEIGHT	621.48
PERCENT RECOVERED	99.32
SIEVE#	WEIGHT IN GRAMS
25	7.54
35	47.57
45	23.36
60	83.74
120	282.42
170	55.26
230	45.35
PAN	76.24

GART 8 8-1	
TIME:	12 minutes
START WEIGHT	300.42
END WEIGHT	298.02
PERCENT RECOVERED	99.20
SIEVE#	WEIGHT IN GRAMS
25	1.83
35	21.04
45	16.57
60	64.58
120	122.41
170	23.57
230	15.82
PAN	32.20

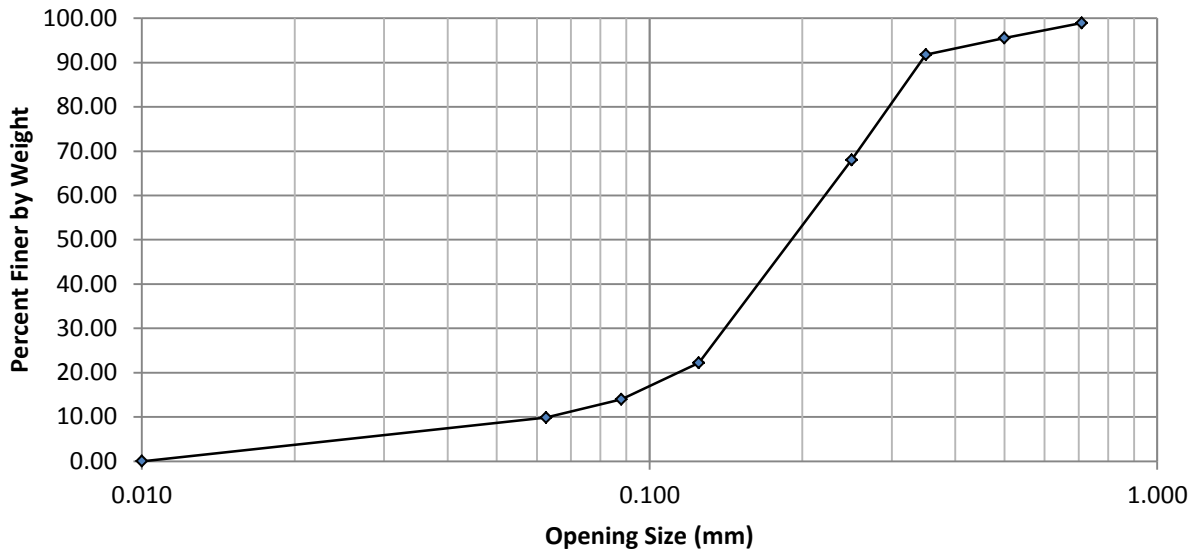
GART 11 3.87-3.92	
TIME:	10 minutes
START WEIGHT	388.96
END WEIGHT	386.31
PERCENT RECOVERED	99.32
SIEVE#	WEIGHT IN GRAMS
25	10.59
35	14.55
45	18.27
60	85.04
120	153.87
170	33.81
230	22.70
PAN	47.48

GART 15 3.60-4.0	
TIME:	15 minutes
START WEIGHT	590.24
END WEIGHT	587.72
PERCENT RECOVERED	99.57
SIEVE#	WEIGHT IN GRAMS
25	3.76
35	25.72
45	49.92
60	153.87
120	251.22
170	42.57
230	19.87
PAN	40.79

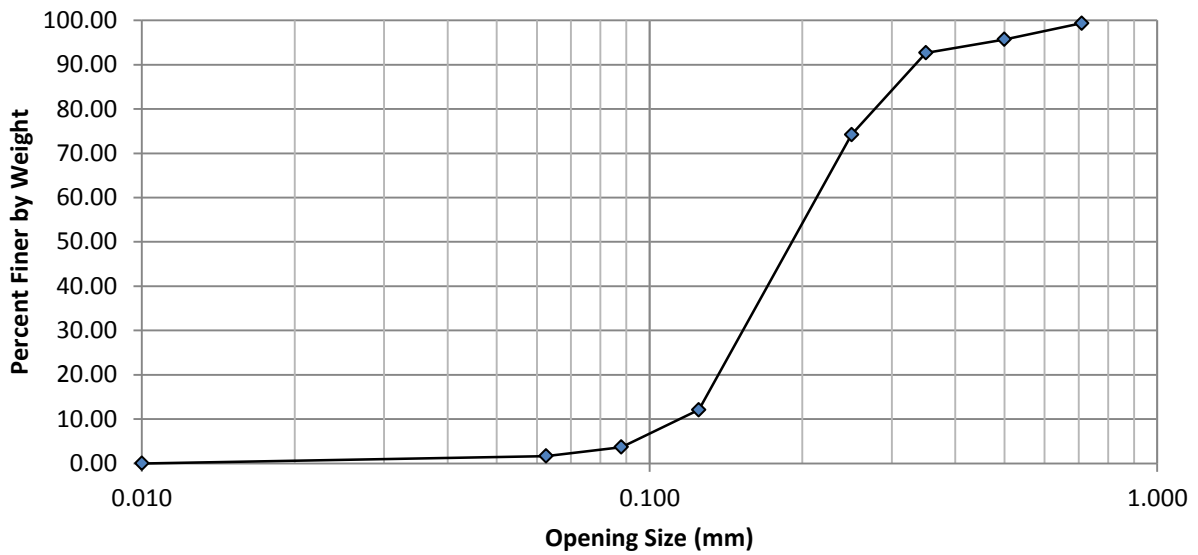
Sieve Analyses Charts



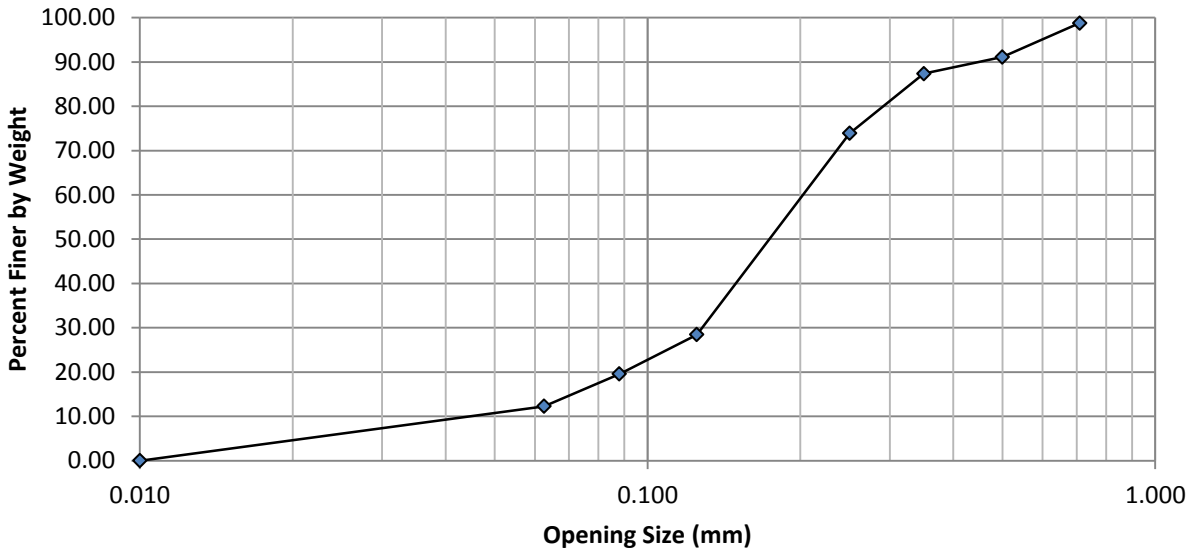
Gart 10, Silty Sand, 5.65 to 6.57 ft



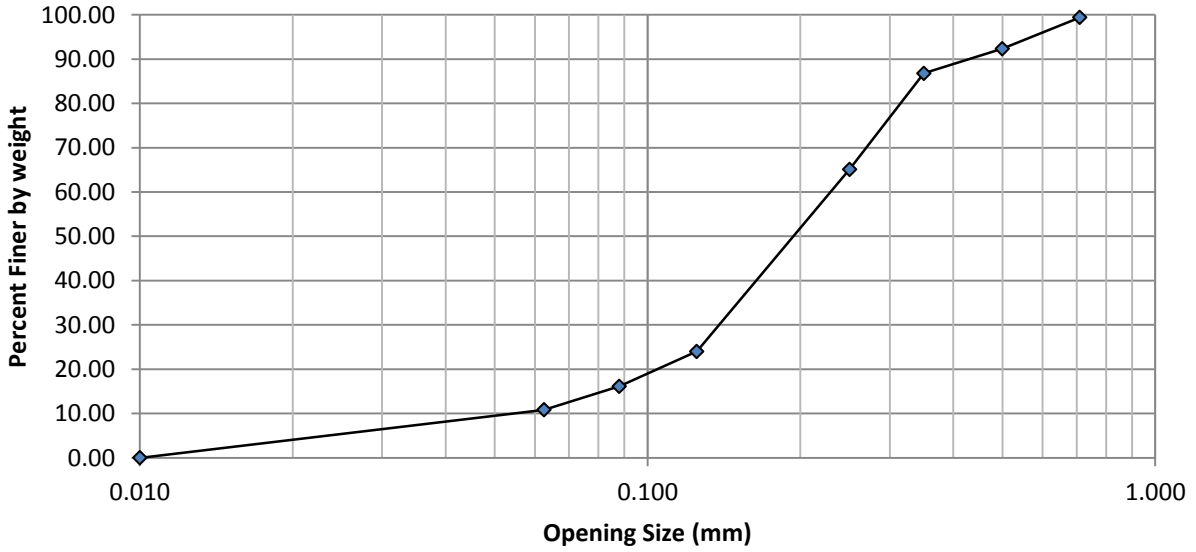
Gart 10, Dark Silty Sand, 7.0-7.67 ft



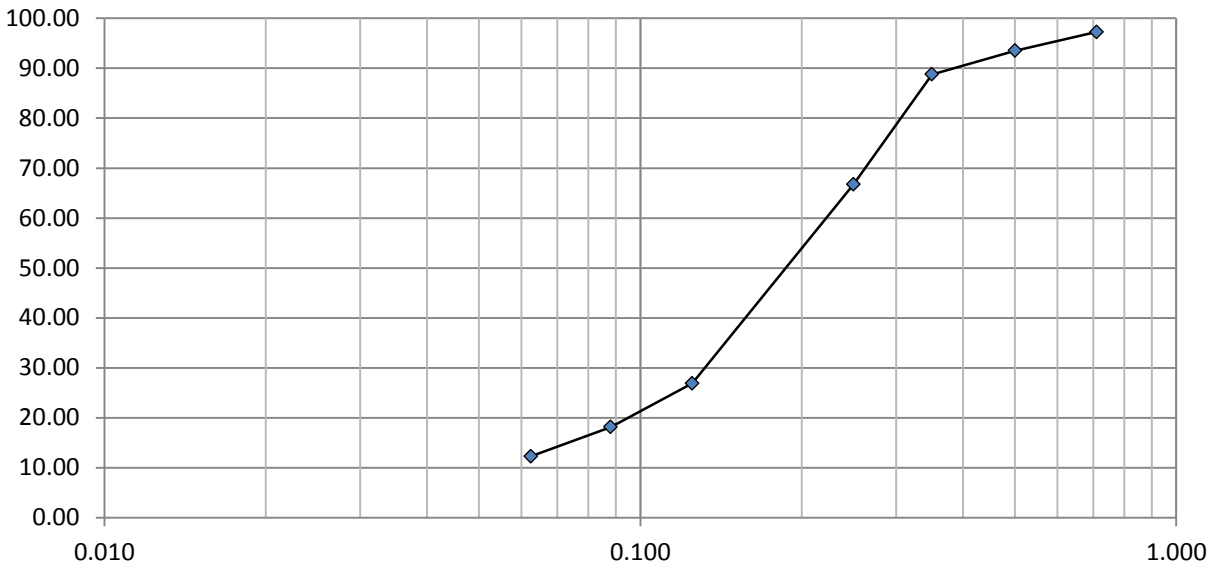
Gart 4, Silty Sand, 18.5-18.8 ft



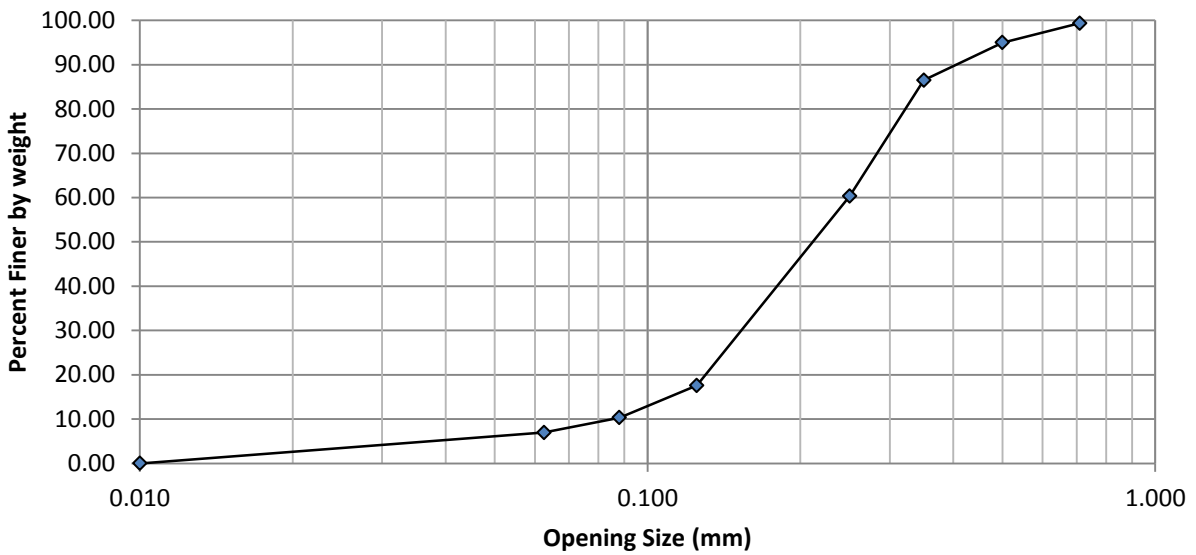
Gart 8, Light Brown Sand, 0.8-1.9 ft



Gart 11, Peat Layer 3.87 to 9.92 ft

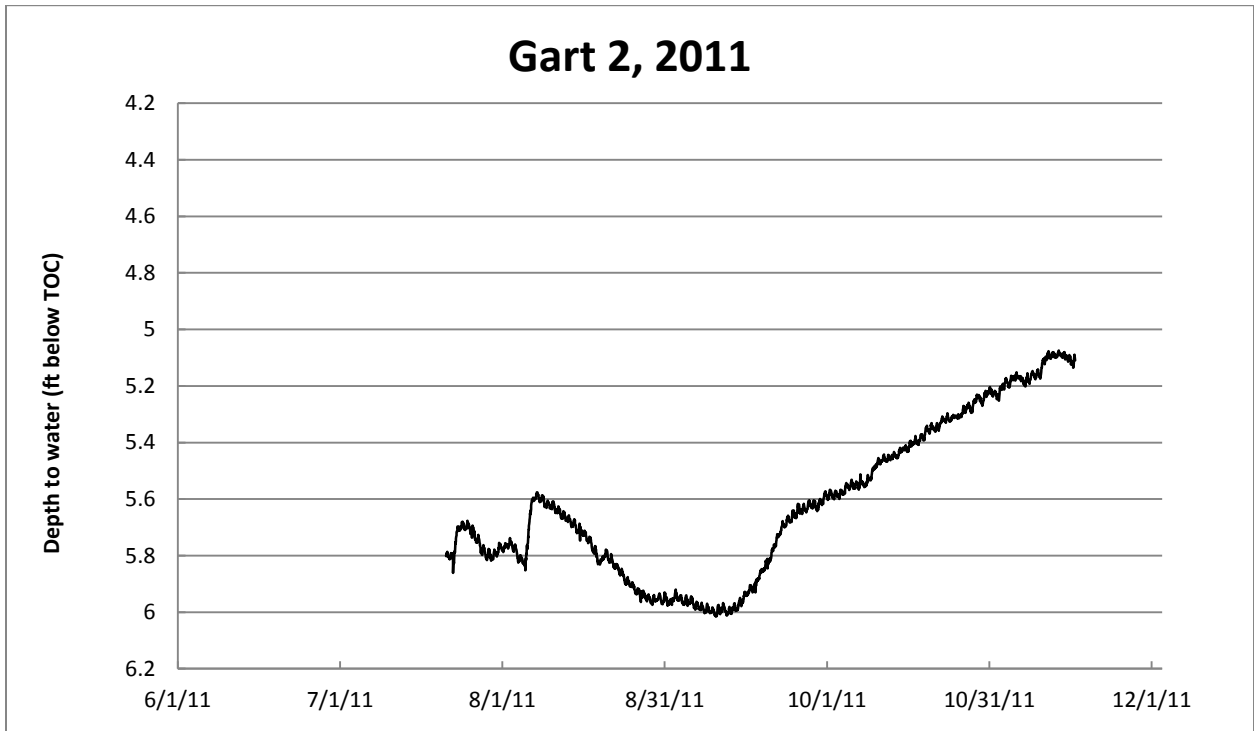
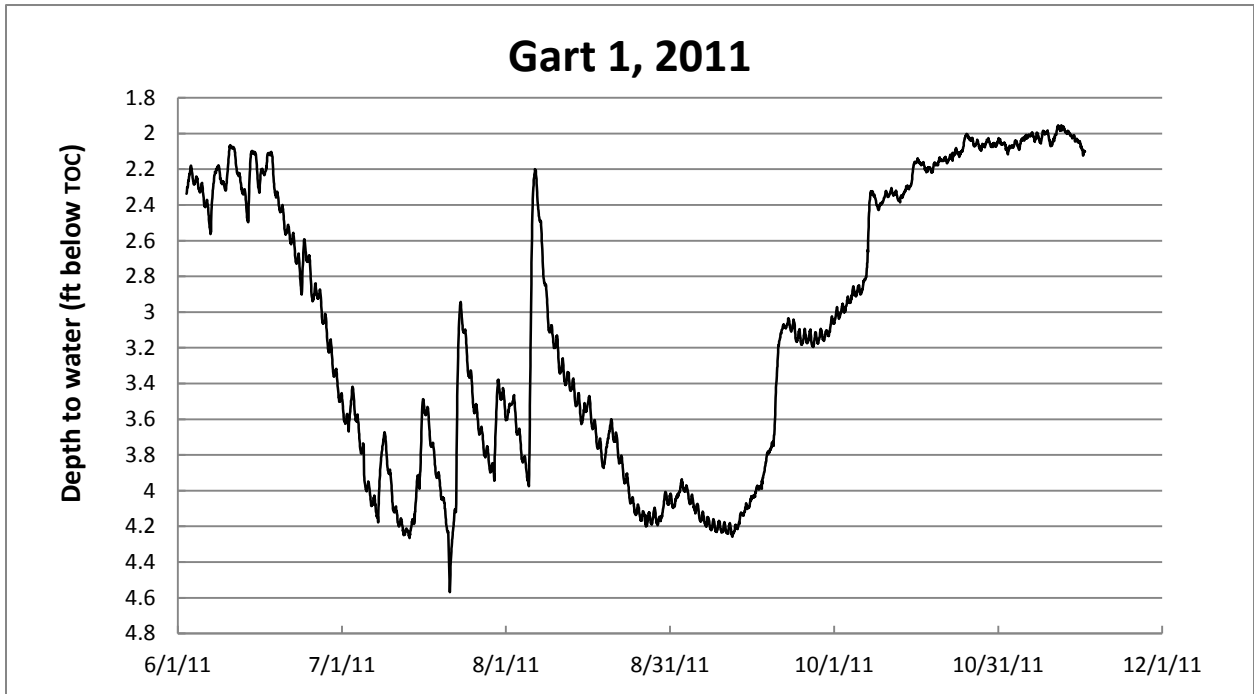


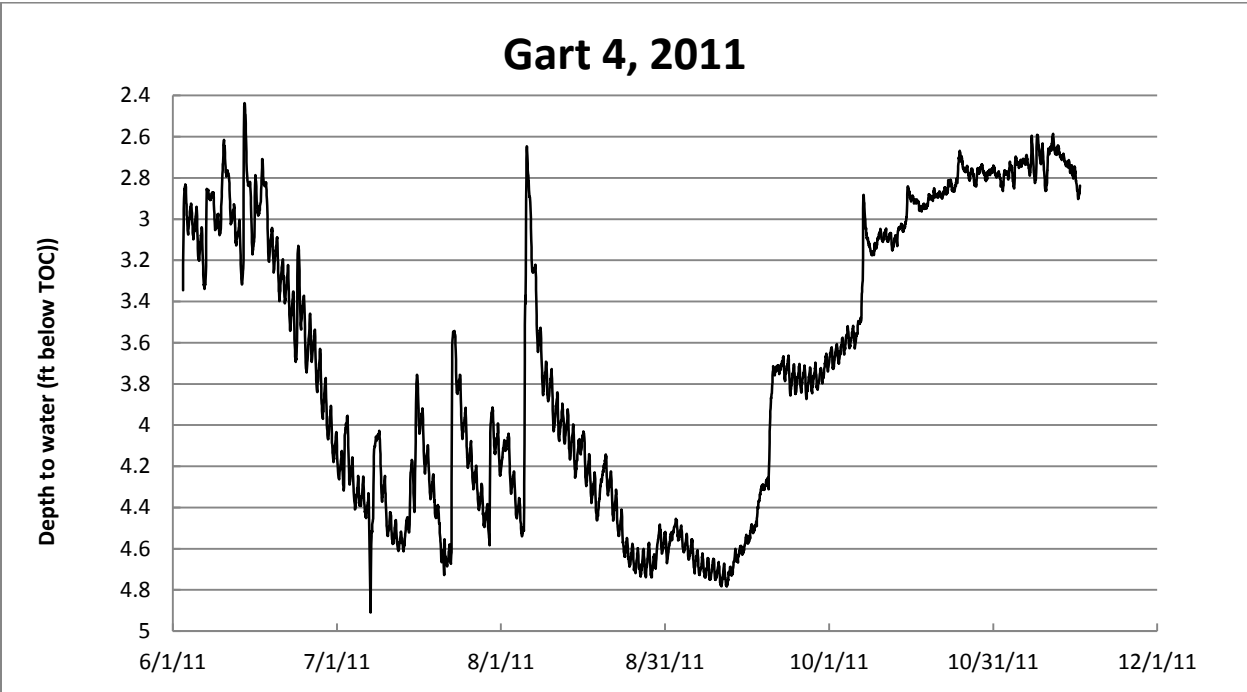
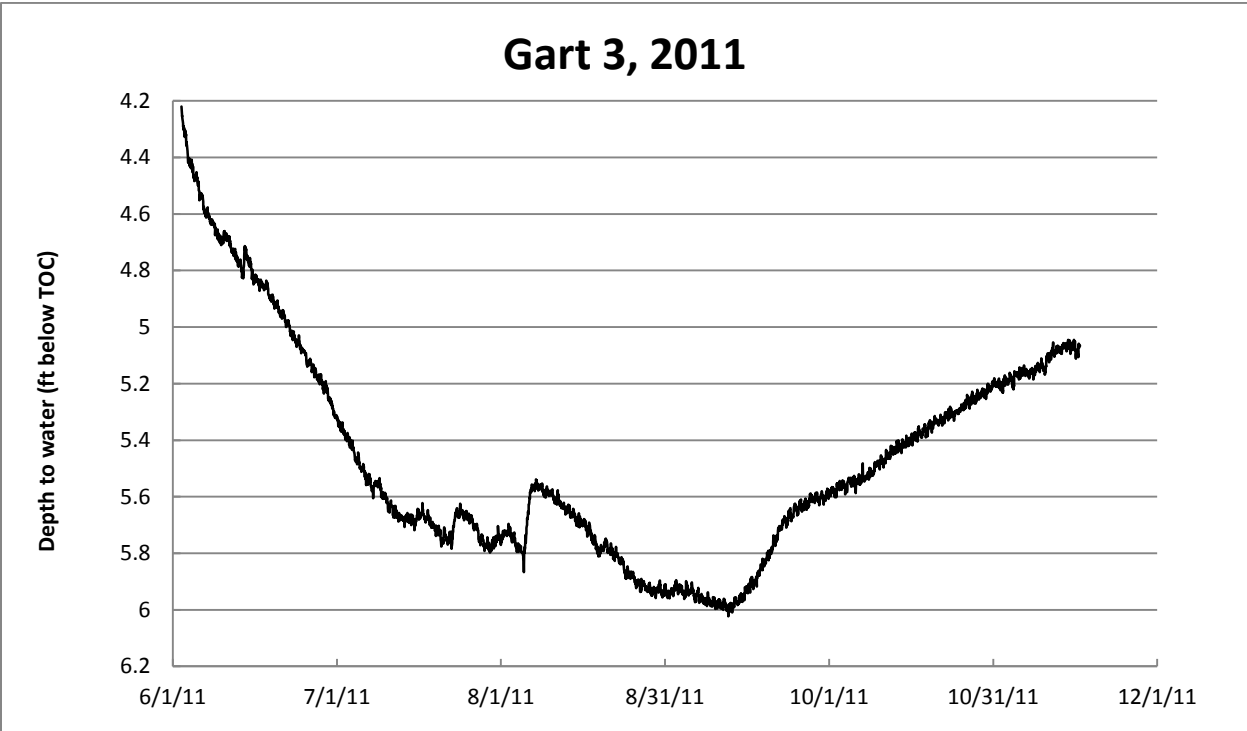
Gart 15, Coarse Brown Sand, 3.60-5.2 ft

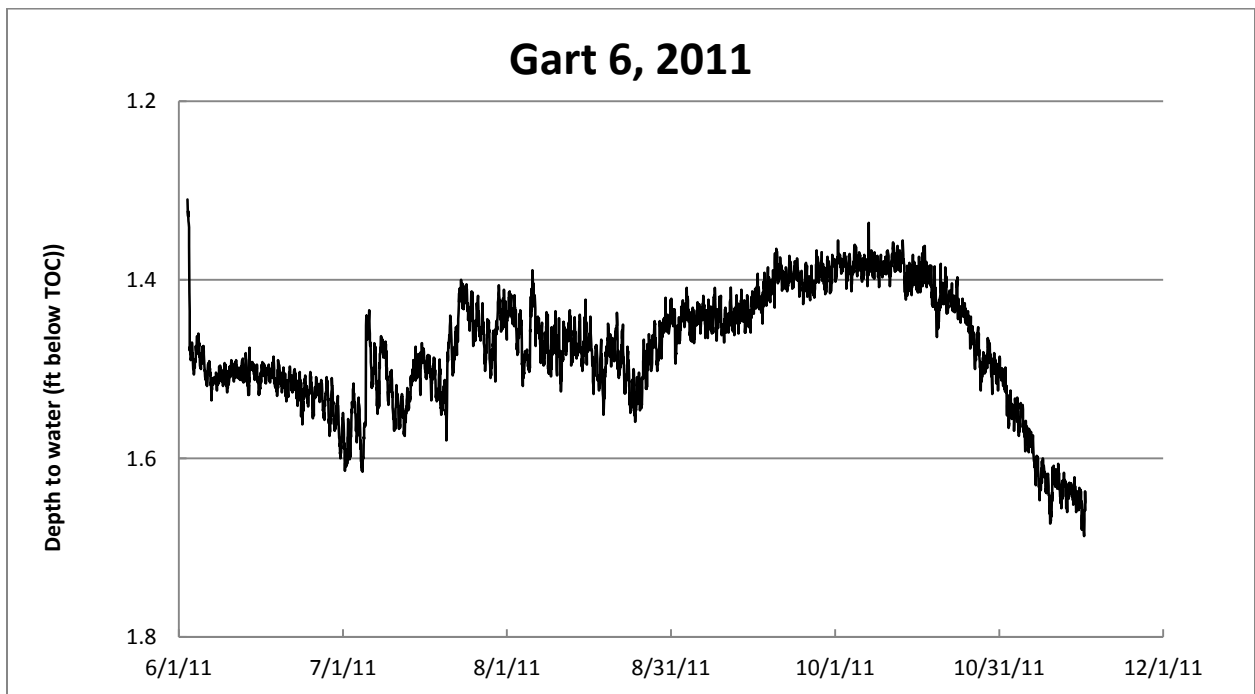
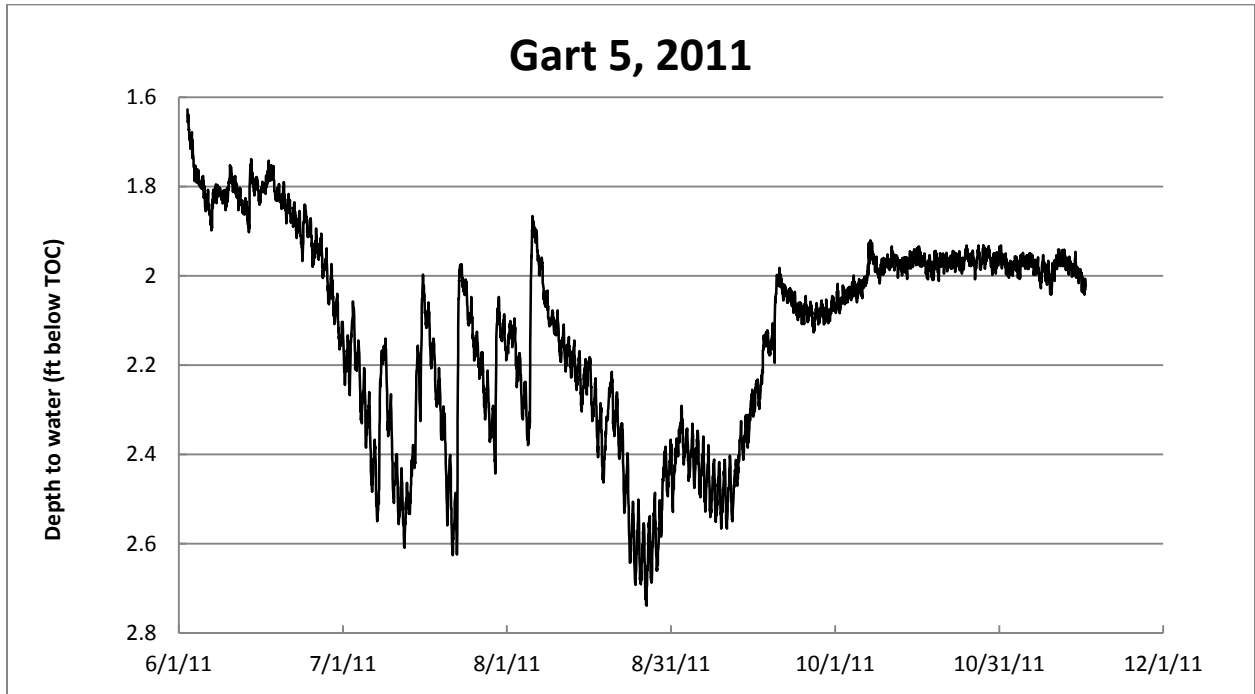


Appendix C: Water Level Charts

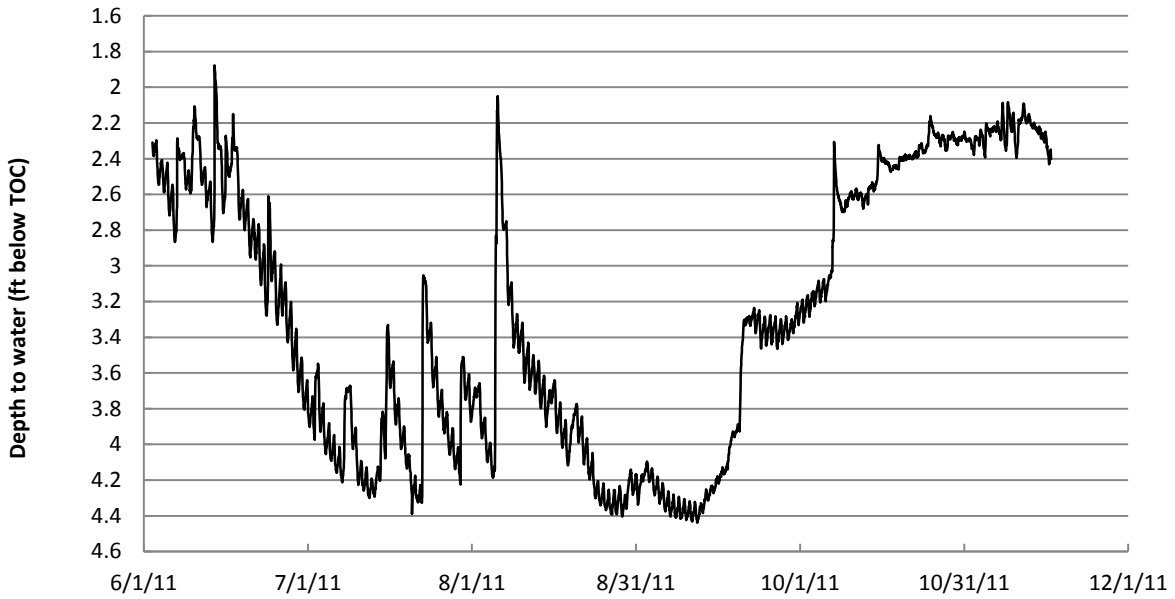
2011 Season



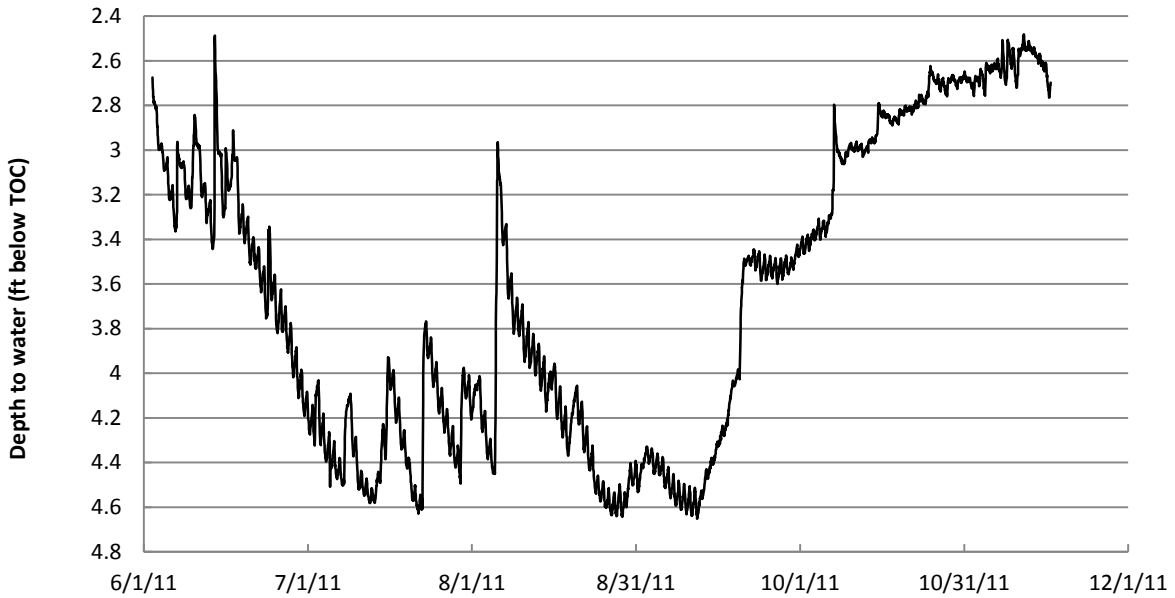


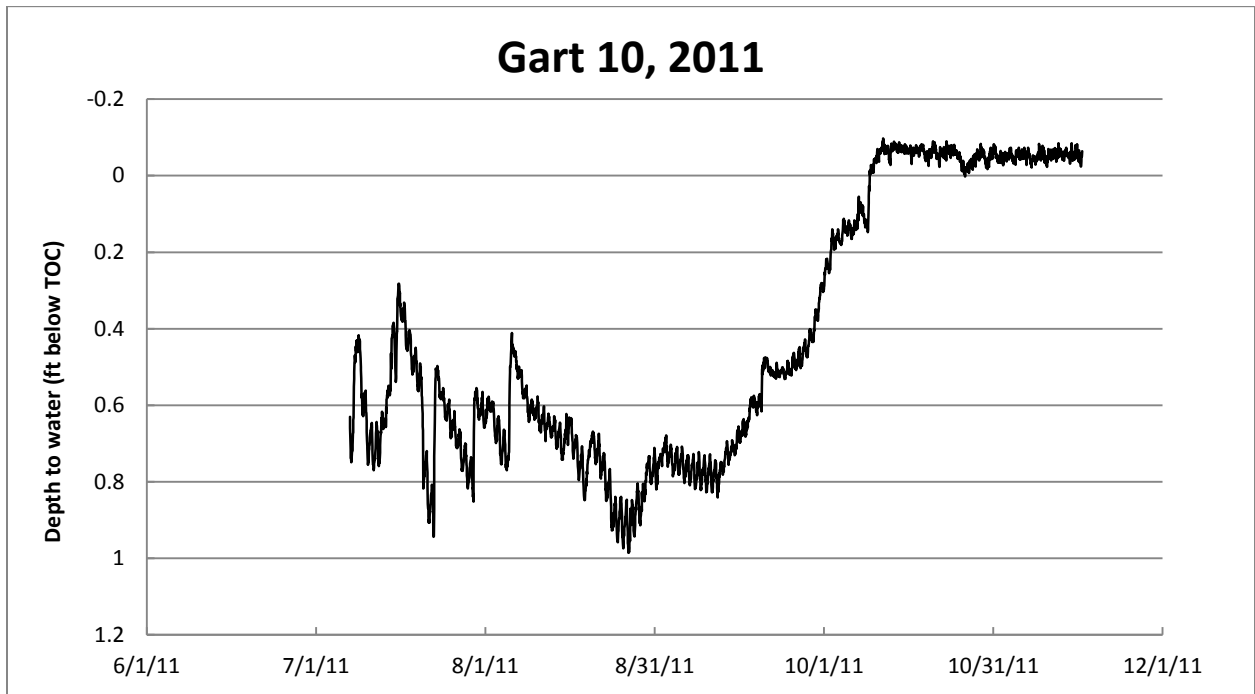
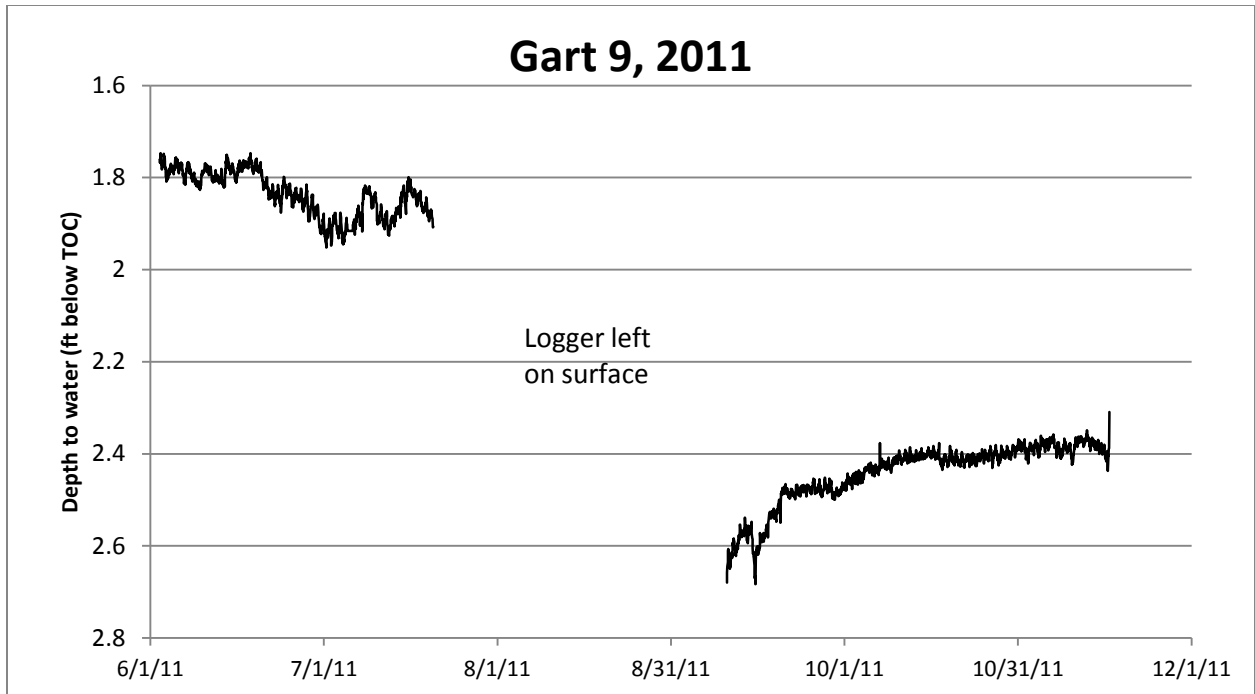


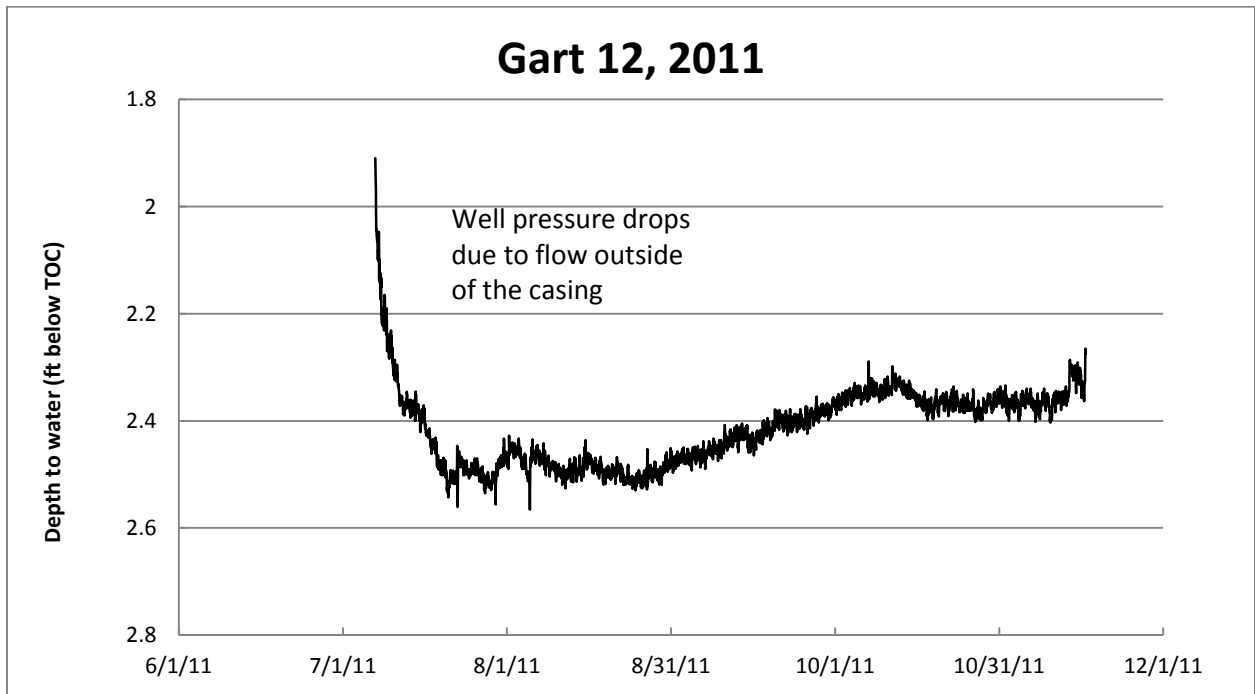
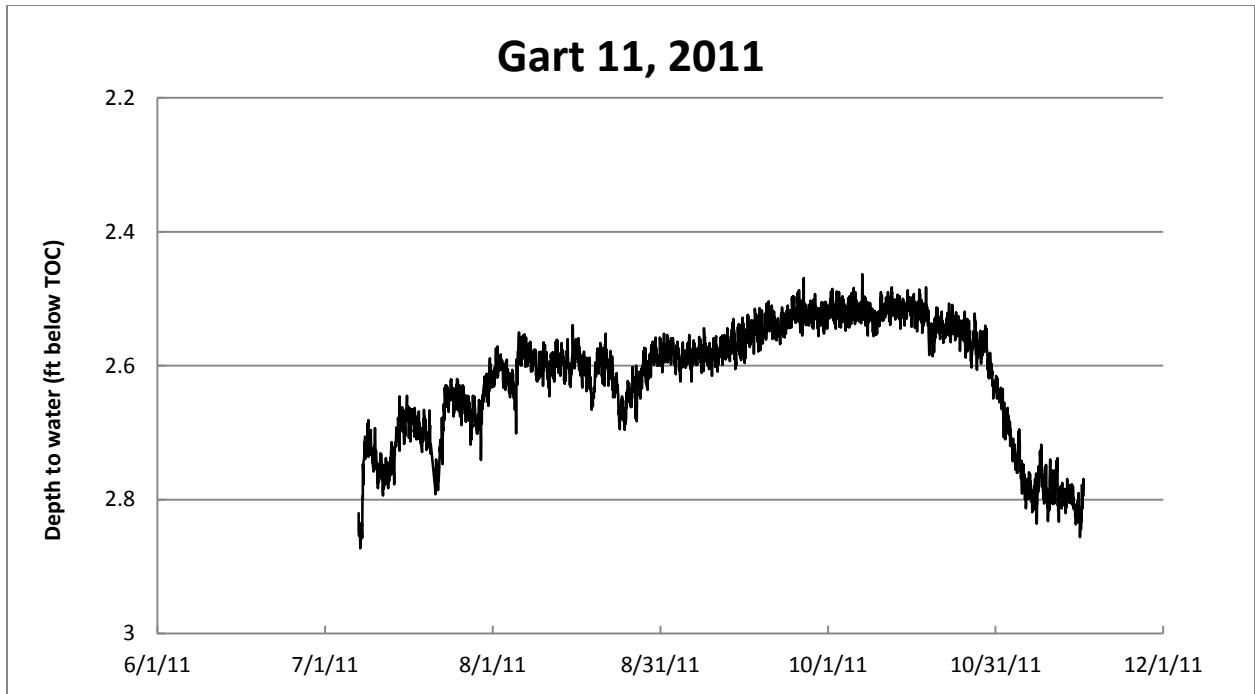
Gart 7, 2011

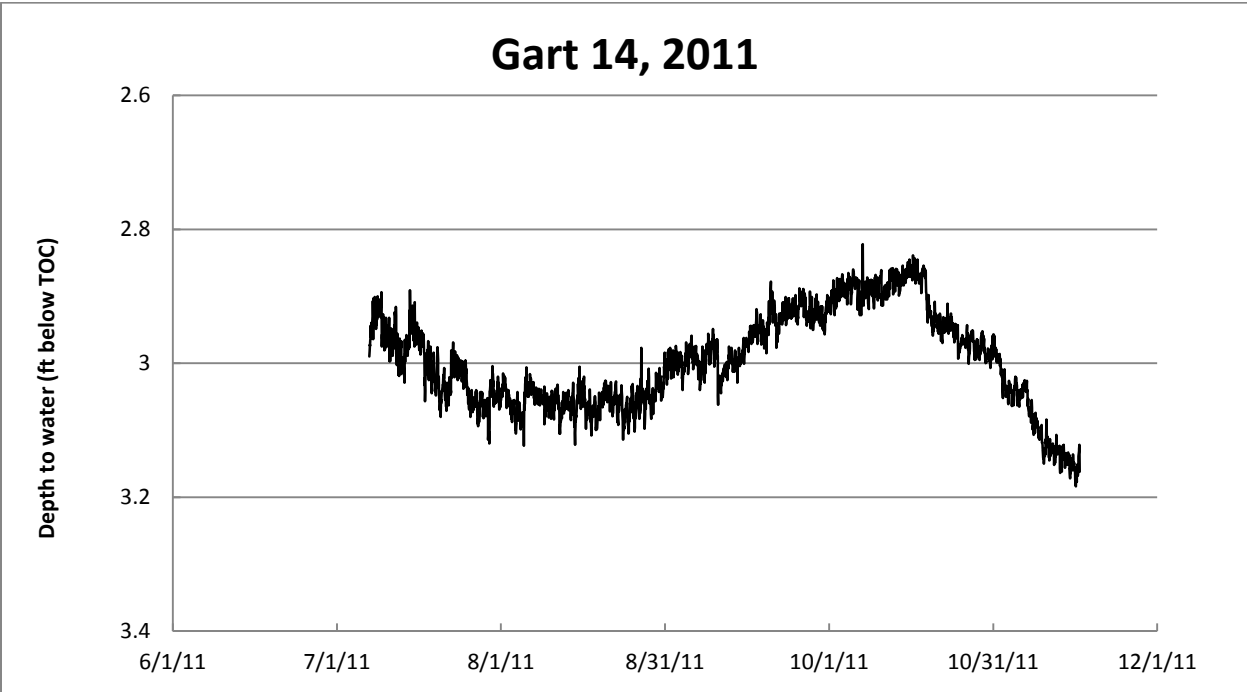
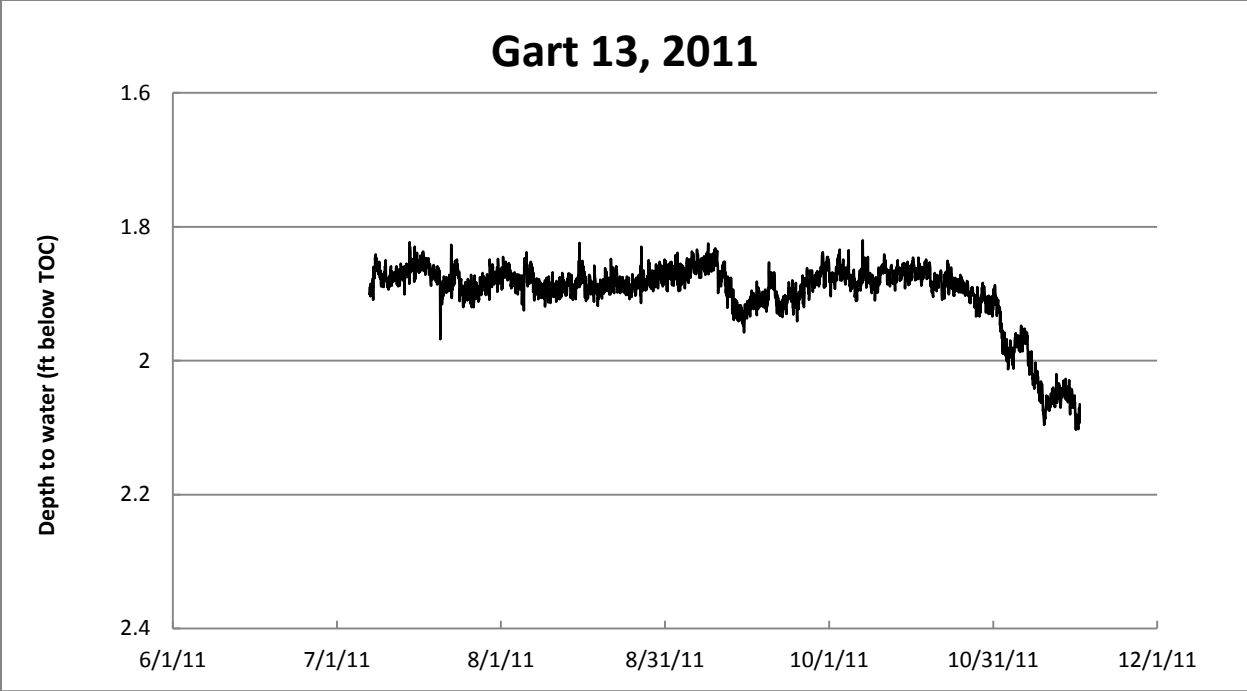


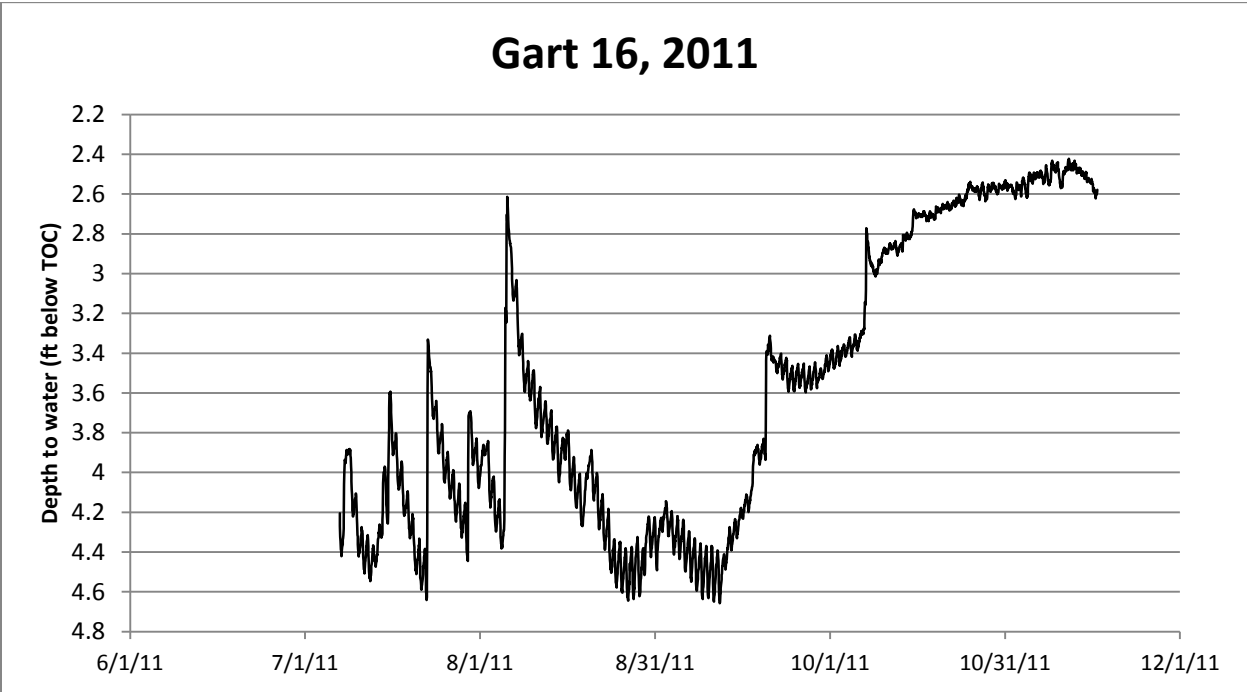
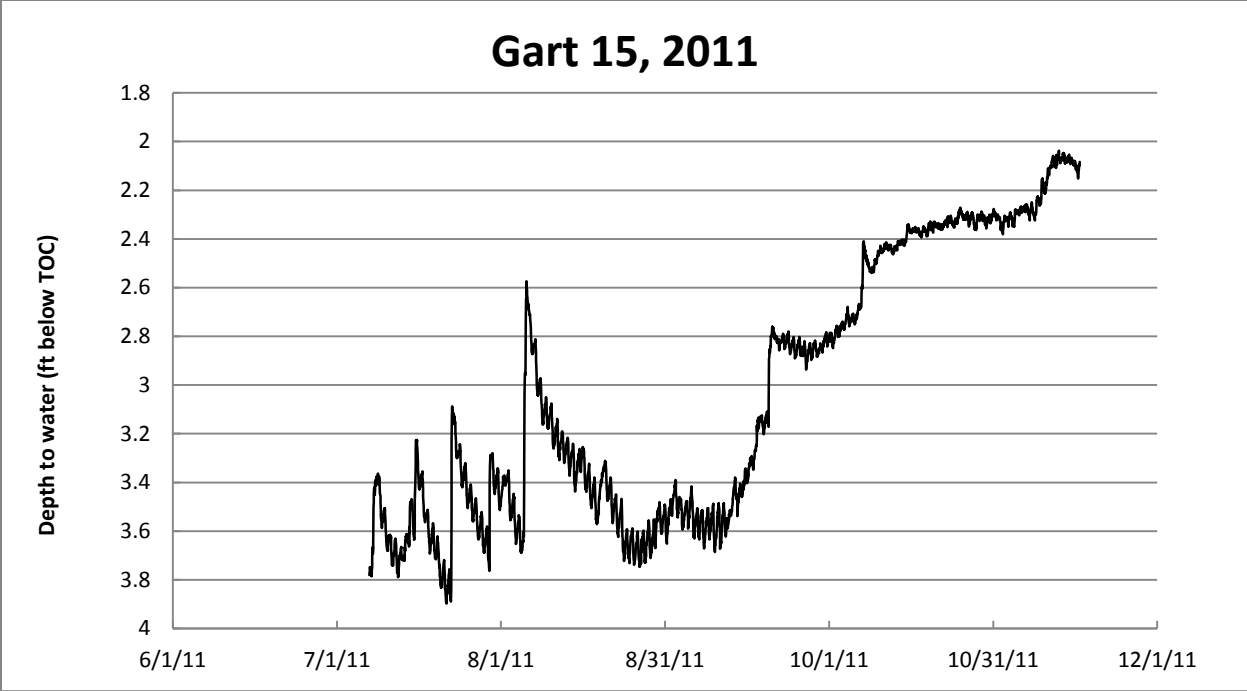
Gart 8, 2011



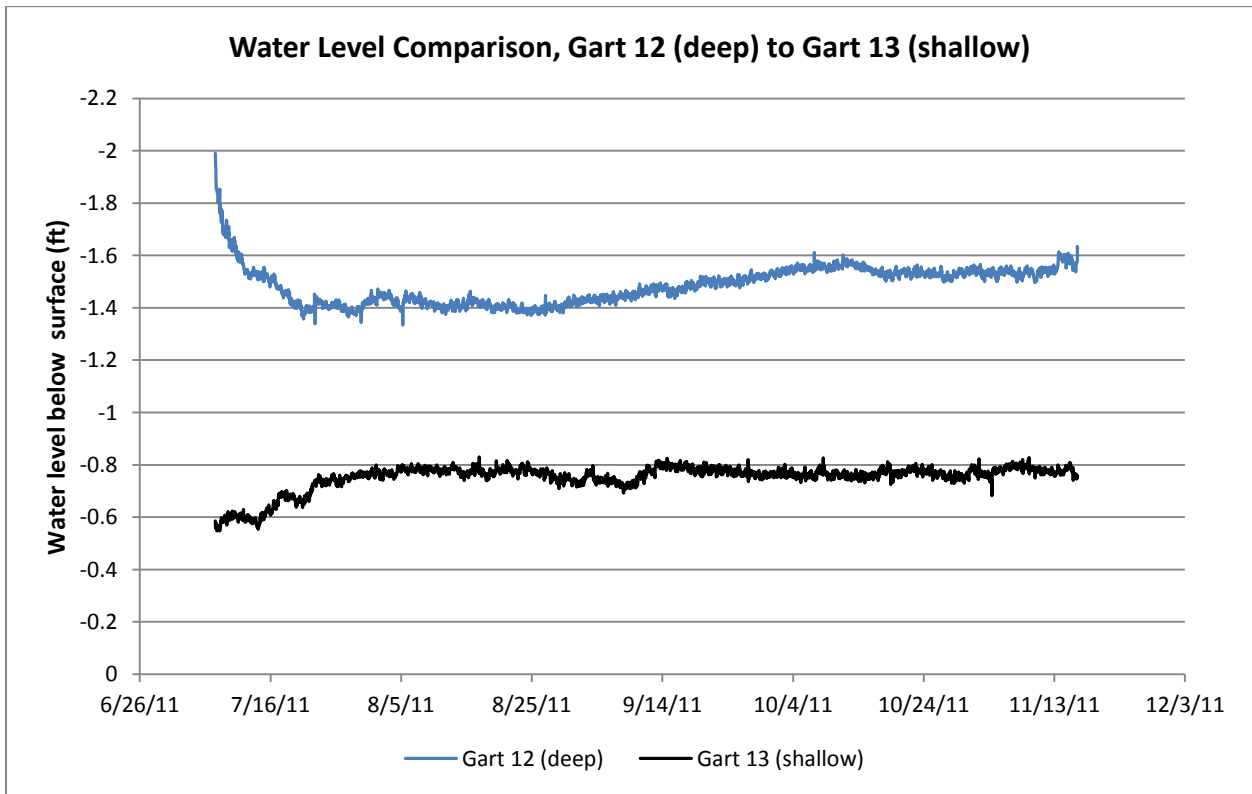
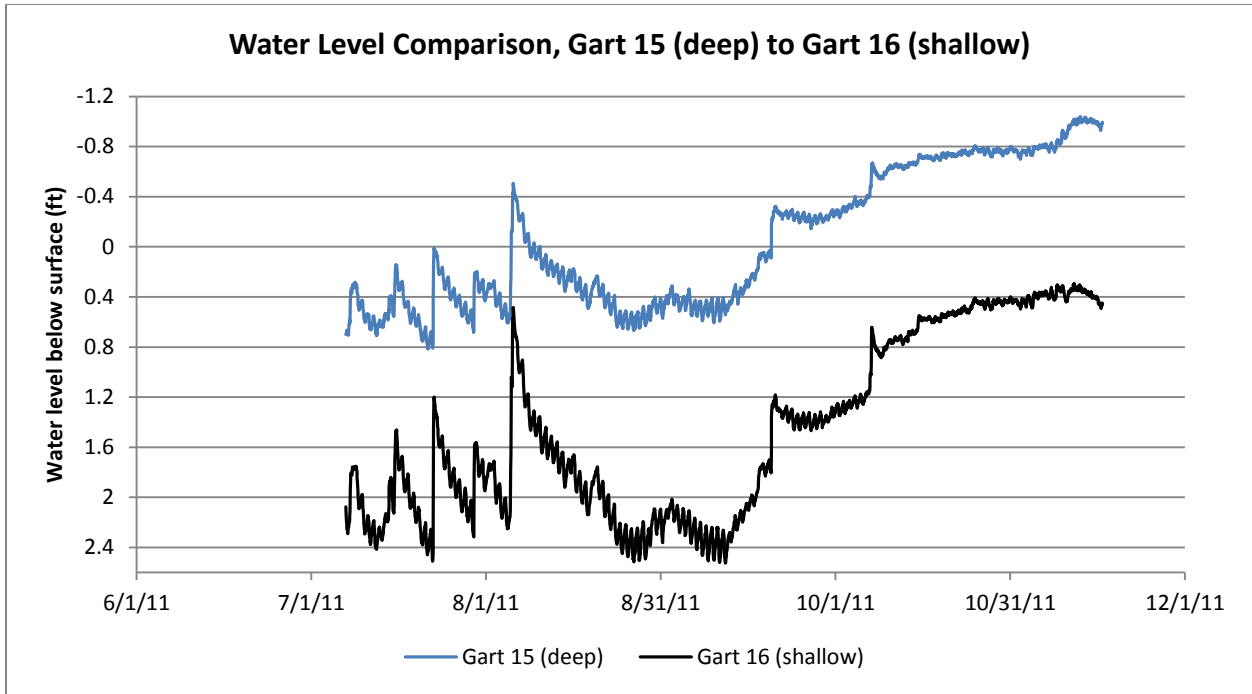




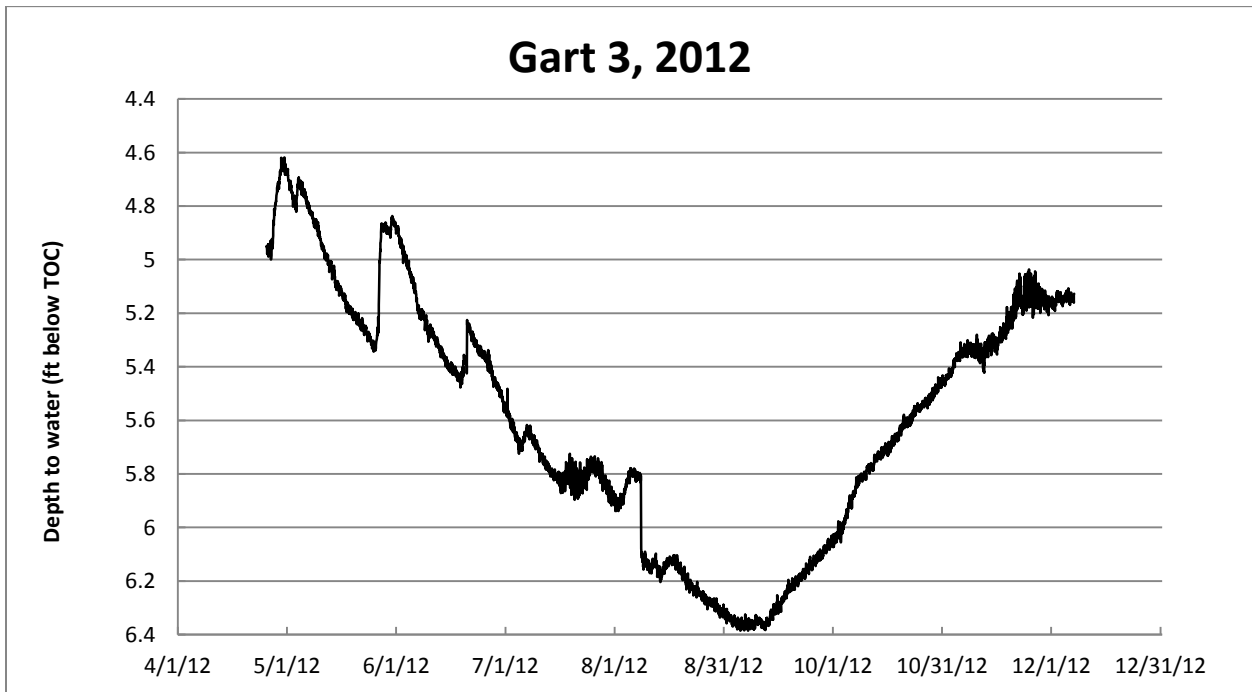
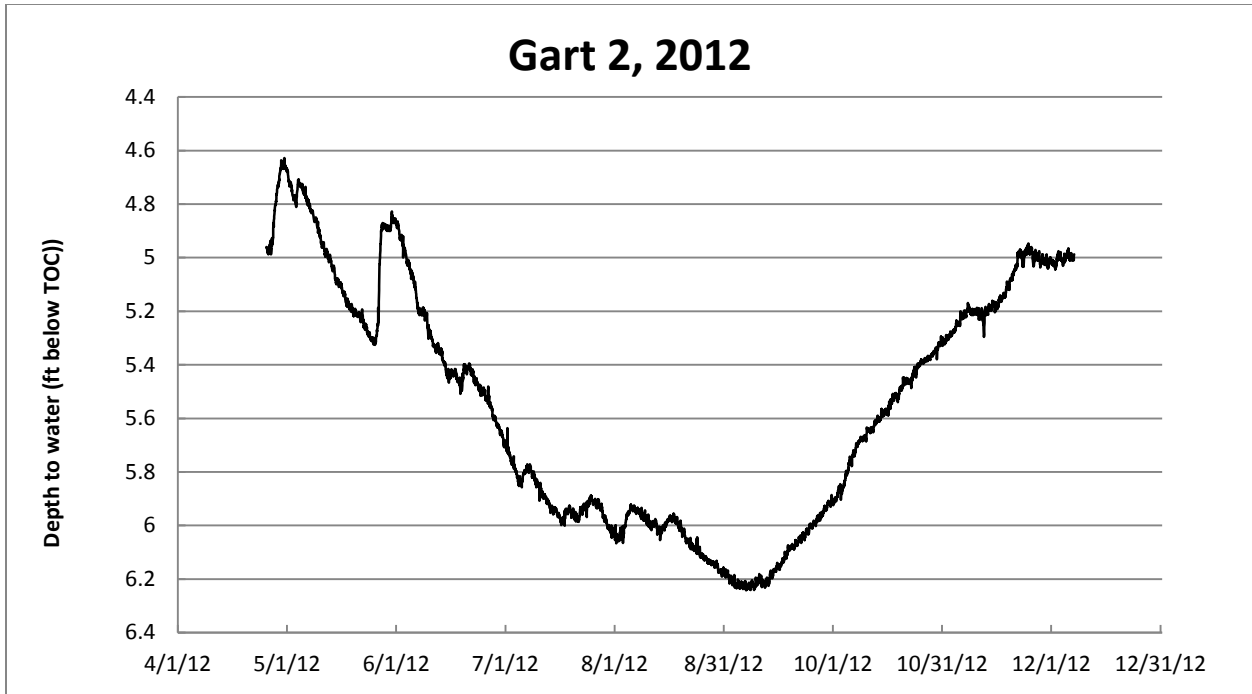


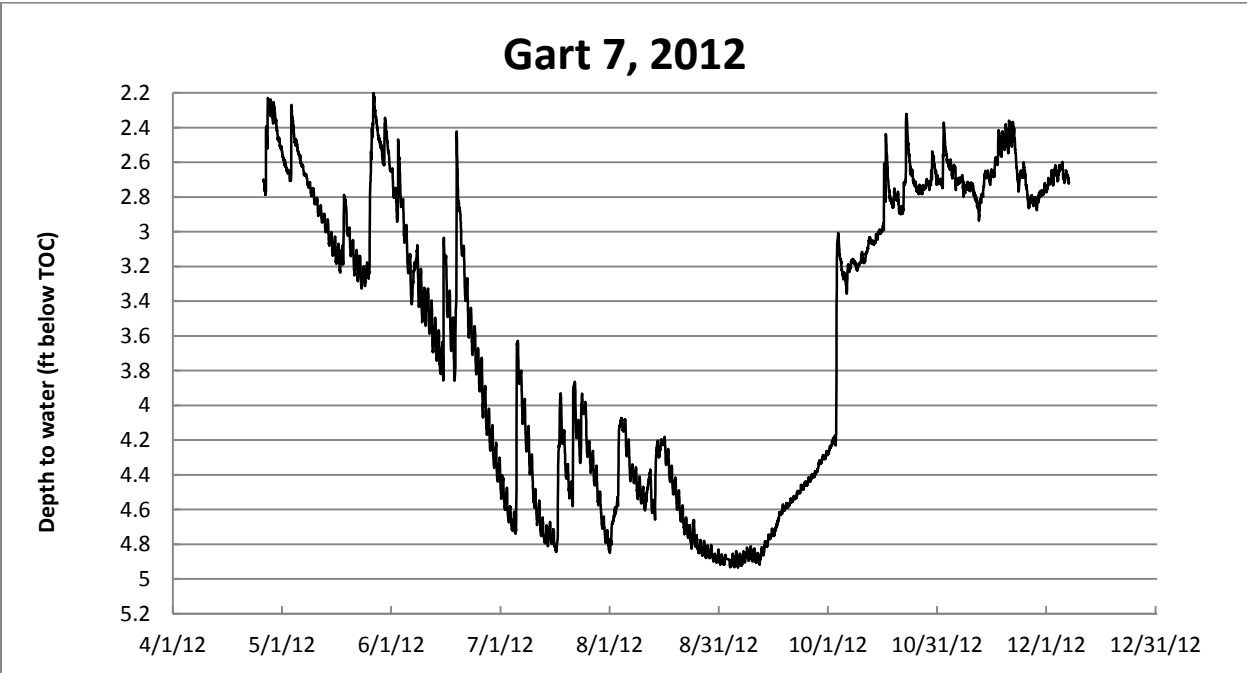
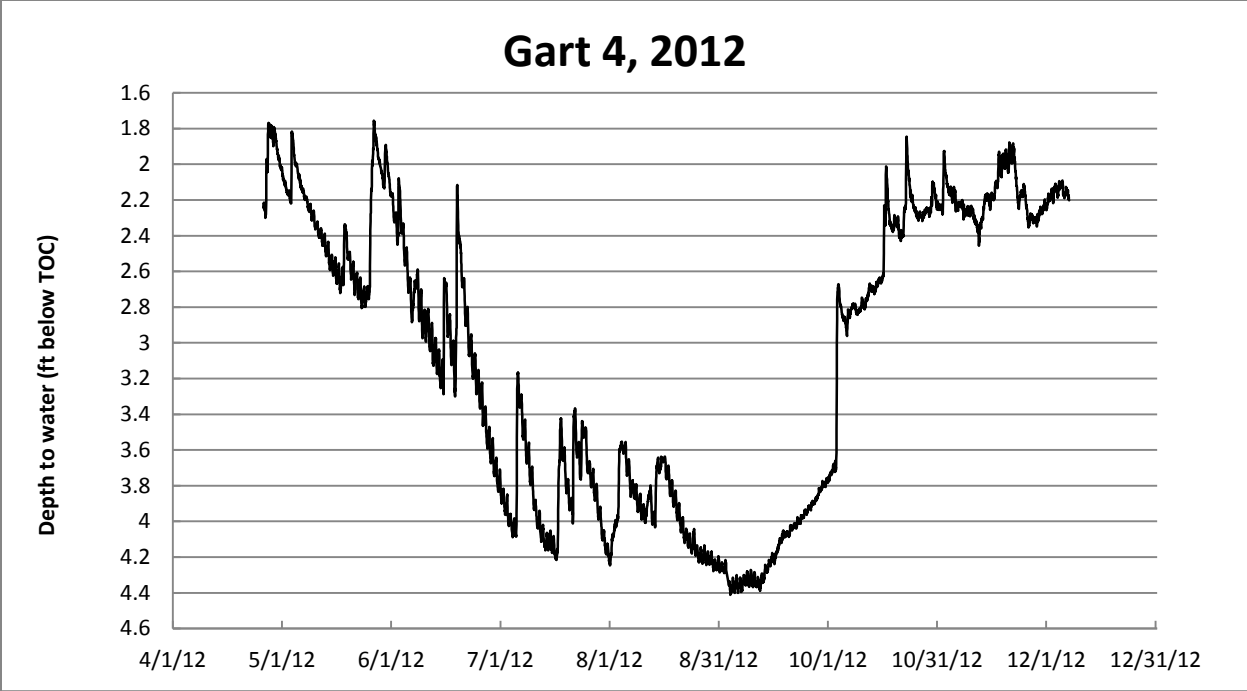


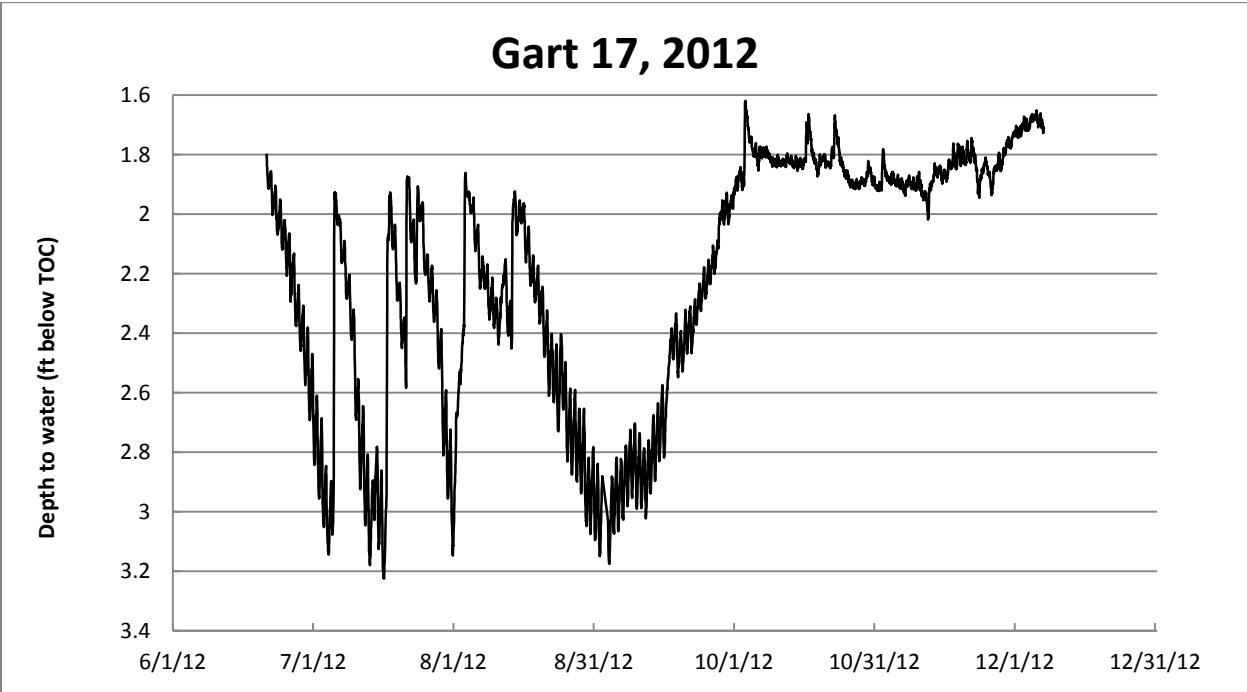
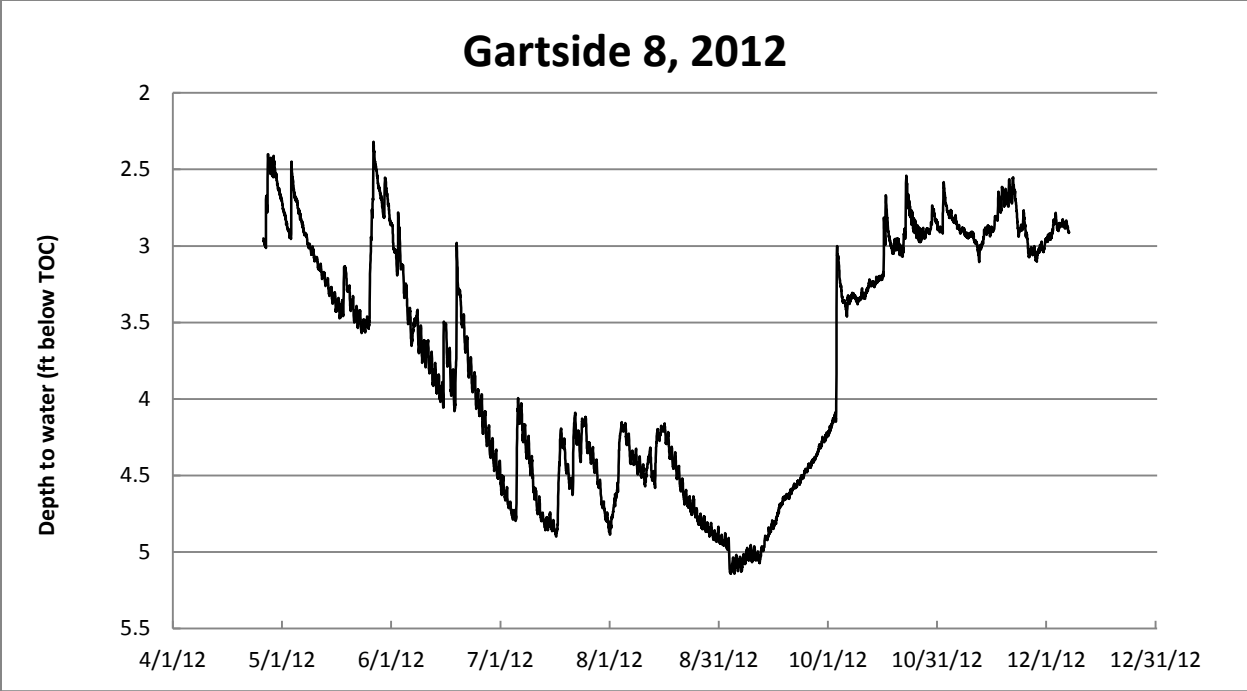
2011 Paired Well Water-level Comparisons



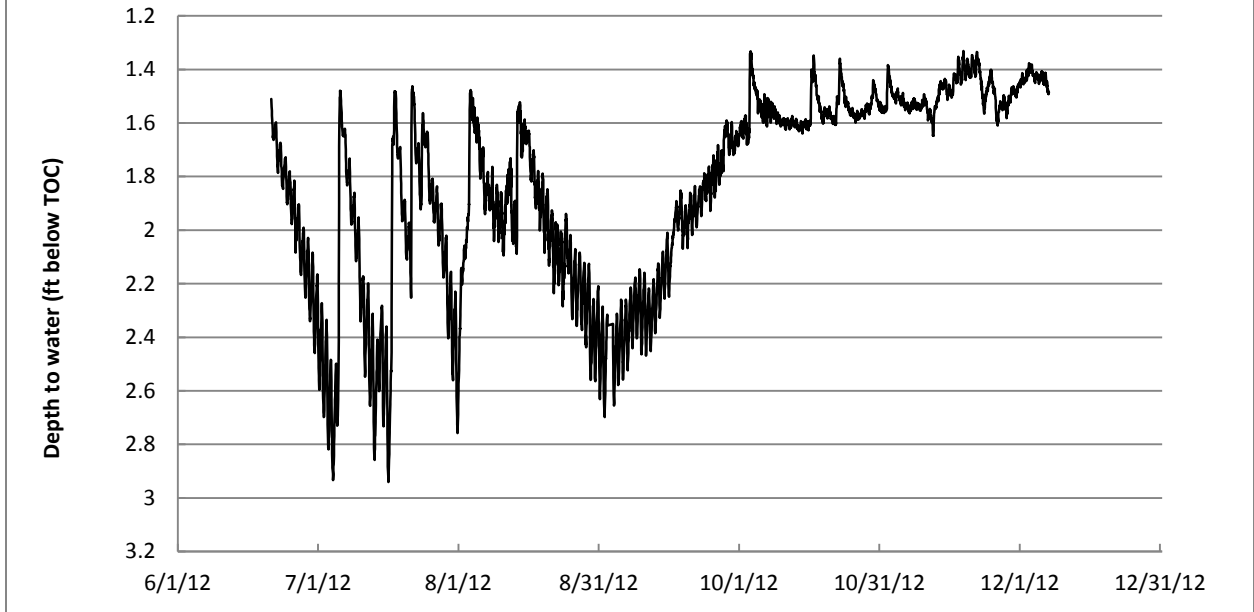
2012 Season







Gart 18, 2012



Appendix D: Ash Content Analyses

Gart 5 (sample depth 1.9-3.7 feet)								
Sample	Time Burned	Crucible Mass (grams)	Crucible + Peat (grams)	Ending Mass (grams)	Sample Mass (grams)	Ash Mass (grams)	% Ash	Observations
A	41 min	11.8333	13.7867	13.2922	1.9534	1.4589	74.69	A reddish flame (strontium?). At 9:14 turned solid black in appearance. At 9:28 turned to a light grey.
B	41 min	9.9976	12.3602	11.7457	2.3626	1.7481	73.99	A reddish flame (strontium?) At 9:14 turned solid black in appearance. At 9:28 turned to a light grey.
C	38 min	13.1950	15.4526	14.8256	2.2576	1.6306	72.23	Turned grey fast.
						Average	73.63	
Gart 4 (sample depth 13.6-14.7 feet)								
G	35 min	19.0000	21.2756	20.2609	2.2756	1.2609	55.41	After 1 min started turning black. Orange flame lasted 2-3 min. At 10:11 turned light grey, white on bottom at 10:24.
D	36 min	16.5318	18.6672	17.6400	2.1354	1.1082	51.90	After 1 min started turning black. Orange flame lasted 2-3 min. At 10:11 turned light grey, white on bottom at 10:24.
Z	36 min	19.2521	21.9005	20.6545	2.6484	1.4024	52.95	After 2 min started turning black. Orange flame lasted 2-3 min. At 10:11 turned light grey, white on bottom at 10:24.
						Average	53.42	
Gart 10 (sample depth 4.36-4.85 feet)								
A	41 min	11.8330	13.1717	12.9138	1.3387	1.0808	80.74	Turned black after 2 min. Orange flame at 11: 14 and very small. At 11:22 still black. At 11:13 turned light grey. At 11:44 no change.
B	42 min	9.9977	11.6374	11.3242	1.6397	1.3265	80.90	Turned black after 2 min. Orange flame at 11: 14 and very small. At 11:22 still black. At 11:13 turned light grey. At 11:44 no change.
C	43 min	13.1949	14.9530	14.6025	1.7581	1.4076	80.06	Turned black after 2 min. Orange flame at 11: 14 and very small. At 11:22 still black. At 11:13 turned light grey. At 11:44 no change.
						Average	80.57	

Using 222Rn and Isotopic Tracers to Trace Groundwater-Lake Interactions

Basic Information

Title:	Using 222Rn and Isotopic Tracers to Trace Groundwater-Lake Interactions
Project Number:	2011MT241B
Start Date:	3/1/2011
End Date:	2/28/2013
Funding Source:	104B
Congressional District:	At-large
Research Category:	Ground-water Flow and Transport
Focus Category:	Groundwater, Surface Water, Nutrients
Descriptors:	None
Principal Investigators:	Glenn Shaw

Publication

1. Shaw, G.D., E.S. White and C. Gammons. 2013. Characterizing groundwater-lake interactions and its impact on lake water quality. *Journal of Hydrology* 492:69-78.

MONTANA WATER CENTER SEED GRANT FINAL REPORT

For

Using ²²²Rn and Isotopic Tracers to Trace Groundwater-Lake Interactions

PI: Glenn Shaw, Ph.D., Assistant Professor, Department of Geological Engineering, Montana Tech, Butte, MT 59701, 406-496-4809 (office), 406-496-4260 (fax), gshaw@mtech.edu.

ABSTRACT

Several geochemical and isotopic tracers were used to investigate groundwater and lake interactions in Georgetown Lake, Granite County, MT. Georgetown Lake is a large high elevation lake experiencing rapid growth and high recreation use. It was classified as eutrophic or mesotrophic in the 1980s. Spatial variations of geochemistry combined with physical measurements were used to develop a conceptual understanding of how groundwater and surface water interact. Radon samples were used to show that groundwater primarily enters the lake along the eastern shore of the lake through karst caverns and fractures. Physical and solute mass balances indicate that the lake is a flow through lake, with groundwater exiting on the western side of the lake. This is consistent with water levels and the west dipping bedrock in the region. Stable isotopes of the water molecule were used to perform an endmember mixing analysis. From this analysis there appear to be three water types mixing in the lake. The first type is precipitation, which represents the overland flow component. The second endmember is groundwater, and the third endmember is lake water that has been highly evaporated. The third endmember was most likely derived from the first two endmembers and represents a process controlling the lake. The western side of the lake has the most evaporated water, which is consistent with the conceptual model of groundwater entering along the eastern shores and exiting along the western shores. The average lake composition suggests that the lake is roughly 27.4% groundwater, 34.8% precipitation, and 38.1% evaporated lake water. These fractions are also consistent with the groundwater and surface water components derived from the mass balances. Spatial variations of nutrients show no direct correlation of groundwater sources of nutrients (i.e. septic systems leaking to the lake). In fact, groundwater inflows appear to bring in oxygenated groundwater to the eastern side of the lake improving water quality of the lake. The western two-thirds of the lake was anoxic near the bottom of the water column with H₂S-S and NH₃/NH₄⁺-N concentrations as high as 1.99 mg/L and 4.0 mg/L respectively. Groundwater samples were low in H₂S-S and NH₃/NH₄⁺-N, PO₄³⁻, but had moderate NO₃⁻-N, and SO₄²⁻ values. There is currently no evidence that high levels of nutrients are entering the lake through groundwater inflows to the lake during late winter, but the conceptual understanding of groundwater flow suggests that groundwater pollution is a greater risk in the southeast portion of the reservoir.

PROBLEM STATEMENT

This report is a final report for the Montana Water Center Seed Grant proposal, “Using ^{222}Rn and Isotopic Tracers to Trace Groundwater-Lake Interactions”; under U.S. Geological Survey contract G11AP20090 and Montana Water Center sub award G208-11-W3491. The funding cycle was from March 2011 to March 2013. The purpose of this project was to investigate groundwater and lake interactions using geochemical and isotopic tracers in Georgetown Lake, Granite County, Montana (Figure 1). Montana. Georgetown Lake is the most highly recreated lentic water body of its size in Montana, and its surrounding lands are under-going subdivision and development and continued expansion is probable (Missoulain, 2010). Land and lake uses include: homes, motels, sight-seeing, boating, water skiing, fishing, hunting, picnicking, camping, snowmobiling, cross-country skiing and downhill skiing at Discovery Basin. Subdivision of land for home sites has remained steady and rapid urbanization could have negative impacts on water quality and quantity. Georgetown Lake was classified as eutrophic or mesotrophic (Knight, 1981), and there are currently concerns about decreasing dissolved oxygen during winter months from increasing biological oxygen demand (BOD) because of nitrogen and phosphorous loading when the lake is covered with ice (Garrett; 1983; Knight, 1981; USEPA, 1983). Several studies have been conducted looking at dissolved oxygen and nutrient dynamics within the lake to better understand the source of nutrients (i.e. Craig Stafford at the University of Montana, Montana Department of Environmental Quality Total Maximum Daily Load Program, and several theses and dissertations from MSU and U of M). Recent work (Henne, 2011) confirms previous studies (Knight 1981; Trabert, 1993) that show DO declines become more severe as winter months proceed. Nutrient sources could include tributary streams and springs, septic effluent, fertilizer application, previous grazing, or geologic sources. Characterizing the groundwater-lake interactions may provide some insight into the possible sources of nutrients or processes controlling nutrient dynamics within Georgetown Lake, helping guide management decisions.

Our interest was primarily to characterizing groundwater dynamics within the lake, but we also investigated nutrients to see if there is any correlation between nutrient loading and groundwater. Groundwater and surface water are accepted as being a single complex and interconnected system (Cook et al., 2008; Loveless et al., 2008; Owor et al., 2011). In order to responsibly develop and manage lakes it is important to understand water fluxes into and out of lakes (Barr et al., 2000; Cherkauer and Nader, 1989). Groundwater and surface water inflow play an important role in controlling lake water chemistry, water quality, aquatic habitat and biodiversity (Hagerthey and Kerfoot, 1998). Groundwater flow to lakes can be especially difficult to determine using traditional techniques, such as well hydraulics and Darcy’s Law, because of the large degree of heterogeneity in geologic material—especially in fractured, faulted, and folded terrain such as that surrounding Georgetown Lake. Darcy’s Law estimates generally cannot be made unless there is sufficient information about aquifer parameters, especially the hydraulic conductivity, which varies over thirteen orders of magnitude in natural geologic material (Freeze and Cherry, 1979) and local heterogeneities can lead to vastly different results (Fetter, 2001). The use of naturally occurring environmental tracers coupled with physical methods has proven to be particularly useful in characterizing groundwater interactions with surface water (Maloszewski and

Zuber, 1982; Maloszewski et al., 1983; Mattle et al., 2001). In this study ^{222}Rn was used to characterize groundwater-surface water interactions (Cook et al., 2008; Genereux et al., 1993).

The objectives for the present study were to i) obtain spatial concentrations of ^{222}Rn and water isotopes ($\delta^{18}\text{O}$ and δD) in Georgetown Lake and surrounding groundwater to develop a conceptual understanding of how groundwater interacts with Georgetown Lake, ii) spatially assess nutrient and other solute concentrations in the Lake groundwater within Georgetown Lake and the surrounding basin, iii) investigate the role of groundwater on nutrient levels.

STUDY AREA

Georgetown Lake is a high elevation Lake sitting at 1960 meter above sea level. It is located in the Flint Creek drainage situated on a high plateau between the Anaconda-Pintler Range and the Flint Creek Range in the upper Clark Fork watershed of western Montana (Figure 1). The plateau was emplaced by the Georgetown Thrust Fault, a low angle, westward dipping fault consisting of allochthonous mid-Proterozoic sedimentary rocks of the Belt Basin on top of mid-Paleozoic sedimentary rocks (Lonn et al., 2003) (Figure 2). Georgetown Lake is underlain by the Georgetown Thrust which separates the Lake into the eastern and western sides. The west side of the Lake is dominated by the middle Belt carbonate (Yc) which consists of dolomitic siltite and quartzites. The east side of the Lake is comprised of sedimentary rocks of the Madison Group (PMs). Surficial deposits, including alluvium and glacial till (Qgk), form a thin, discontinuous layer above the bedrock. The Madison is a fossiliferous limestone underlain by a flaggy limestone and shale (Figure 2). Rock units dip $\sim 40^\circ$ - 60° to the northwest and strike northeast/southwest and have been folded, faulted, and metamorphosed by intrusion of late Cretaceous granitic bodies.

The hydrogeology of Georgetown Lake is highly influenced by upland terrain. The Lake is fed by two major tributaries, several springs, and groundwater within its 13,720 ha drainage area. Stuart Mill Spring has an average year-round flow of roughly 0.5 m³/s from a 4,222 ha drainage area (Figure 1), and it discharges from karst limestone a short distance from the lake. Flint Creek (North Fork) is a free-stone creek that discharges into the Lake from an approximate drainage area of 4,895 ha, and shows large seasonal variation in flow.

The study area includes 22,680 meters of a highly embayed Lake shoreline. The deepest point in the Lake is 10.7 meters and the average depth is 4.9 meters. The Lake has an irregular shape with a surface area of 1,219 ha and a volume of 38.3×10^6 m³ of water (Knight, 1981). At Silver Lake, which is nearby Georgetown Lake, the mean annual precipitation for 1950- 1983 was 47.5 cm and the average annual snowfall was 352.0 cm (Western Regional Climate Center, <http://www.wrcc.dri.edu/cgi-bin/cliMAIN.pl?mt7605>). Higher elevations around the Lake receive a much greater amount of precipitation in the range 89- 144 cm/yr (Western Regional Climate Center, 2011). The Lake typically freezes in early-to mid-November, and ice-off usually occurs in May.

METHODS

Seventy Lake samples were collected around the perimeter of Georgetown Lake between March 12 and April 12, 2011 (Figure 3). An additional 46 ^{222}Rn samples were collected in the middle of the lake along linear transects extending from the lake shore to the center of the lake during February and March, 2013. Sampling locations were roughly evenly spaced around the perimeter of the Lake, but occasionally samples were collected more closely spaced together if there was geomorphic evidence of groundwater seepage to the Lake (e.g. near locations where ice was melted near the shore, in the neck of inlets, or near tributary or spring confluences). A gas powered ice auger was used to drill holes in the ice for sampling. A 12 volt geosub purge pump was used to sample Lake water from near the bottom of the Lake. Hydrolab MS5 measurements were also collected near the bottom of the Lake where lake samples were collected. DO and pH were calibrated each day the Hydrolab MS5. A 2-point pH 7 and pH 10 calibration was conducted. Sc was not calibrated for each use, but was checked against a 1413 $\mu\text{S cm}^{-1}$ KCl standard before each use. If results were more than $\sim 2\%$ off, then the meter was calibrated. Lake sampling was conducted during the late winter months to ensure that ice cover would prevent ^{222}Rn from degassing and/or being dispersed by wind driven mixing. During summer, degassing and mixing would be significant because of daily turnover resulting from high winds and the large surface area to volume ratio of the Lake.

From June 2011 to September 2011, additional samples were collected from 16 residential groundwater wells, two springs (Emily Spring and Stuart Mill Creek), and Flint Creek inflow and outflow. Stuart Mill Spring samples were collected 200 ft. from the discharge location. The samples come from a spigot plumbed to the spring. Closed plumbing was necessary to avoid degassing of radon samples. Samples at the Flint Creek inflow were taken just upstream of MT Highway 1, and the Flint Creek outflow samples were collected 0.1 mi from the dam outlet. Groundwater samples were collected around the perimeter of the Lake (Figure 3). Groundwater samples were collected from hydrants or spigots connected to domestic wells. Three well volumes of water were purged from the well before sample collection, and no treated water was sampled. All sampling locations had temperature, specific conductivity, pH, and dissolved oxygen measured in the field using a HydroLab MS5 multi-parameter meter. Major cations (Na^+ , K^+ , Mg^{2+} , Ca^{2+}), major anions (F^- , Cl^- , Br^- , NO_2^- , NO_3^- -N, SO_4^{2-}), alkalinity, nutrients (H_2S -S, PO_4^{3-} , and $\text{NH}_3/\text{NH}_4^+$ -N), stable isotopes of water ($\delta^{18}\text{O}$ and $\delta 2\text{H}$), and ^{222}Rn were also sampled at each location. Nutrients, cations and anions were collected by filtering with a 0.2 μm PES syringe filter into separate 60 ml HDPE bottles. Each bottle was triple rinsed with filtered water from the source being sampled (e.g. Lake or well water) prior to sampling. Major anions, nutrients, and cations were stored at 4 °C, and cations were also preserved with 2% nitric acid. Alkalinity samples were collected unfiltered in 250 ml HDPE bottles. Stable isotopes of water were collected unfiltered in 30 ml HDPE bottles with no headspace, and ^{222}Rn was sampled in 250 ml gas-tight glass bottles and samples were kept refrigerated at 4 °C. To insure degassing of ^{222}Rn was kept to a minimum, the water was pumped into a two gallon plastic bucket and the bottle was fully submerged until all air had been purged from the bottle. No field blanks or duplicate samples were collected.

Water ion samples were analyzed at the Murdock Environmental Biogeochemistry Lab at the University of Montana. Anions were analyzed on Dionex DX-500 Ion Chromatograph using EPA Method 300.0.

Cations were analyzed using a Perkin-Elmer Optima 5300DV optical inductively-coupled plasma atomic emission spectroscopy (ICP-AES) using EPA Method 200.7. Ammonium-N, H₂S-S, and PO₄³⁻ were analyzed at Montana Tech Biogeochemistry Lab using a HACH 9600 spectrophotometer using EPA Methods and 8038, 8131, and 8048 respectively. Alkalinity was analyzed using bromocresol green-methyl red indicator powder and a HACH digital titrator in the Montana Tech Biogeochemistry Lab. Stable isotopes of water samples were analyzed at the University of Wyoming Stable Isotope Facility using a Los Gatos Liquid Water Isotope Analyzer (LGR-LWIA). Radon was analyzed at the Montana Bureau of Mines and Geology using a 6000 series Beckman Liquid Scintillation counter. Standard EPA Method 913 for ²²²Rn was followed and measured concentrations were decay-corrected for the date and time of sample collection. Detection limits for major ions and nutrients are listed in Table 1.

In order to answer the objective questions, several spatial samples were collected for a variety of analytes. Several mass balance approaches were used to help develop a conceptual understanding of groundwater-lake interactions and quantify groundwater inflows and outflows. Radon was used to determine the locations where groundwater enters the lake. Radon, Sc, and Cl⁻ mass balance approaches were combined with a physical hydrologic budget to quantify groundwater inflows and outflows. Stable isotopes were used in an endmember mixing analysis (EMMA) to identify the sources of water or processes controlling lake water. Each sample in the lake was separated into their respective endmembers. The following is a summary of these methods. Spatial variations of nutrients were also investigated to help answer research question.

RESULTS

Water Quality and Major Ion Chemistry

All samples and water quality measurements collected in Georgetown Lake were collected less than 0.5 m from the Lake bottom. Georgetown Lake temperature in this study ranged between 0.00 and 4.84 °C, with an average value of 1.67 °C (Table 2). Specific conductivity ranged between 208.1 and 418.0 μS/cm, with an average value of 234.6 μS/cm. Dissolved oxygen concentrations ranged between 0.38 and 8.25 mg/L. The average dissolved oxygen was 2.95 mg/L, indicating that much of the Lake bottom was suboxic at the time of sampling. Lake pH ranged from 6.17 to 9.89, and the average Lake pH was 7.5.

The 16 groundwater wells sampled had well depths ranging from 6 to 98 m, and the depths to water from top of casing ranged from 1 to 17 m (Table 3). Temperature in groundwater wells and springs ranged from 6.39 to 7.3 °C, with an average value of 7.19 (Table 4). Specific conductivity ranged between 153.3 and 553.0 μS/cm with an average value of 325.7. Dissolved oxygen in groundwater ranged from 5.51 to 12.15 mg/L, with an average value of 8.47 mg/L. Thus, relative to the inshore bottom water in winter, influent groundwater was warmer, more saline, and more oxygenated. In groundwater pH ranged between 7.30 and 6.39 with an average value of 6.83.

Major ion results show that both the Lake and groundwater were primarily calcium/magnesium bicarbonate dominated-water (Figure 4). This is typical of water in western Montana, especially since Georgetown Lake is partially underlain by the Madison Limestone. Tables 4-6 show individual water

quality field parameters, major cations and major anions for collected for individual groundwater samples.

Stable Isotopes

The mean stable isotopic composition of Georgetown Lake water was -15.2 ‰ and -123.0 ‰ for $\delta^{18}\text{O}$ and δD respectively (Figure 5). Groundwater $\delta^{18}\text{O}$ ranged from -17.6 to -13.4 ‰, and δD ranged from -116.5 to -135.4 ‰. Groundwater samples averaged -18.2 and -136.2 ‰ for $\delta^{18}\text{O}$ and δD respectively (Table 7). Groundwater $\delta^{18}\text{O}$ ranged from -19.7 to -15.2 ‰, and δD ranged from -141.9 to -119.9 ‰. Georgetown Lake shows a range of isotopic compositions that plot along the global meteoric water line (GMWL) and also show various degrees of evaporation (Figure 5). Samples that have undergone the most evaporation plot the furthest to the right of the GMWL in Figure 5. These results are similar to other meteoric water collected in Southwest Montana (Gammons et al., 2006). In general, water samples collected to the west of the Georgetown Thrust Fault plot further away from the GMWL suggesting water that has undergone higher evaporation. Given the extensive mixing in the Lake without ice cover, the entire Lake most likely undergoes significant evaporation during the summer and early fall months. After the Lake is covered with ice and all through the winter months, the evaporated signal in the Lake apparently is diluted in the southeastern portion of the Lake from inflowing groundwater. In contrast, the H and O isotopes revealed that groundwater had undergone little to no evaporation (Figure 5).

Radon

Mean ^{222}Rn activity in Georgetown Lake was 31.5 pCi/L. Radon-222 activity varied extensively around Georgetown Lake ranging between 3.5 pCi/L and 194.0 pCi/L (Figure 6). Activities were highest along the east side of the Lake indicating groundwater seepage to the Lake. The highest radon activities correspond with samples that were collected near the projected trace of the Georgetown Thrust Fault. Locations nearest to the fault on the east side of the Lake had ^{222}Rn concentrations of 141.2, 153.5, and 194.0 pCi/L, while ^{222}Rn activities were 61.0 and 72.9 pCi/L near the fault on the southern shore of the Lake (Figure 6).

The ^{222}Rn activity of groundwater ranged between 145.8 and 990.4 pCi/L with a mean activity of 576 pCi/L (Table 7). Groundwater had higher ^{222}Rn activity on the west side of the Lake, with values ranging between 441.6 to 990.9 pCi/L. Radon-222 activity of groundwater on the east side of the Lake, ranged between 145.8 and 624.3 pCi/L.

The ^{222}Rn activities in Emily Spring and Stuart Mill Spring were 228.4 and 188.1 pCi/L respectively. Emily Spring was sampled right at the spring orifice and Stuart Mill Spring sampled from a residential water supply piped from the spring. It is possible that even with the efforts to prevent sampling degassed water, there could be some degassing as groundwater discharges to the spring orifice. Both of these

springs discharge from karst limestone on the southeastern side of the study area. Radon activity at the mouth of the Flint Creek inflow was 10.2 pCi/L. Just downstream of the Lake outlet to Flint Creek, the radon activity was 6.5 pCi/L.

Nutrients

Phosphate concentrations in Georgetown Lake from near the bottom ranged from 0.09 to 0.40 mg/L, and in groundwater ranged from 0.04 to 0.14 mg/L (Figure 7). Mean PO_4^{3-} concentrations were 0.09 mg/L and 0.07 mg/L in the Lake and groundwater respectively. In general, PO_4^{3-} concentrations were elevated in the Lake in comparison with groundwater. There was one location along the east side of the Lake that has a value of 0.40, whereas all other Lake water had concentrations less than 0.30 mg/L (Figure 7).

Hydrogen sulfide-S ranged from non-detect to 1.99 mg/L in Georgetown Lake, and all groundwater samples were non-detect. Our method of detection for $\text{H}_2\text{S-S}$ was if the sampler could smell $\text{H}_2\text{S-S}$ in the sample bottles then we would analyze for $\text{H}_2\text{S-S}$. If not, we assumed the sample was non-detect. In the Lake the $\text{H}_2\text{S-S}$ concentrations had a mean concentration of 0.11 mg/L. The method used to measure $\text{H}_2\text{S-S}$ has an upper detection limit of 2.00 mg/L, and it may be that the sample with 1.99 mg/L $\text{H}_2\text{S-S}$ actually exceeds the detection limit (site 6 in Figure 3). This suggests an internal source of $\text{H}_2\text{S-S}$ —most likely generated from bacterial reduction of SO_4^{2-} brought into the Lake by surface water, groundwater and/or in the Lake sediments. Hydrogen sulfide-S concentrations varied spatially around the perimeter of Georgetown Lake (Figure 8). In general, $\text{H}_2\text{S-S}$ concentrations were highest along the northern and western portion of the Lake where ^{222}Rn activity was low and there were no groundwater inflows to the Lake.

In general, groundwater had elevated SO_4^{2-} in comparison to the Lake. Sulfate concentrations in Georgetown Lake ranged from 1.72 to 5.89 mg/L with a mean value of 3.94 mg/L. Groundwater ranged from 0.95 to 22.3 mg/L with a mean value of 7.9 mg/L (Figure 9). Accordingly, locations in the Lake where ^{222}Rn activity was the highest also had relatively high concentrations of SO_4^{2-} (Figures 6 and 9), reflecting the groundwater inputs.

Ammonium-N concentrations in Georgetown Lake ranged from non-detect to 4.0 mg/L, with a mean concentration of 0.15 mg/L. Ammonium-N was virtually absent in groundwater (ranging from non-detect to 0.02 mg/L) (Figure 10). Like $\text{H}_2\text{S-S}$, $\text{NH}_3/\text{NH}_4^+\text{-N}$ appears to be generated primarily within the Lake and concentrations were lowest where groundwater seepage was highest along the eastern portion of the Lake. Similar to $\text{H}_2\text{S-S}$, the maximum $\text{NH}_3/\text{NH}_4^+\text{-N}$ concentration was located at site 6 (Figure 3) and had a value at the maximum detection for the analytical method used. This is the only sample where $\text{NH}_3/\text{NH}_4^+\text{-N}$ and $\text{NH}_3/\text{NH}_4^+\text{-N}$ may have actually been elevated in comparison to the reported value in this report.

Nitrate-N levels generally were low in the Lake (less than 0.07 mg/L), and vary from non-detect to 5.2 mg/L in groundwater (Figure 11). There was no distinction between the east and west sides of the Lake for NO_3^- -N concentrations, and the source of NO_3^- -N is unknown.

Dissolved oxygen concentrations ranged from 0.3 to 8.25 mg/L in Georgetown Lake and from 5.51 to 12.15 mg/L in groundwater (Figure 12). Mean DO values were 2.95 mg/L and 8.04 mg/L in the Lake and groundwater respectively. Three of the wells had greater than 100% saturation in DO. This could be from either incorporation of air

during sampling or from supersaturation of oxygen from excess air trapped in groundwater during recharge. The latter is the most likely scenario because DO was continuously measured while discharging the pump. Samples were either measured in a flow through cell where there was no contact with the atmosphere or they were collected by continuously pumping laminar flow to the bottom of a 5 gallon bucket. During well purging, DO was measured at the bottom of the bucket preventing contact with the atmosphere. Rapid recharge in a groundwater system has been known to lead to supersaturation of dissolved gases from incorporation of tiny air bubbles that later dissolve into groundwater (Cey et al., 2008). For future reference, the best method to determine if this occurs in the Georgetown Lake watershed is to sample noble gases to determine quantities of supersaturated excess air.

Alkalinity ranged from 110 to 227 mg/L in Georgetown Lake and from 88 to 240 mg/L in groundwater (Figure 13). Mean alkalinity values were 132 mg/L and 177 mg/L in the Lake and groundwater respectively.

DISCUSSION

Groundwater-Lake Interactions

Radon-222 activity in Georgetown Lake can be used as a surrogate for groundwater inflows. Combining ^{222}Rn with the local geology allows one to develop a simple conceptual model of how groundwater interacts with the Lake. In general, groundwater seepage to Georgetown Lake occurs along the east side of the Lake which consists of karst limestone (PMs) and glacial till (Qgtk). Groundwater seepage appears to be greatest near the boundary of the thrust fault (Figure 6). This could be from the fault acting as a conduit for groundwater flow to the Lake, as groundwater from the east encounters the fault. The Precambrian "upper plate" might also act like a confining layer, thus forcing groundwater entering from the east to discharge near the Georgetown Thrust Fault. One other possibility for the higher rates of groundwater flow near the thrust fault is that the Madison Limestone outcrops occur next to the thrust fault, while glacial till covers the limestone along the majority of the eastern shoreline between the Madison Limestone outcrops (figure 2). Although thin, the till has a lower hydraulic conductivity relative to the limestone, and therefore could act as a submerged semi-confining layer to upwards groundwater flow. Stuart Mill Spring discharges on the order of 0.5 m³/s and emerges from fractures and voids within karst limestone.

On the west side of the Lake, which consists of fractured and folded Belt rock, the radon concentration was lower suggesting that there is little to no influent groundwater seepage from the west to the east. The low ^{222}Rn activity on the west side of the Lake (<10 to 29 pCi/L) may be from radioactive decay of dissolved ^{226}Ra within the Lake, or diffusion of ^{222}Rn from Lake bottom sediments or sediment pore water and not from groundwater seepage. In general the primary dip orientation of the bedrock throughout the entire region is to the west (Figure 2). If groundwater was following bedding planes, then there would be essentially no groundwater seepage from the west side because bedding planes dip steeply away from the lake. It may even be the case that the west side of the Lake recharges groundwater flow to the associated Precambrian metasedimentary rocks, resulting in a flow-through-Lake system where groundwater enters the Lake from the east and exits the Lake to the west.

The stable isotopes of water results provide an additional understanding of groundwater and Lake flow paths. The more highly evaporated water on the western side of the Lake suggests that water in the western bays is not replenished by incoming groundwater or surface water, and that it takes substantial time for this water to exit the Lake either as groundwater along the western shore or as surface water through the dam during the winter. Isotope samples were used in an endmember mixing analysis. The lake samples tend to plot in a triangular shape when plotted against the meteoric water line (Figure 14). The three corners of the triangle represent source waters mixing, or processes occurring on the lake water. These endmembers are described as:

EM1:	Groundwater, isotopically depleted which is representative of fresh snowmelt recharge. Position on Figure 13: $\delta^{18}\text{O} = -18.3 \text{ ‰}$, $\delta^2\text{H} = -136 \text{ ‰}$
EM2:	Evaporated water, isotopically enriched Position on Figure 13: $\delta^{18}\text{O} = -12.8 \text{ ‰}$, $\delta^2\text{H} = -121 \text{ ‰}$
EM3:	Average annual precipitation Position on Figure 13: $\delta^{18}\text{O} = -15.5 \text{ ‰}$, $\delta^2\text{H} = -115 \text{ ‰}$

Precipitation samples from Butte, MT were used to define the precipitation end member. Samples were reported from Gammons et al. (2006). The groundwater endmember concentrations were derived from average groundwater values in this study, and the evaporated water was taken from the most extremely evaporated water sample within the lake. Each sample in the lake falls within this triangle and represents a mixture of each of these endmembers. The three endmember mixing results are plotted on a trilinear diagram, and shows that the most highly evaporated samples are located on the west side of the lake (Figure 15). The east side continues to receive groundwater and Flint Creek water that is not highly evaporated, but the water on the west side tends to be more stagnant and is influenced more from evaporative processes prior to exiting the lake as groundwater or surface water. These results fit with our conceptual understanding from radon and the mass balances. When all lake samples are averaged, the calculated fractions suggest that the lake is 27.4% groundwater, 34.8% precipitation, and 38.1 percent evaporated lake water (this last endmember could be water that was originally groundwater or precipitation).

Four mass balance approaches were used to determine the rates of groundwater inflow and outflow within the lake. The first mass balance approach was derived from a physical water balance. This

approach uses values of precipitation, evaporation, surface water inflows and outflows, and is used to solve for the difference between groundwater inflows and outflows. Chemical mass balances were used to separate the groundwater inflows and outflows.

The physical mass balance is as follows:

$$\frac{\partial V}{\partial t} = PA - EA + Q_{gwi} - Q_{gwo} + Q_{si} - Q_{so} \quad (1)$$

where:

$$\begin{aligned} \frac{\partial V}{\partial t} &= \text{Change in Volume with time; Storage} \\ A &= \text{area of the lake (ft}^2\text{)} \\ P &= \text{precipitation (ft/day)} \\ E &= \text{evaporation (ft/day)} \\ Q_{gwi} &= \text{groundwater flux into the lake (ft}^3\text{/day)} \\ Q_{gwo} &= \text{groundwater flux out of the lake (ft}^3\text{/day)} \\ Q_{si} &= \text{surface water flux into the lake (ft}^3\text{/day)} \\ Q_{so} &= \text{surface water flux out of the lake (ft}^3\text{/day)} \end{aligned}$$

A chemical mass balance is as follows:

$$\frac{\partial C_L V}{\partial t} = Q_{gwi} C_{gw} + Q_{si} C_{si} + F A_b - Q_{gwo} C_{gwo} - Q_{so} C_{so} - k A C_w - \lambda V C_L \quad (2)$$

where:

$$\begin{aligned} F &= \text{diffusive flux from underlying sediments} \\ A_b &= \text{area of lake bottom} \\ k &= \text{gas transfer velocity} \\ \lambda &= \text{radioactive decay constant (0.18 day}^{-1}\text{)} \\ V &= \text{volume of the lake (ft}^3\text{)} \\ C_L &= \text{concentration of the lake (pCi/L)} \end{aligned}$$

Sc and Cl⁻ mass balances use equation 2, but the decay term and diffusion terms are not included. The radon mass balance included the decay term, but diffusion was assumed to be negligible. Parameters for the mass balance were determined from direct measurements in this study or from a DNRC report submitted to the Georgetown Lake Homeowners Association (Amman, 2011). The parameters used are shown in Table 8, and the calculated results are for groundwater inflows and outflows are found in Table 9.

Groundwater inflow and outflows estimated from the radon mass balance approach are too high, but the results from the Cl⁻ and Sc mass balances are within the correct order of magnitude (with total flows similar to surface water flows). One possible explanation for the discrepancy could be from not including a diffusive flux of radon from the sediment pore water. One should note that the solute mass balance approach may also be just an order of magnitude estimate as diffusion of solutes from sediment was

also not included in the study. Further, the lake samples were collected at the bottom of the lake during a time when the lake was stratified. This may also result in groundwater inflows and outflows that are either too high or too low.

Groundwater and Lake Water Quality

The correlation between groundwater inflows and nutrients is not exact, but one must consider that each sample was taken near the Lake bottom, and the Lake depth at each location varied. Georgetown Lake was classified as a mesotrophic or eutrophic Lake (Knight, 1981). During late spring the Lake is inversely stratified under the ice, and there are significant vertical variations in water quality and chemistry throughout the Lake (Henne, 2011). Although, vertical and temporal variations in water quality were captured at two locations by Henne (2011), this study only captured the Lake chemistry at the Lake bottom for one time period.

Phosphate concentrations in groundwater were significantly lower than in the Lake and did not exceed 0.09 mg/L (Figure 7; Table 6). The majority of Lake samples also had similar PO_4^{3-} values; however, 25 of the 67 Lake samples ranged between 0.10 and 0.40 mg/L. There appears to be no visual correlation between PO_4^{3-} concentrations along the eastern and western shores. This suggests that groundwater inflows do not control PO_4^{3-} concentrations. It is interesting that the most elevated sample falls near the mouth of Emily Spring, which provides a major spawning habitat for rainbow trout. The elevated PO_4^{3-} concentrations may be a result of breakdown of organic matter transported to the site by spawning fish.

$\text{H}_2\text{S-S}$ was below detection in all groundwater samples, but generally was higher within Georgetown Lake (Figure 8). In the Lake, $\text{H}_2\text{S-S}$ concentrations were low where groundwater inflows enter the Lake on the eastern shores, but they were elevated west of the thrust fault where there were no groundwater inflows. $\text{H}_2\text{S-S}$ concentrations in the Lake often far exceeded the EPA's 2.0 $\mu\text{g/L}$ chronic criteria for freshwater life. SO_4^{2-} concentrations, on the other hand, were elevated in Georgetown Lake where groundwater discharges to the Lake, and were low or absent where there were no groundwater inflows (Figure 9; Table 6). SO_4^{2-} concentrations in groundwater wells were generally elevated in comparison to the Lake and there were no obvious distinctions between groundwater concentrations on the east or west side of the Lake. These results suggest that the groundwater was a source of SO_4^{2-} to the Lake. The source of $\text{H}_2\text{S-S}$ is unknown, but likely comes in the Lake as SO_4^{2-} and is later reduced to $\text{H}_2\text{S-S}$ from sulfate reducing bacteria or the $\text{H}_2\text{S-S}$ is generated from S present in the Lake sediment.

NO_3^- -N and $\text{NH}_3/\text{NH}_4^+$ -N concentrations also show a similar pattern as SO_4^{2-} and $\text{H}_2\text{S-S}$ (Figures 10 and 11; Tables 5 and 6). $\text{NH}_3/\text{NH}_4^+$ -N in groundwater wells was mostly below detection, but sometimes had concentrations of 0.02 mg/L, which is consistent with the low $\text{NH}_3/\text{NH}_4^+$ -N concentrations in the Lake where groundwater discharges. $\text{NH}_3/\text{NH}_4^+$ -N levels varied around the Lake, but the higher values most often observed in areas lacking major groundwater inputs. Ammonia-N levels in the Lake often exceeded water quality standards. The EPA's 2009 draft ammonia criteria for chronic exposure is 0.26 mg/L or 1.8 mg/L, with the more protective standard used when mussels are present. Nitrate-N in groundwater ranged between non-detect and 5.2 mg/L, all of which were below the EPA's drinking

water standard of 10 mg/L. Although groundwater samples were sparsely sampled from the area surrounding the SE part of the Lake, it appears that the groundwater along the eastern part of the study area has the lowest NO_3^- -N values in comparison to the other regions of the study area (i.e. NO_3^- -N in groundwater samples collected in wells east of the Georgetown Thrust Fault did not exceed 0.99 mg/L). This may be important from a water quality standpoint suggesting that groundwater may not contribute significantly to sources of NO_3^- -N to the Lake.

Although, DO was generally lower in the Lake, no groundwater samples show dissolved oxygen levels below 5.5 mg/L, suggesting that low DO is not contributing to the winter DO sags measured in the Lake (Figure 12). The DO levels observed in groundwater around Georgetown Lake are higher than typically observed elsewhere, and likely help create DO refuges for the fish during the winter months. In general, DO was a little more elevated where there were significant groundwater inflows, but a full vertical profile of DO would be appropriate to determine the shape of the chemocline. The state's 6 mg/L criteria for cold water fisheries were often exceeded in these Lake samples taken near the bottom.

The connection between elevated DO, N and S species in an oxidized state and groundwater inflows is an interesting part of this study. There appears to be a direct correlation between groundwater inflows and elevated DO in the Lake during the late winter months just prior to ice off. The locations where N and S species are reduced $\text{NH}_3/\text{NH}_4^+$ -N and H_2S -S sometimes have concentrations far exceeding the maximum contaminant levels (MCL). This occurs in the poorly oxygenated locations of the Lake where there were no groundwater inflows detected. These findings suggest that groundwater play an important role in supplying DO to the Lake during the winter months when the Lake is closed to the atmosphere.

Alkalinity was elevated in groundwater in comparison to the Lake (Figure 13). There appears to be no correlation between groundwater and Lake alkalinity.

Potential Impacts on Lake Water Quality

Although there appears to be little connection between nutrient concentrations in the Lake and groundwater discharge of nutrients, we can use our current understanding of groundwater inflows to the Lake to generate locations where groundwater quality may need to be more carefully considered. Protection of Georgetown Lake water quality may be prioritized by identification of groundwater inflow locations to the Lake. These results show that we have not identified any major groundwater sources of nutrients to the Lake except perhaps SO_4^{2-} and a little NO_3^- -N, but there were no exceedances of the MCLs in groundwater and springs. Furthermore, nutrient concentrations were not uniform or concentrated within one region of the watershed. However, because groundwater seems to enter the Lake on the east and southeastern shores, it is especially important to prevent groundwater up gradient of this region from getting contaminated from septic systems or other potential sources. For example, groundwater wells and septic systems installed on the east side of the Georgetown Thrust Fault pose a greater risk for providing a nutrient source, or interfering with water resources that would normally discharge to the Lake.

Our results cannot be interpreted as a complete absence of groundwater flow to the western/northern region of the Lake. We simply have not identified any discharge locations along this region. Regardless of the regional geology and groundwater flow paths, there can still be isolated shallow flow paths discharging to the Lake along the west side. Although the bedrock bedding planes dip to the west, there could be isolated fractures connected to the lake (often times perpendicular to bedding planes in several directions) that may periodically fill up and flow towards the lake during wet periods of the year. There could also be shallow soil through flow in some of the drainage patterns that could result in temporary subsurface flow paths to the Lake during storm event and snowmelt (our study was conducted prior to snowmelt). In addition, the low nutrient concentrations in groundwater and lack of correlation between groundwater inflows and negatively impacted water quality does not translate to an absence of seepage from septic systems. We suspect that diffusion of nutrients may play an important role in controlling the nutrient dynamics in the lake.

More groundwater investigations need to be conducted to fully understand water flow pathways, the potential for nutrient transport to the Lake, and for identifying critical DO refuges for the fish during the winter months. Establishing an accurate water table elevation around the basin would provide much needed information about the nature of groundwater flow to and perhaps from the Lake. For example, sample GW 15 shows groundwater quality and isotope concentrations which were very similar to average Georgetown Lake water chemistry. This suggests that the Lake may be losing water along portions of the Lake that are west of the Georgetown Thrust Fault. A better understanding of groundwater flow paths would also help refine nutrient risk assessment and also locate areas in the Lake which are critical for fish during the late winter period of oxygen stress.

PRODUCTS AND OUTREACH

The following list summarizes reports, theses, incoming graduate students, presentations and posters that resulted or are pending from this project.

Papers, Theses and Reports

1. Shaw, Glenn, and Elizabeth White, (2013) Characterizing groundwater-lake interactions and its impact on lake water quality, *Journal of Hydrology*, 492, 69-78.
2. Shaw, Glenn, and Elizabeth White, (2013) Nutrients and Groundwater-Lake Interactions at Georgetown Lake, MT, *Montana Department of Environmental Quality Report*, pp. 30., (In Review).
3. White, Elizabeth, (2012) Using Naturally Occurring Geochemical Tracers to Track Groundwater-Lake Interactions at Georgetown Lake, Granite County, Montana, M.S. Thesis, Montana Tech of the University of Montana, Butte, Montana, pp 89.

Presentations and Seminars

1. Clint Barkell, Jessica Scanlan, Heidi Reid, and Linda Bone, (2013) Groundwater Inflows and Water Quality of Georgetown Lake, *Montana Tech Undergraduate Research Fair, Techxspo*, Butte, Montana, April 2013.
2. Shaw, Glenn (2012) Groundwater-Lake Interactions at Georgetown Lake, Montana. BYU Idaho Geology Department Seminar, Rexburg Idaho, September 2012.
3. Shaw, Glenn, and E. White, (2012) Using ^{222}Rn , Water Isotopes and Major Ions to Investigate a Large Alpine Through-Flow lake, *Goldschmidt Spring Meeting*, Montreal, Canada, June 26, 2012.
4. Bramlett, E., and G. Shaw, (2011) Using geochemical tracers to trace groundwater interactions with Georgetown Lake, Granite County, Montana, *American Water Resources fall meeting poster*, October 2011, Great Falls, MT.
5. Malsom, Jacob, and Robyn Fisher, (2011) Groundwater/Lake Interactions at Georgetown Lake, MT. Presentation at the Montana Tech Undergraduate Research Fair.

Outreach

6. Shaw, Glenn, and Elizabeth White, (2011) Source Water and Water Quality of Stewart Mill Spring. Personal Report to Ms. Diana Neely (Home Owner who provided access to a large spring discharging to Georgetown Lake).
7. Shaw, Glenn, (2011) Groundwater and Surface Water at Georgetown Lake, MT. Presentation at the Georgetown Lake Homeowners Association.

Student Involvement

Graduate Researchers

Elizabeth Bramlett White (January 2011-May 2012), M.S. student geoscience with a hydrogeology option at Montana Tech. Elizabeth came to Montana Tech in January 2011 and completed her M.S. degree in three semesters. She was funded by the Alfred Sloan Foundation on a Native American Sloan Scholarship. Elizabeth was the first graduate student and primary researcher on this project. She received a B.S. in Geology from the University of Wyoming in 2010, and an M.S. in Geoscience with a hydrogeology option at Montana Tech in 2012.

Katie Mitchell (August 2012-Present), M.S. student in geoscience with a hydrogeology option at Montana Tech. Katie began graduate studies at Montana Tech in Geoscience with a Hydrogeology option in August 2012. She graduated with a B.S. in Geology and a B.S. in Public Administration in December 2011 from Stephen F. Austin State University-Nacogdoches, TX. Katie served in the Army National Guard from 2002 to 2008 and earned the rank of Sgt. She was deployed in Iraq from 2003 to 2005. She has an anticipated graduation date of May 2014 .

Undergraduate Researchers

Each of these students were Involved with field and laboratory analyses. They were all freshman at Montana Tech and paid stipends by the Montana Tech Undergraduate Research Program. They were part of the “Research Assistant Mentorship Program” designed to involve students in research early in their undergraduate programs.

<u>Name</u>	<u>Dates Worked</u>	<u>Major</u>
Jacob Malsom	January 2011-May 2011	Geological Engineering.
Robyn Fisher	January 2011-May 2011	Geological Engineering.
Jessica Scanlan	January 2013-May 2013	Geological Engineering
Clinton Barkell	January 2013-May 2013	Geological Engineering
Linda Bone	January 2013-May 2013	Geological Engineering
Heidi Reid	January 2013-May 2013	Mechanical Engineering

CONCLUSIONS

The use of ^{222}Rn as a groundwater tracer combined with the physical geology was useful in developing a conceptual model for how groundwater interacts with a high elevation Lake in geologically complex terrain. Groundwater inflows were spatially mapped, and groundwater appears to discharge into the Lake primarily along the southeastern and eastern shoreline to the east of the Georgetown Thrust Fault. The westward dipping bedrock suggests that the western portion of the Lake may discharge to groundwater, but groundwater inflow and outflow rates cannot be quantified without additional information. Groundwater clearly influences the water chemistry and nutrient dynamics within the Lake during winter months, and this has substantial implications for aquatic life including the fishery resource. Where groundwater enters the Lake a less reducing relatively well-oxygenated environment exists, as illustrated by lower H_2S -S and $\text{NH}_3/\text{NH}_4^+$ -N concentrations in these zones. Based on data collected in this study and previous work, the majority of water in Georgetown Lake has DO concentrations that are suboxic to anoxic by late winter. Therefore, groundwater flows are critical in providing DO refuge zones within the Lake where fish and other aquatic species may thrive during the late winter and early spring months prior to ice-off in the Lake. Without the groundwater refuges, aquatic life would have little respite from the low oxygen and associated accumulation of toxic, reduced substances such as H_2S -S and $\text{NH}_3/\text{NH}_4^+$ -N.

Our conceptual understanding of groundwater flow to the Lake may help in determining locations where groundwater may act as a conduit to bring septic and other pollution into the Lake. Although we did not see overt evidence of nutrient loading on the Lake from groundwater sources in winter, wastewater impacts to groundwater flowing to the Lake could be more substantial during summer when usage of shoreline residences is higher.

In general, this study shows the importance of groundwater - surface water interactions in understanding and managing freshwater resources. In particular, the findings highlight the importance of spatial variations in water quality under ice cover in a lentic system, influence of groundwater in generating this variation, and how understanding groundwater flow paths can be useful for assessing the pollution risk to the receiving water body.

REFERENCES

Amman, D., 2011. *Georgetown Lake Homeowners Association*. Retrieved from Flint Creek Dam Advisory Committee Update: April 14, 2011:

www.georgetownlakehomeowners.com/files/86711303233131SnoPackApril11-2011Sum.pdf

Barr, A.D., Turner, J.V., Townley, L.R., 2000. WSiBal: a coupled water, conservative solute and environmental isotope mass balance model for lakes and other surface water bodies. *IHAS Publication (International Association of Hydrological Sciences)*. 262, 539-544.

Cey, B.D., G. B. Hudson, J. E. Moran, and B. R. Scanlan, 2008, Impact of artificial recharge on dissolved noble gases in groundwater in California, *Environmental Science and Technology*, 42 (4), 1017-1023.

Cherkauer, D.S., Nader, D.C., 1989. Distribution of groundwater seepage to large surface -water bodies- the effect of hydraulic heterogeneities. *Journal of Hydrology*. 109, 151-165.

Cook, P. G., Wood, C., White, T., Simmons, C.T., Fass, T., Brunner, P., 2008. Groundwater inflow to a shallow, poorly -mixed wetland estimated from a mass balance of radon. *Journal of Hydrology*. 354, 213-226.

Fetter, C. W., 2001. *Applied Hydrogeology* 4th Ed. Prentice Hall, Upper Saddle River, NJ. 598 pp.

Freeze, R.A., Cherry, J.A., 1979. *Groundwater*. Prentice Hall, Englewood Cliffs, NJ. 604 pp.

Gammons, C., Pellicori, D., Reed, P., Roesler, A., Petrescu, E., 2006. The hydrogen and oxygen isotopic composition of precipitation, evaporated mine water, and river water in Montana, USA. *Journal of Hydrology*. 328, 319-330.

Garrett, P. A., 1983. *Relationships Between Benthic Communities, Land Use, Chemical Dynamics, and Trophic State in Georgetown Lake*. Ph.D. Dissertation, Montana State University. 149 pp.

Genereux, D.P., Hemond, H.F., Mulholland, P.J., 1993. Use of radon -222 and calcium as tracers in a three-end-member mixing model for stream flow generation on the west fork of Walker Branch watershed. *Journal of Hydrology*. 142, 167-211.

Hagerthey, S.E., Kerfoot, W.C., 1998. Groundwater flow influences the biomass and nutrient ratios of epibenthic algae in a north temperate seepage lake. *Limnology and Oceanography*. 43, 1227-1242.

Henne, W., 2011. *Using Chemical and Isotopic Tracers to Track Biogeochemical Processes Under Ice Cover at Georgetown Lake, Montana*. M.S. Thesis, Montana Tech of the University of Montana. 81 pp.

Knight, J.C., 1981. An Investigation of the General Limnology of Georgetown Lake, Montana. Ph.D. Dissertation, Montana State University. 139 pp.

Lonn, J.D., McDonald, C., Lewis, R.S., Kalakay, T.J., O'Neill, J.M., Berg, R.B., Hargrave, P., 2003. Preliminary Geologic Map of the Philipsburg 30' x 60' Quadrangle. Western Montana. *Montana Bureau of Mines and Geology*.

Loveless, A.M., Oldham, C.E., Hancock, G.J., 2008. Radium isotopes reveal seasonal groundwater inputs to Cockburn Sound, a marine embayment in Western Australia. *Journal of Hydrology*. 351, 203-217.

Maloszewski, P. W., Zuber, A., 1982. Determining the turnover time of groundwater systems with the aid of environmental tracers. 1. models and their applicability. *Journal of Hydrology*. 57, 207-231.

Maloszewski, P, Rauert, W., Stichler, W., Herrmann, A., 1983. Application of flow models in an alpine catchment area using tritium and deuterium data. *Journal of Hydrology*. 66, 319-330.

Mattle, N., Kinzelbach, W., Beyerle, U., Huggenberger, P., Loosli, H.H., 2001. Exploring an aquifer system by integrating hydraulic, hydrogeologic and environmental tracer data in a three-dimensional hydrodynamic transport model. *Journal of Hydrology*. 242, 183-196.

Missouliau, 2010. Crowd details wildlife, water concerns in meeting on Georgetown Lake subdivision. http://missouliau.com/news/state-and-regional/article_3a0cabac-113d-11df-b362-001cc4c002e0.html.

Owor, M., Taylor, R., Mukwaya, C., Tindimugaya, C., 2011. Groundwater/surface-water interactions on deeply weathered surfaces of low relief: evidence from Lake Victoria and Kyoga, Uganda. *Hydrogeology Journal*. 19, 1403-1420.

Shaw, G. D., E. S. White, and C. Gammons, 2013, Characterizing groundwater-lake interactions and its impact on lake water quality, *Journal of Hydrology*, 492, 69-78.

Trabert, M. J., 1993, The Depletion of Oxygen in Georgetown Lake, Montana During Winter Months, M.S. Thesis, Montana College of Mineral Science and Technology, Butte, MT., 52 pp.

U.S. Environmental Protection Agency, Environmental Management Report, 1983. Region 8, EPA-908/9-83-001. Denver Colorado.

Western Regional Climate Center, 2011. Retrieved from Precipitation Maps for Western United States: www.wrcc.dri.edu/pcpn/mt.gif.

FIGURES AND TABLES

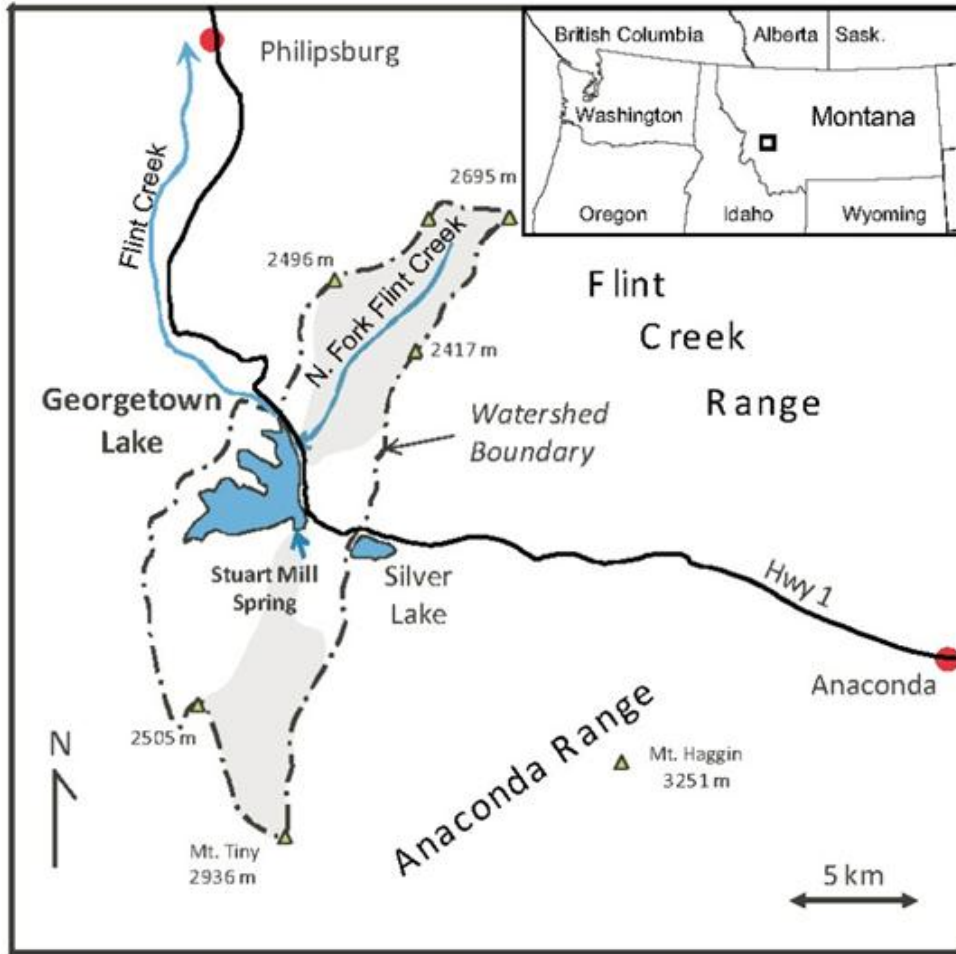


Figure 1: Map of the Georgetown Reservoir area relative to the state of Montana (from Shaw et al., 2013).

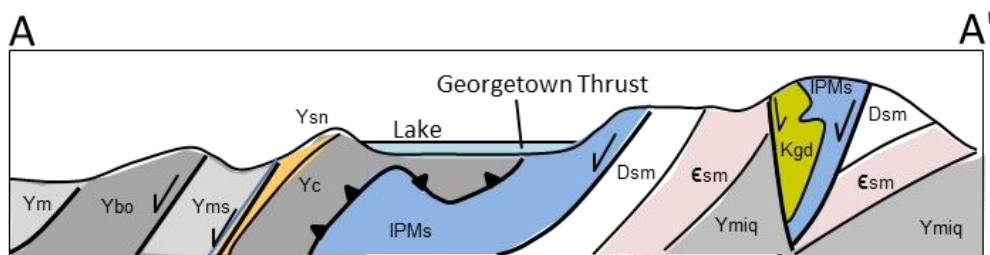
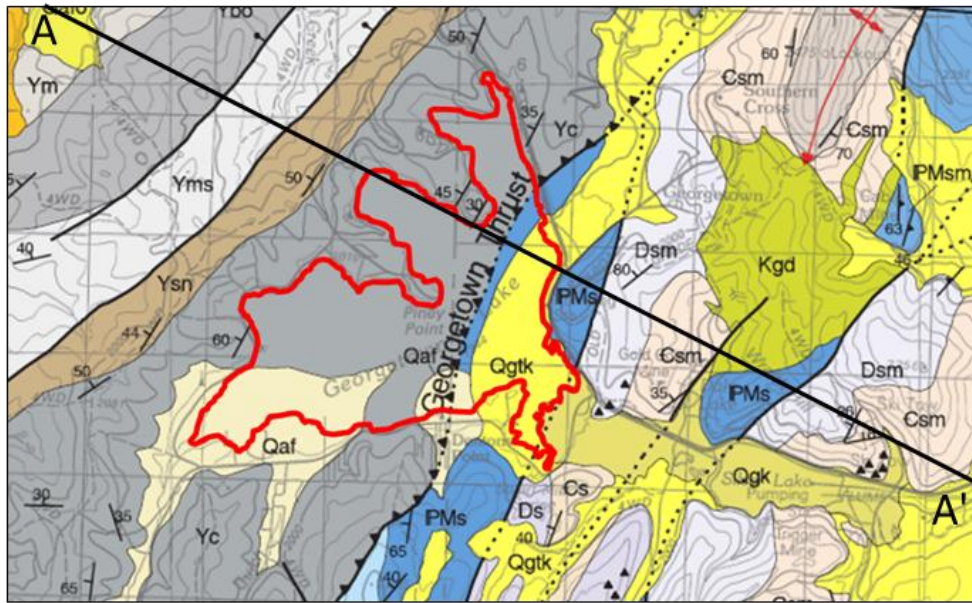


Figure 2: Geologic map (top, Lonn et al., 2003) and schematic cross-section for the region surrounding Georgetown Reservoir. Key to rock ages: Y = Proterozoic; ϵ = Cambrian; D = Devonian; IPM = Pennsylvanian and Mississippian (includes Madison Limestone); K = Cretaceous; Q = Quaternary. Quaternary units are omitted from the cross section (from Shaw et al., 2013).

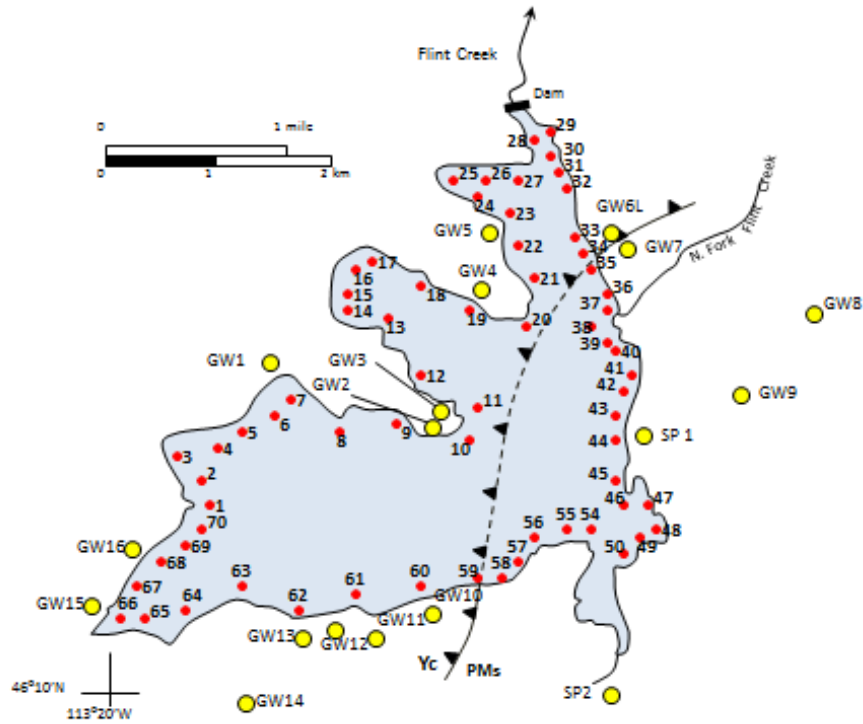


Figure 3: Lake (red circles) and groundwater/spring (yellow circles) sampling locations. The number by the sampling point represents the sample location ID..

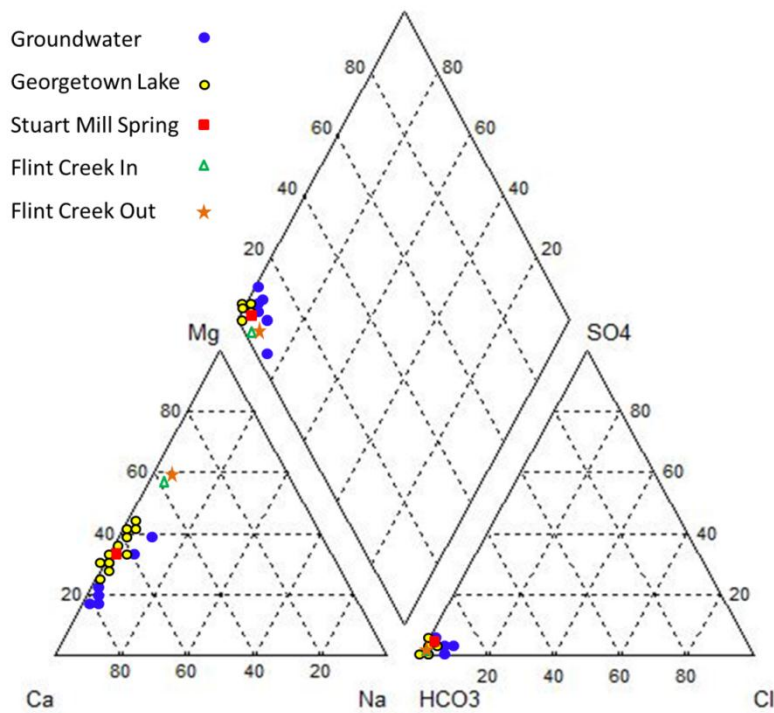


Figure 4: Piper diagram illustrating the water chemistry of Georgetown Reservoir (light circles), groundwater (dark circles), Stuart Mill Spring (square), Flint Creek inflow (open triangle), and Flint Creek outflow (star) (from Shaw et al., 2013).

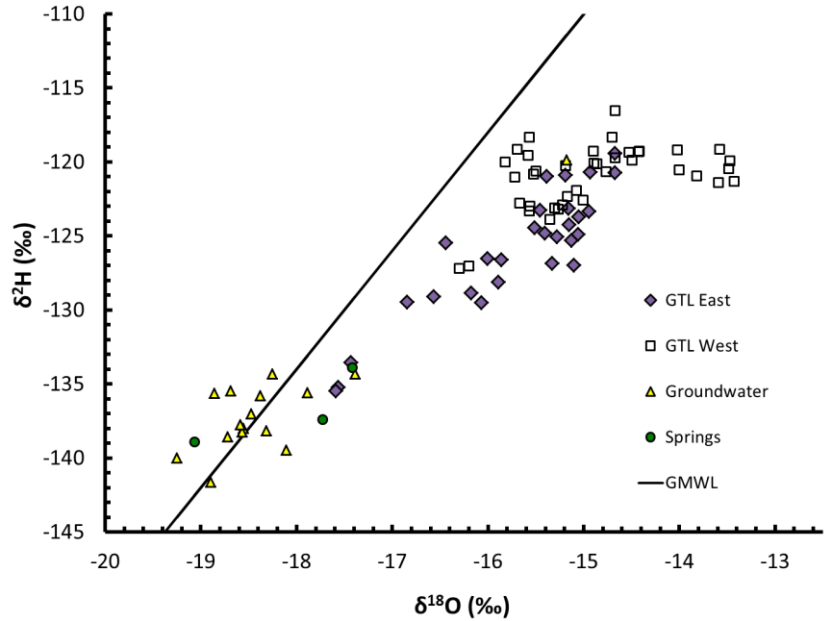


Figure 5: Stable isotopes in Georgetown Reservoir and nearby groundwater (triangles) and springs (circles). GTL East (diamonds) and GTL West (open squares) represent lake samples that were collected on the east and west sides of Georgetown Reservoir respectively. The Global Meteoric Water Line (GMWL) and a local evaporation line (LEL) are also labeled on the figure (from Shaw et al., 2013).

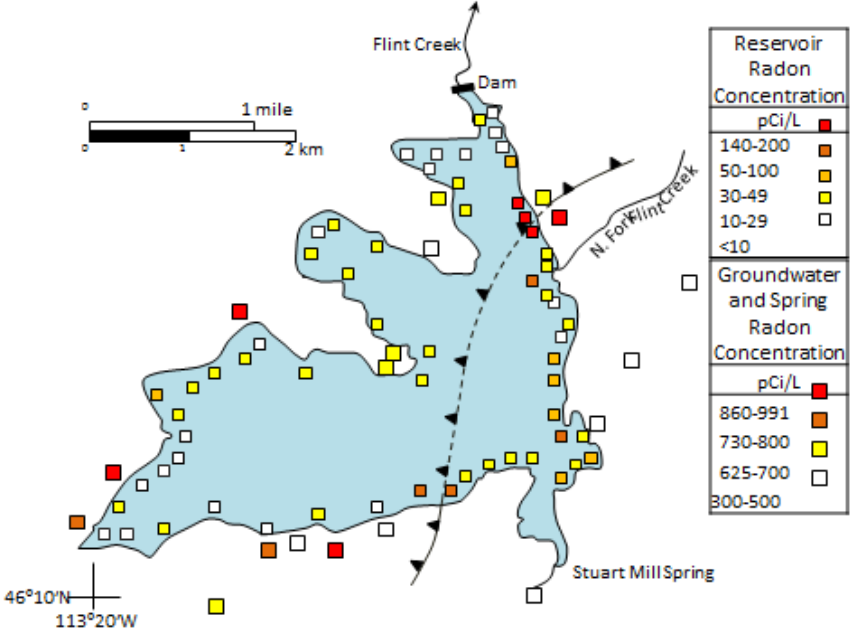


Figure 6: Spatial distribution of ^{222}Rn activity in Georgetown Reservoir and surrounding groundwater (from Shaw et al., 2013).

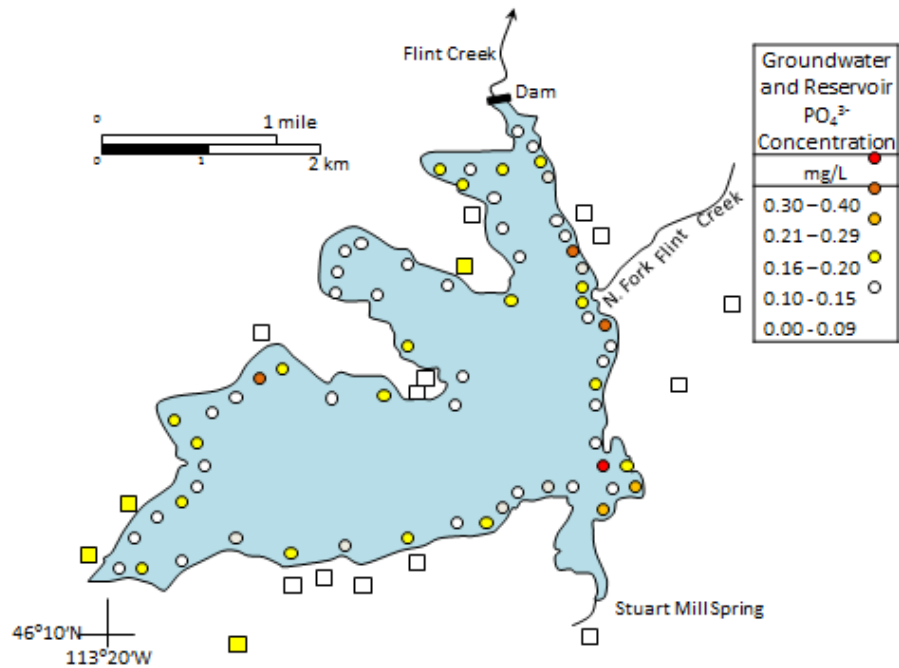


Figure 7: Spatial distribution of PO₄³⁻ concentrations in Georgetown Reservoir and surrounding groundwater (modified from Shaw et al., 2013).

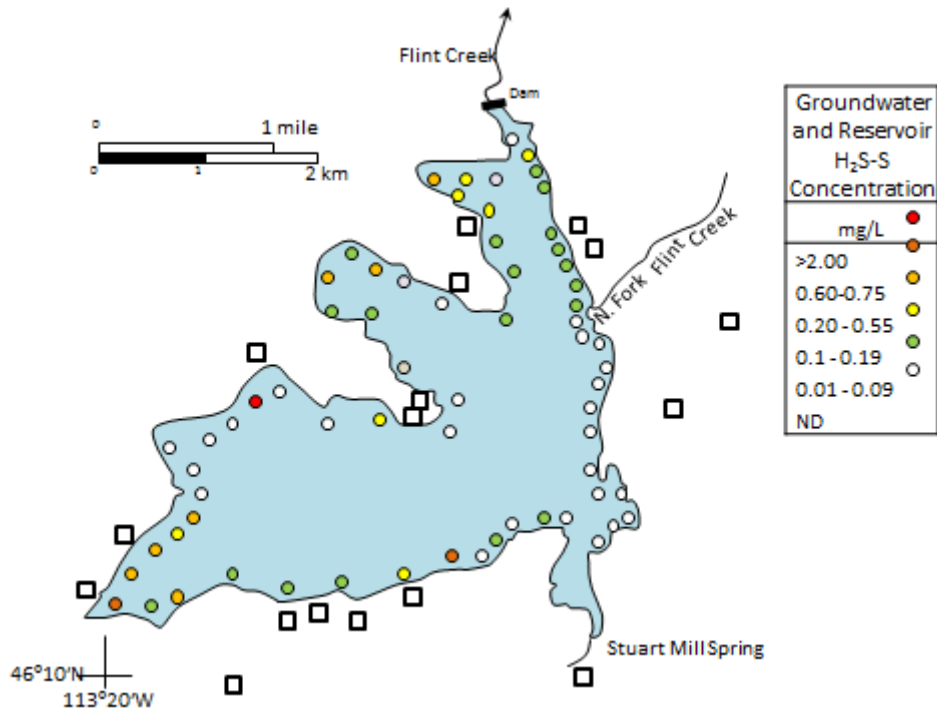


Figure 8: Spatial distribution of H₂S-S concentrations in Georgetown Reservoir and surrounding groundwater (modified from Shaw et al., 2013).

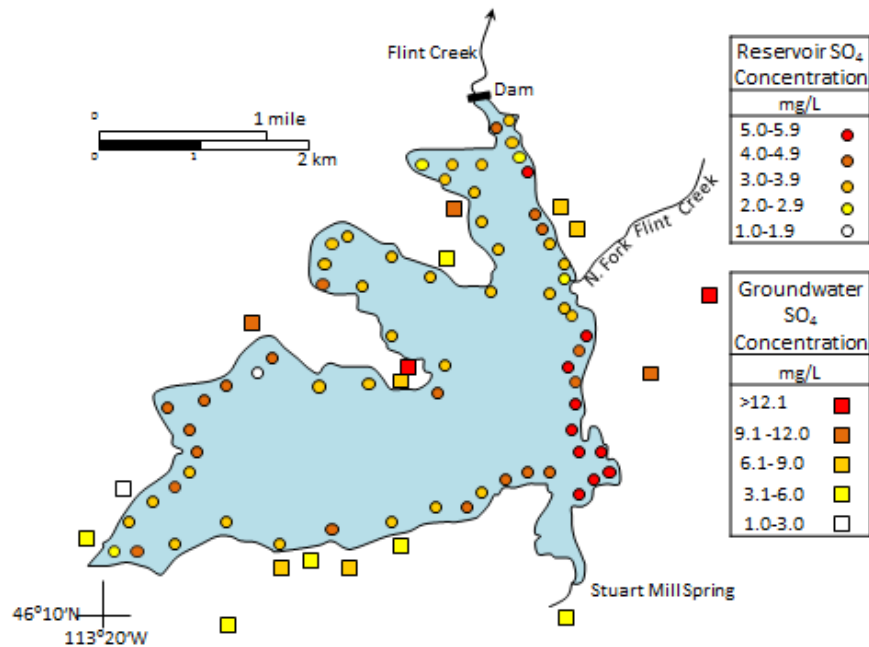


Figure 9: Spatial distribution of SO_4^{2-} concentrations in Georgetown Reservoir and surrounding groundwater (modified from Shaw et al., 2013).

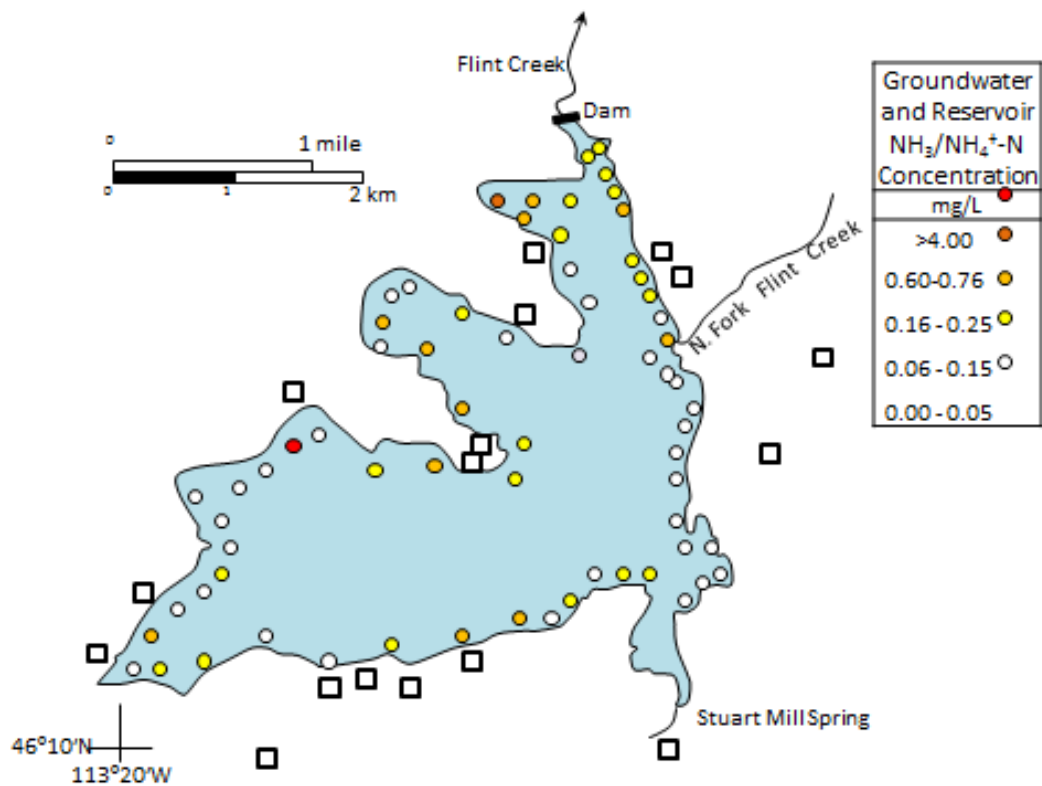


Figure 10: Spatial distribution of $\text{NH}_3/\text{NH}_4^+-\text{N}$ concentrations in Georgetown Reservoir and surrounding groundwater (modified from Shaw et al., 2013).

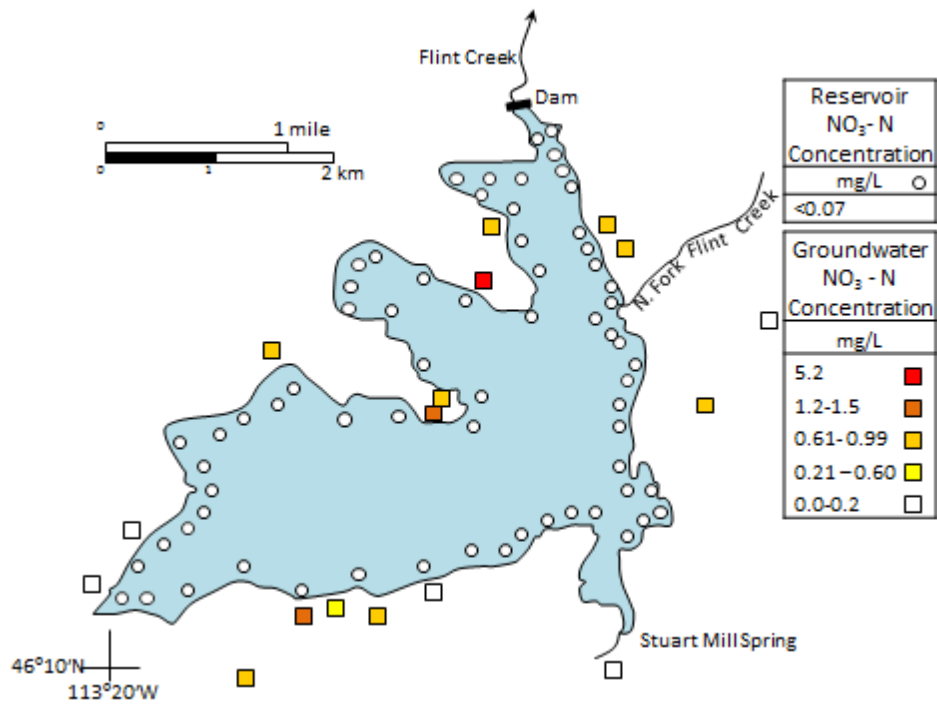


Figure 11: Spatial distribution of NO₃⁻-N concentrations in Georgetown Reservoir and surrounding groundwater.

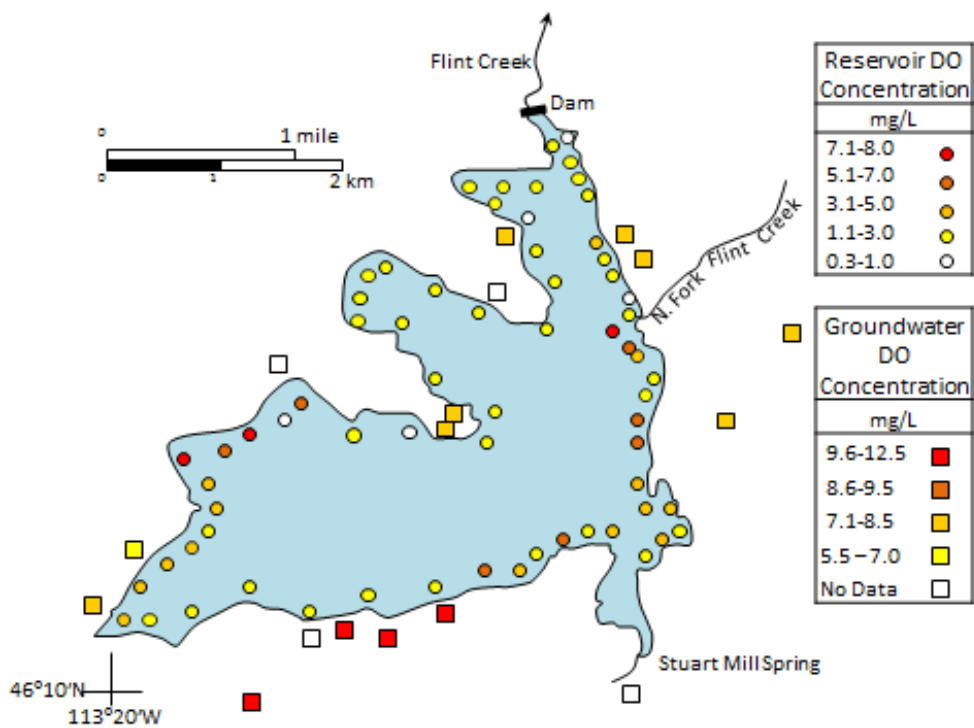


Figure 12: Spatial distribution of DO concentrations in Georgetown Reservoir and surrounding groundwater

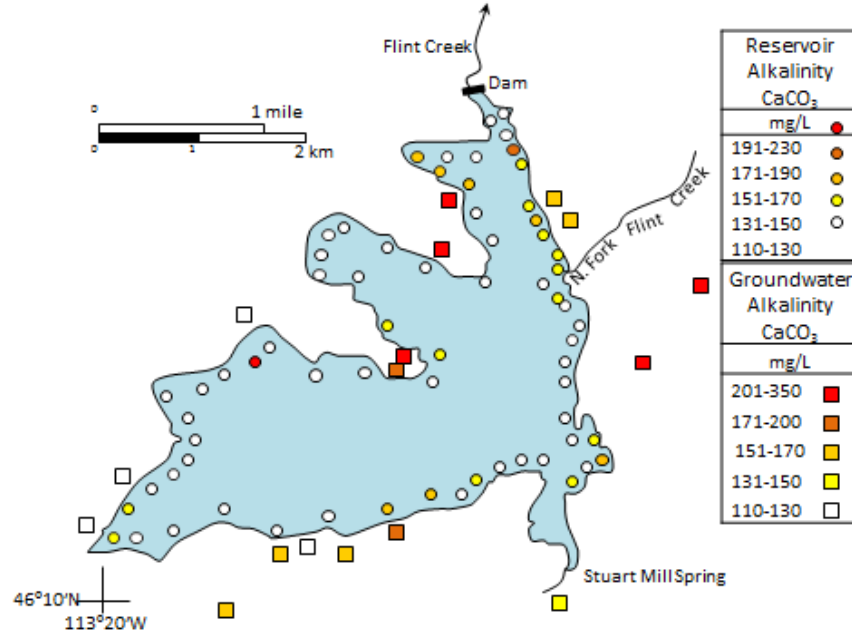


Figure 13: Spatial distribution of alkalinity concentrations in Georgetown Reservoir and surrounding groundwater.

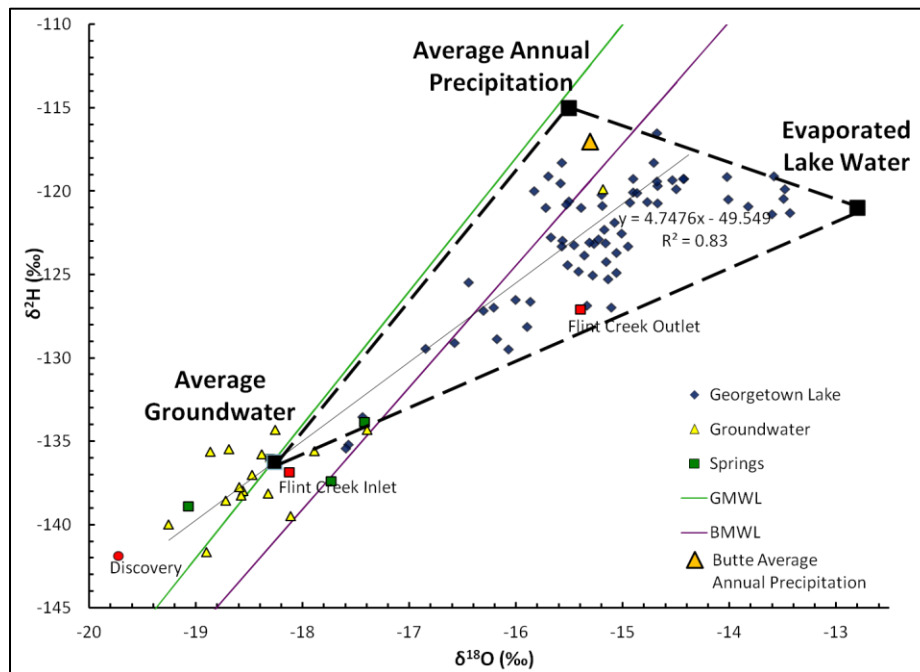


Figure 14: End Member Mixing Analysis. Three sources are identified: average groundwater, average annual precipitation and evaporated lake water.

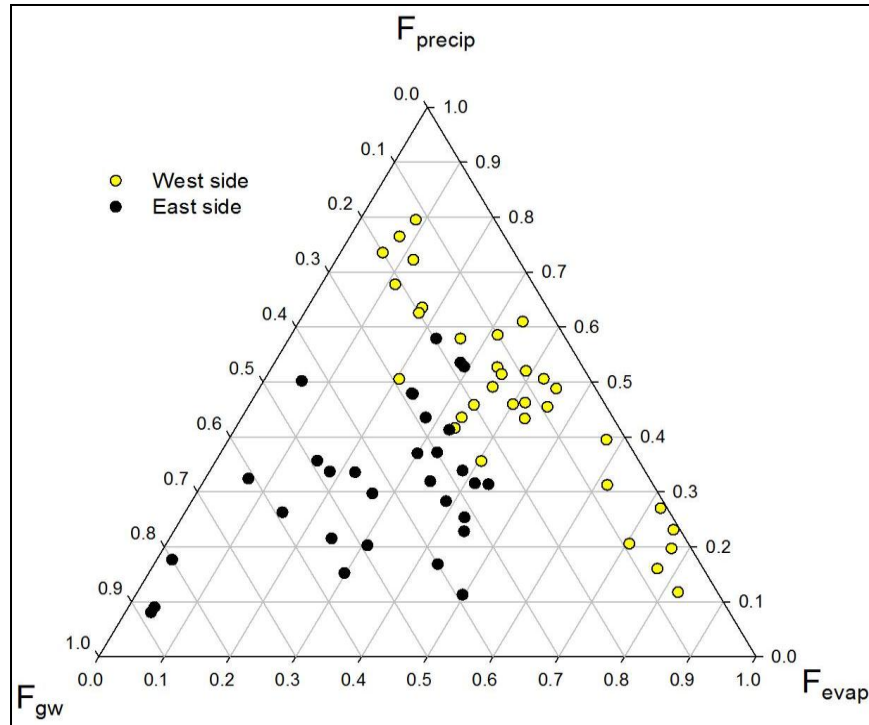


Figure 15: Ternary Plot showing origin of lake water three end members (groundwater, precipitation, and evaporated lake water).

Table 1: Analytical detection limits for major ions and nutrients

Parameter	Detection Limit (mg/L)
Ca ²⁺	0.10
Mg ²⁺	0.10
Na ⁺	0.50
K ⁺	0.50
F ⁻	0.05
Cl ⁻	0.30
SO ₄ ²⁻	0.60
H ₂ S-S	Human smell
NO ₂ ⁻ N	0.10
NO ₃ ⁻ N	0.07
NH ₃ /NH ₄ ⁺ -N	0.01
PO ₄ ³⁻	0.03

Note: H₂S-S and NH₃/NH₄⁺-N had upper limits of 2.00 and 4.00 mg/L respectively.

Table 2: Georgetown Reservoir Water Quality

Georgetown Reservoir Water Quality					
	Maximum	Minimum	Average	Median	Standard Deviation
pH	9.89	6.17	7.47	7.44	0.67
DO (mg/L)	8.25	0.38	2.95	2.45	1.87
SC (µS/cm)	418	208.1	240	234.6	30.3
Temp (°C)	4.84	0.00	1.67	1.56	0.88

Table 3: Groundwater and spring sampling dates and times and well information.

ID	Date	Time	Well Depth (ft)	DTW
GW1	8/16/2011	19:00	19	4.6
GW2	9/5/2011		150+	21.8
GW3	9/4/2011		46	
GW4	8/16/2011	17:10	142	28.9
GW5	7/29/2011	17:15	120	8.6
GW6	7/29/2011	15:15	40	17.0
GW7	7/29/2011	13:50	60	9.0
GW8	9/4/2011	0.72	80	
GW9	9/4/2011	0.54	220	
GW10	9/5/2011	0.52		
GW11	7/28/2011	13:00	60	3.0
GW12	8/16/2011	12:45	75	5.7
GW13	8/16/2011	15:00	89	locked
GW14	8/17/2011	13:00	120	56.6
GW15	9/5/2011		170	
GW16	9/5/2011		320	
SP2				spring
SP2	7/28/2011	14:00		spring
SP1	6/6/2011	16:10		spring

Table 4: Groundwater and spring field water quality parameters.

ID	pH	DO(mg/L)	DO %	SC (μ S/cm)	Temp ($^{\circ}$ C)
GW1				276.0	7.6
GW2	6.96	7.62	80.1	362.4	8.1
GW3	6.65	8.06	84.4	441.2	7.7
GW4				553.0	7.0
GW5	6.80	7.42		412.0	6.1
GW6	7.02	7.30		323.0	7.4
GW7	6.77	7.90		326.0	6.8
GW8	6.92	7.61	75.8	315.6	6.0
GW9	6.64	7.57	75.6	402.5	6.2
GW10	6.92	10.60	108.1	323.7	6.8
GW11	7.13	9.85		324.0	5.1
GW12	7.30	10.34	119.6	156.3	10.8
GW13				314.0	8.2
GW14	6.88	12.15	122.5	321.6	4.8
GW15	6.39	8.13	88.9	166.7	9.8
GW16	6.44	5.51	57.6	193.8	6.7
SP2					
SP2	7.14	8.94		262.0	7.8
SP1	7.77	6.29	66.5	282.9	7.8

Table 5: Groundwater and spring major cation concentrations.

ID	NH ₃ -N (mg/L)	Na (mg/L)	K (mg/L)	Ca (mg/L)	Mg (mg/L)	Fe (mg/L)	Mn (mg/L)	Si (mg/L)	Sr (mg/L)
GW1	0.01	2.12	0.57	38.52	11.58	0.01067	0.00047	6.78	0.048
GW2	0.01	3.35	1.09	46.43	18.92	0.01326	0.00197	5.60	0.075
GW3	0.00	1.81	0.83	82.53	9.944	0.00204	0.00038	4.54	0.050
GW4	0.00	2.59	1.04	63.83	29.69	0.00169	0.00022	5.72	0.077
GW5	0.01	2.41	0.61	64.62	12.58	0.00028	0.00058	4.74	0.047
GW6	0.01	1.65	1.10	44.57	13.96	0.00336	0.00098	4.90	0.045
GW7	0.00	3.02	1.03	44.5	12.00	0.00144	0.00082	5.21	0.042
GW8	0.00	2.40	1.21	49.46	12.71	0.00050	0.00061	7.23	0.063
GW9	0.02	1.90	1.59	60.87	17.72	0.00121	0.00051	6.42	0.058
GW10	0.00	1.13	0.94	49.41	14.4	0.00587	0.00151	4.31	0.095
GW11	0.01	1.67	0.66	54.3	9.22	0.00221	0.00014	4.90	0.047
GW12	0.00	1.83	0.19	45.69	5.32	0.00389	0.00102	5.40	0.056
GW13	0.00	1.77	0.59	51.51	7.81	0.00056	0.00027	5.05	0.045
GW14	0.00	1.65	1.31	58.84	8.88	0.00208	0.00005	5.94	0.050
GW15	0.01	2.54	0.71	21.58	8.25	0.00004	0.00093	8.95	0.072
GW16	0.00	6.71	1.27	20.95	10.14	0.11080	0.03587	10.88	0.053
SP2	0.02	0.89	1.37	45.16	13.87	0.01341	0.00204	3.78	0.044
SP2	0.01	0.86	1.48	36.85	11.71	0.00225	0.00023	3.83	0.042
SP1	0.01	1.73	1.42	42.24	12.96	0.01003	0.00162	4.87	0.062

Table 6: Groundwater and spring major anion concentrations.

ID	Alkalinity (mg/L)	PO ₄ ³⁻ (mg/L)	NO ₂ ⁻ N (mg/L)	F ⁻ (mg/L)	Cl ⁻ (mg/L)	NO ₃ ⁻ N (mg/L)	SO ₄ ²⁻ (mg/L)
GW1	124	0.05	0.001	<0.05	2.2	0.78	11.9
GW2	194	0.04	0.002	0.093	2.1	1.5	8.6
GW3	229	0.05	0.001	<0.05	2.8	0.52	22.3
GW4	240	0.1	0.001	0.52	<0.3	5.2	5.7
GW5	200	0.05	0.001	<0.05	5.1	0.93	12.0
GW6	166	0.06	0	0.068	1.6	0.74	8.0
GW7	165	0.04	0	0.061	5.6	0.73	6.9
GW8	351	0.09	0.000	<0.05	0.90	0.13	13.9
GW9	221	0.07	0.000	<0.05	3.0	0.71	11.0
GW10	178	0.09	0.002	<0.05	0.66	0.16	4.6
GW11	166	0.04	0	0.052	2.0	0.61	6.6
GW12	125	0.06	0.001	0.13	1.3	0.27	3.2
GW13	168	0.09	0.003	0.064	5.5	1.2	8.1
GW14	168	0.1	0	<0.05	1.6	0.70	3.7
GW15	88	0.14	0.000	0.080	0.99	0.12	3.8
GW16	110	0.11	0.002	0.24	1.3	<0.07	1.1
SP2	160	0.05	0.002	<0.05	0.48	0.077	4.9
SP2	130	0.05	0.001	<0.05	0.36	<0.07	5.3
SP1		0.07	0.000	<0.05	1.5	0.21	8.6

Table 7: Groundwater and spring radon and isotope concentrations.

ID	Radon (pCi/L)	δD (‰)	δD (‰)
GW1	791.0	-139	-18.1
GW2	640.0	-139	-18.7
GW3	658.3	-135	-18.7
GW4	596.3	-134	-17.4
GW5	661	-134	-18.3
GW6	624.3	-137	-18.5
GW7	730.7	-138	-18.6
GW8	145.8	-136	-18.9
GW9	294.0	-136	-18.4
GW10	387.4	-140	-19.3
GW11	990.4	-138	-18.6
GW12	743.6	-142	-18.9
GW13	441.6	-138	-18.6
GW14	651.4	-136	-17.9
GW15	729.1	-120	-15.2
GW16	869.3	-138	-18.3
SP2		-137	-17.7
SP2	188.1	-139	-19.1
SP1	228.4	-134	-17.4

Table 8: Parameters used in Radon mass balance and Sensitivity Analysis

	March & April	Sensitivity on Model
Q_{SI}	$2.87 \times 10^6 \text{ ft}^3/\text{day}$	High
Q_{SO}	$2.16 \times 10^6 \text{ ft}^3/\text{day}$	High
V	$2.8 \times 10^9 \text{ ft}^3$	High
A	$1.31 \times 10^8 \text{ ft}^2$	
Storage	$3.36 \times 10^5 \text{ ft}^3/\text{day}$	Low
P	0	Low
E	0	Low
λ	0.18 day^{-1}	
C_{gwi}	449.7 pCi/L	High
C_{gwo}	24.7 pCi/L	High
C_{SO}	6.51 pCi/L	High
C_{SI}	10.2 pCi/L	High
C_L	24.7 pCi/L	High

Table 9: Estimated Groundwater Flux from Mass Balance Methods

	Groundwater Influx (ft^3/day)	Groundwater Outflow (ft^3/day)	Outflow - Influx (ft^3/day)
Radon	2.18×10^7	2.25×10^7	7.13×10^5
Specific Conductivity	1.31×10^6	2.36×10^6	1.04×10^6
Cl^-	9.47×10^5	1.99×10^6	1.04×10^6

Assessing Hydrologic, Hyporheic, and Surface Water Temperature Responses to Stream Restoration

Basic Information

Title:	Assessing Hydrologic, Hyporheic, and Surface Water Temperature Responses to Stream Restoration
Project Number:	2012MT263B
Start Date:	3/1/2012
End Date:	2/28/2014
Funding Source:	104B
Congressional District:	MT01
Research Category:	Climate and Hydrologic Processes
Focus Category:	Hydrology, Groundwater, Surface Water
Descriptors:	None
Principal Investigators:	Geoffrey Poole

Publications

There are no publications.

Project Title: Assessing Hydrologic, Hyporheic, and Surface Water Temperature Responses to Stream Restoration.

Principal investigator: Geoffrey Poole, Department of Land Resources and Environmental Sciences, Montana State University, Bozeman, MT, ph: (406) 994-5564, fax: (406) 994-3933
gpoole@montana.edu

Student: Byron Amerson, Department of Land Resources and Environmental Sciences, Montana State University, Bozeman, MT, (415) 912-8792, byron.amerson@gmail.com

Groundwater and Surface Water Hydrologic and Temperature Monitoring

This research project combines a variety of field and numeric modeling techniques to create a complete picture of the residence time distribution for hyporheic water at the restoration site for both pre- and post- restoration conditions and will document the effects of channel re-alignment on hyporheic exchange (rates, magnitude, and volume), hyporheic flow path lengths, residence time, and ultimately, channel temperature. This research was designed to meet the following three objectives:

1. Quantify ground the rate and magnitude of surface water - groundwater exchange and groundwater residence time both prior to and after restoration actions to assess changes in recharge and discharge between Meacham Creek and its alluvial aquifer (hyporheic exchange).
2. Establish a monitoring network of stream temperature loggers and water level loggers to measure changes in the surface and subsurface water elevation and temperature due to restoration actions.
3. Pilot a new method of stream restoration monitoring that will have broad utility to other restoration efforts in the region.

Actions to meet these objectives to date are presented below.

Actions and Methods to Date

Groundwater Modeling Methods and Preliminary Model Analysis

In late 2010 and early 2011, groundwater hydrology of the baseline and restored channel alluvial aquifers was modeled using the USGS groundwater modeling software MODFLOW (Harbaugh, 2005), where the main input into the aquifer was the water surface elevation of the creek plan form. Surface water elevation was derived from first-return LiDAR for the baseline condition, and under the restored condition it was based on "filling" the design channel pools and the riffle ground elevations. In either case, aquifer thickness was assumed to be 5 m in the valley center, tapering to .5 m at the valley wall using the LiDAR terrain model as the surface. Once the potentiometric flow surface was developed, subsurface flow path lines through the potentiometric flow field were generated by releasing "particles" along the creek using the USGS solute modeling software MODPATH (Pollock, 1994)

Based on the groundwater modeling, we predicted that there would be a substantial shift in groundwater surface elevation, as well as in the pattern and magnitude of exchange between groundwater and surface water in the project reach. Based on these initial hydrologic simulations of the site (Figure 1), we predicted that the residence time distribution of hyporheic water will shift to include a higher number of intermediate duration hyporheic flow paths, but that the magnitude of gross hyporheic exchange may either increase or decrease, depending on the change in hydraulic conductivity (Figure 2).

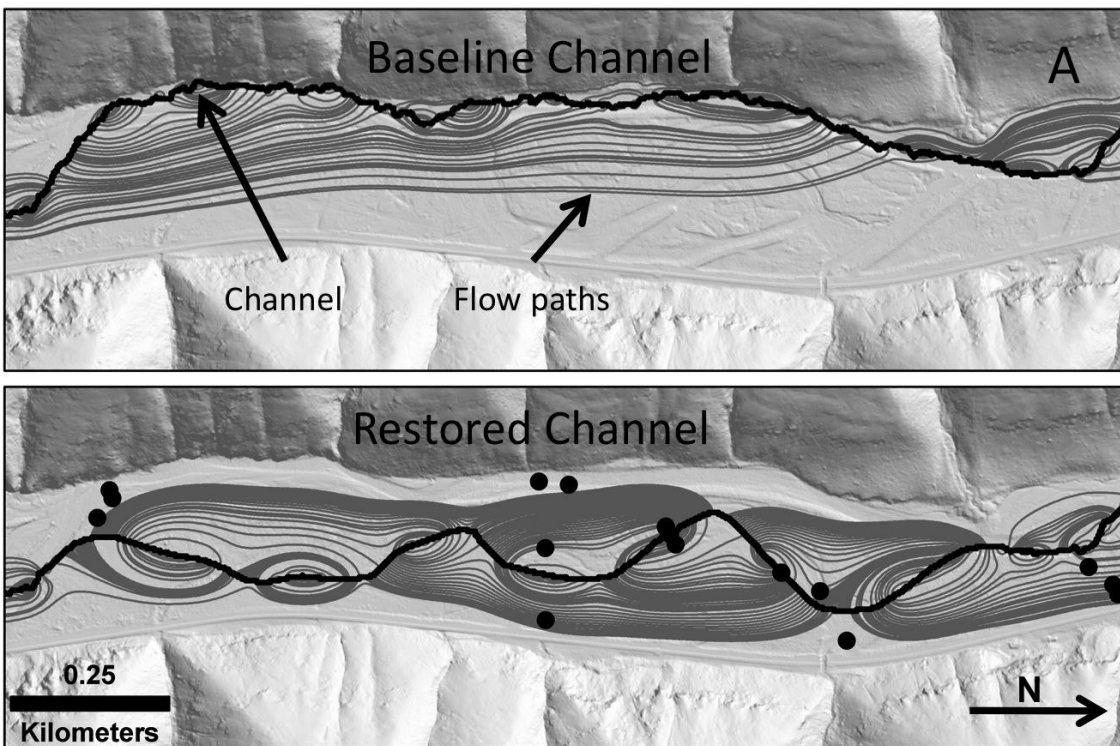


Figure 1. Results from MODFLOW simulation showing expected influence of restoration on hyporheic flow paths (grey lines) on the Meacham Cr. restoration site. Dots show locations of installed monitoring wells in the project site area (This figure is reproduced from the 2011 Seed Grant Proposal).

Groundwater Elevation and Temperature Monitoring

During the spring and summer of 2011 and 2012, a series of 32 monitoring wells were established prior to and during stream restoration activities. In each well a water temperature and level data logger was deployed (Onset HOBO U20 Water Level Data Logger model U20-001-01 [pressure accurate to 0.05% and temperature to 0.1 °C] or Solinst Model 3001 Levellogger Junior Edge [pressure accurate to 0.1% and temperature to 0.1 °C]). Twenty of the well loggers were deployed six weeks before the restoration project began, and another twelve were deployed just prior to diversion of flow to the new channel, and two were install in July 2012. Twenty-two wells remain active, while the

remainder were either accidentally broken or were removed during construction or prior to the onset of seasonal high flows.

Results from the initial MODFLOW simulations with the restored channel planform (Figure 2) were used to select well locations that captured the expected range of hyporheic residence times across the alluvial aquifer. Because daily and seasonal temperature signals are useful tracers of groundwater movement as well as indicators of systematic changes in the temperature status of water as it moves through the hyporheic zone (Arrigoni et al., 2008; Hoehn & Cirpka, 2006; Stonestrom & Constantz, 2003), it is expected changes in the patterns of water temperature across this well network that reflect the restructuring of hyporheic hydrology within the alluvial aquifer.

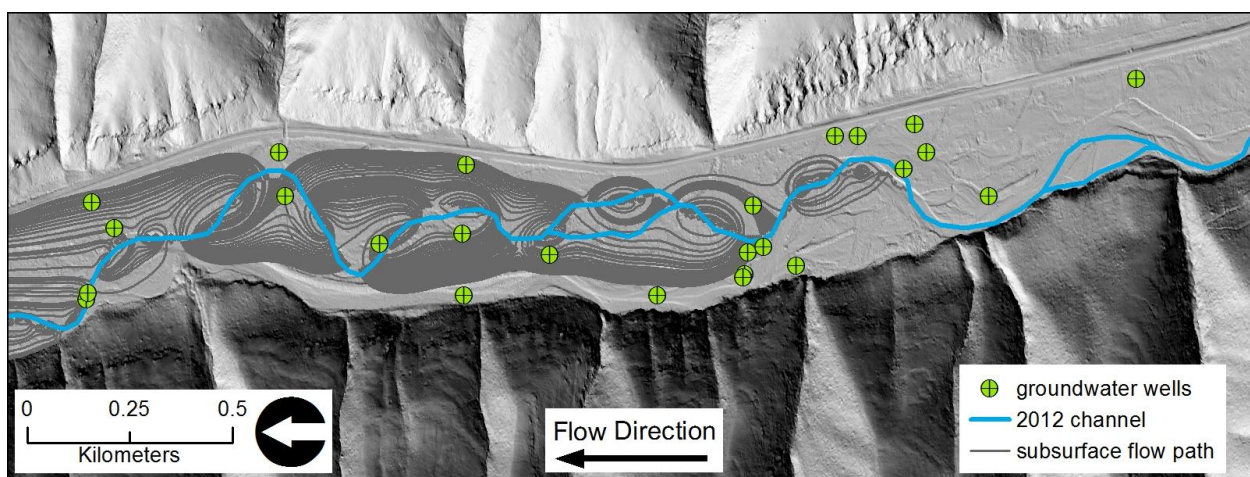


Figure 2. The location of groundwater monitoring wells in juxtaposition to modeled groundwater flow paths of the restored channel at the Meacham Creek Restoration site in 2012.

Surface Water Temperature Monitoring

In 2011 thirty temperature loggers were deployed in surface water features along the restored stream channel prior to diversion of flow into it (Onset HOBO Pendant Temperature/Light Data Logger model 64K - UA-002-64 (accurate to 0.53 °C), or Maxim Dallas iButton model DS1922L (accurate to 0.5 °C) encased in waterproof resin (sold as iBcod by Alpha Mach, Inc.). In addition to those loggers deployed along the restored channel reach, approximately 20 more temperature loggers were deployed in the main channel above and below the project reach as well as in groundwater upwelling features near the channel and in the floodplain. The groundwater upwelling features include springs, flowing backwater areas, and spring brooks far-removed from the channel. In 2012, 54 surface water temperature loggers were deployed (Figure 3). Twenty-eight of those were placed in the main flow of Meacham Creek along the restored reach at hydrologic breaks roughly corresponding to typically-defined aquatic habitat features (e.g.

pool, riffle, etc.). The remaining temperature loggers were deployed in groundwater upwelling features similar to 2011. In September 2012, all of the surface water loggers in the main channel were removed to protect them from being lost in high winter flows. However, all of the loggers in off-channel springs off from the main channel were re-deployed after being downloaded. In addition, a temperature logger was placed in the open channel flow bolted to a bedrock outcrop. These latter deployments were to record over-winter temperatures and capture the full seasonal cycle of surface water temperature variation at the restoration site.

Radon-222 activity and geochemistry

Radon-222 concentration will be measured to verify simulated and observed groundwater residence times across the post-restoration site. Radon-222 concentration is a reliable indicator of subsurface water residence time up to ~20 days (Hoehn and Cirpka 2006, Lamontagne and Cook 2007). In October 2011, we measured Radon-222 activity and collected geochemistry samples at twenty wells, five open channel locations, and four spring brook source waters using methods described by Schubert *et al.* 2006. In March 2013 repeat sampling for radon-222 and geochemistry was repeated at all wells and three open channel locations. Geochemistry data will be used to determine the magnitude of mixing between hyporheic and deep groundwater (Freeze and Cheery 1979, Hoehn and Cirpka 2006, Jones et al. 2008), a prerequisite for estimating hyporheic residence time from Radon-222. An additional value that is required to determine residence time using radon-222 is the equilibrium concentration of the dissolved radon-222 gas in the aquifer of interest. This value is related to radon-222 production by the aquifer material, and is generally idiosyncratic to the system in question; hence literature values do not serve well. Therefore, 8 250 ml pickling jars have been filled up completely with aquifer material from the study material and degassed tap water. After six weeks, samples from the middle of the volume of sediment will be collected and the concentration of radon will be measured by scintillation counter. This method has proved reliable in similar studies (Sebastian LaMontagne, personal communication, March 2013).

Results to Date

Work on the Groundwater and Surface Water Hydrologic and Temperature Monitoring is ongoing, and aside from the preliminary hydrologic modeling, no substantive results are yet available. However, observation of over 25 groundwater upwelling features along the restored channel (Figure 4) demonstrate that there has been a shift in groundwater hydrology at the restoration site. These features include a range of types from strongly flowing springs to seeps along the downstream margin of point bars marked by filamentous algae growing in these nutrient-enriched outflows. In addition, observations of groundwater flow into the exposed portions of the baseline channel and in other areas throughout the floodplain suggest substantial changes in groundwater hydrology. It is

expected that there has been concomitant changes in the thermal processes of the aquifer as well. cursory exploration of level logger data confirms these observations.

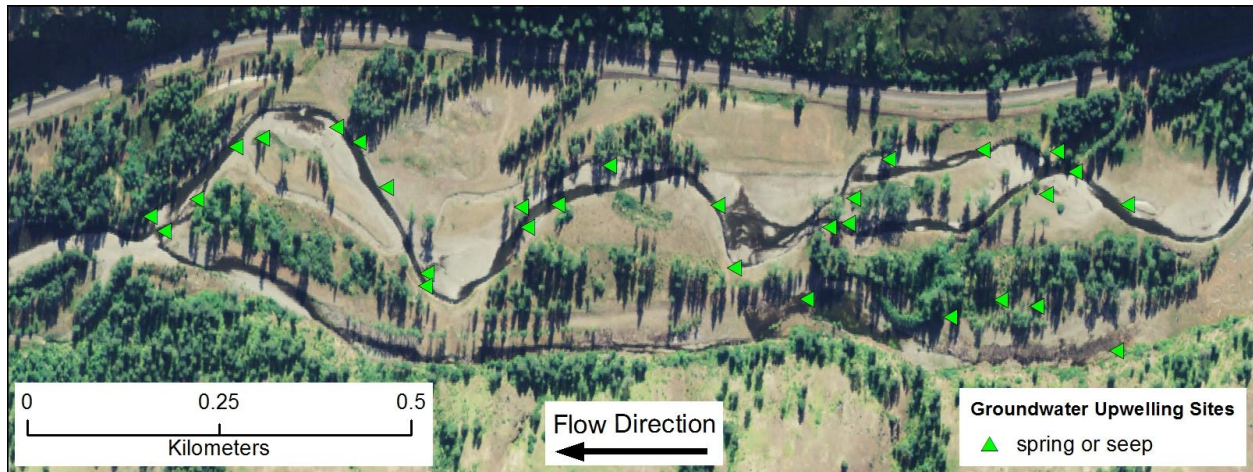


Figure 4. The location of easily-observed groundwater upwelling features along the restored reach of Meacham Creek observed in summer 2012.



Figure 5. An actively flowing groundwater spring and seep (note filamentous algae growing in nutrient-rich outflow) along the restored reach of Meacham Creek in summer 2012.

Database

A database containing over 1.7 million records has been created from the data collected to date. The database software being used is PostgreSQL 9.1.8 (www.postgresql.org), a

powerful enterprise-capable database that is spatially-enabled, allowing retrieval of data in ESRI shapefile format. The database has been carefully designed to allow retrieval of temperature or water level information by date range, location, data logger serial number, data logger make, etc.

Future Actions and Methods

In 2013 and 2014 an updated groundwater hydrology model, a groundwater thermal model, and an energy balance for the restored reach of Meacham Creek will be developed. Temperature and water level data collected to date and in the future will be used to develop, corroborate, and check the models and energy balance.

Hydrogeologic modeling

Modeling of hyporheic hydrology using updated as-built topographic surveys will allow stream-reach scale comparison of the change in magnitude and residence time of hyporheic flux for pre- vs. post-restoration scenarios. As with the preliminary hyporheic hydrologic models, the updated model will be developed using the USGS groundwater models MODFLOW (Harbaugh, 2005) and MODPATH (Pollock, 1994). The simulations will use updated model parameters for aquifer properties measured from aquifer stress tests to be carried out in spring 2013 (see aquifer properties section below for more detail). Observations of groundwater elevations, hyporheic temperature patterns measured to date will be used to help parameterize the model and verify results.

Aquifer heat flux modeling

Advection and dispersion of heat flux through the alluvial aquifer under pre-restoration and post-restoration scenarios will be simulated to determine groundwater heat flux at the reach scale and refine predictions of how heat flux will change in response to the change in channel planform as a result of the restoration. The heat flux simulations will be run with the USGS groundwater solute and energy flux model MT3DMS (Zheng *et al.* 2010, Zheng and Wang 1999). MT3DMS couples groundwater flow solutions from MODFLOW with the canonical advection-dispersion solute and energy transport solutions (Zheng *et al.* 2010, Zheng and Wang 1999).

Aquifer properties (model parameter estimation)

Detailed field data collection of key aquifer properties will be used to refine the input parameters to the hydrogeologic (Figure 2) and temperature models. Key parameters include hydraulic conductivity, porosity, thermal conductivity, bulk heat capacity, thermal conductivity at saturation, thermal conductivity at residual moisture content and volumetric heat capacity. These latter thermal properties are difficult to measure in the field. However, unpublished research on the Umatilla floodplain within 10 miles of the

Meacham Creek study site establishes benchmark values for the parameters (Brian Boer, unpublished manuscript 2005).

In spring 2013, physical properties of the aquifer will be measured, including hydraulic conductivity via stress tests on monitoring wells (Freeze and Cheery 1979, Fetter 1994, Fetter 2008), and hyporheic sediment porosity via comparison of the saturated and oven-dried bulk samples collected on site (Freeze and Cheery 1979, Stonestrom and Constantz 2003).

References

- Alicia S. Arrigoni, A.S., Poole, G.C., Mertes, L.A.K., O'Daniel, S.J., Woessner, W.W., Thomas, S.A. 2008. Buffered, lagged, or cooled? Disentangling hyporheic influences on temperature cycles in stream channels. *WATER RESOURCES RESEARCH*, VOL. 44, W09418, 13 PP.
- Fetter, C. W., *Applied Hydrogeology*, 3rd ed., 1994. 691 pp., Prentice-Hall, Englewood Cliffs, N. J.
- Freeze, A. R., & Cherry, J. A. (1979). *Groundwater*. Prentice Hall.
- Harbaugh, A.W., 2005, MODFLOW-2005, The U.S. Geological Survey modular ground-water model—the Ground-Water Flow Process: U.S. Geological Survey Techniques and Methods 6- A16
- Hoehn, E., and Cirpka, O.A., 2006, Assessing residence times of hyporheic ground water in two alluvial flood plains of the Southern Alps using water temperature and tracers: *Hydrology and Earth System Sciences*, v. 10, p. 553-563.
- Pollock, D.W. 2008. User's guide for MODPATH/MODPATH-PLOT, version 3: a particle tracking post-processing package for MODFLOW, the U.S. Geological Survey finite-difference ground-water flow model. USGS Open-File Report 94-464.
- Stonestrom, D. A. and Constantz, J., 2003. Heat as a tool for studying the movement of ground water near streams. U.S. Geological Survey Circular 1260, 96 p
- Wondzell, S.M., LaNier, J., and Haggerty, R. 2009. Evaluation of alternative groundwater flow models for simulating hyporheic exchange in a small mountain stream. *Journal of Hydrology*, v. 364, p. 142-151.
- Zheng, C., and Wang, P. P., 1999, MT3DMS, A modular three-dimensional multi-species transport model for simulation of advection, dispersion and chemical reactions of contaminants in groundwater systems; documentation and user's guide, U.S. Army Engineer Research and Development Center Contract Report SERDP-99-1, Vicksburg, MS, 202 p.

Zheng, C., Weaver, J., and Tonkin, M., 2010. MT3DMS, A Modular Three-dimensional Multispecies Transport Model and User Guide to the Hydrocarbon Spill Source (HSS) Package. Athens, Georgia: U.S. Environmental Protection Agency.

Thresholds in fluvial systems: Flood-induced channel change on Montana rivers

Basic Information

Title:	Thresholds in fluvial systems: Flood-induced channel change on Montana rivers
Project Number:	2012MT264B
Start Date:	3/1/2012
End Date:	2/28/2014
Funding Source:	104B
Congressional District:	MT01
Research Category:	Climate and Hydrologic Processes
Focus Category:	Floods, Geomorphological Processes, Climatological Processes
Descriptors:	None
Principal Investigators:	Andrew Wilcox

Publications

There are no publications.

Montana Water Center / USGS Interim report

Project title: "Thresholds in fluvial systems: Flood-induced channel changes on Montana rivers "

Start Date: March 1, 2012

End Date: February 28, 2014

Principal Investigator: Andrew Wilcox, Assistant Professor
Department of Geosciences, University of Montana
andrew.wilcox@umontana.edu; 406-243-4761

Our research has been investigating geomorphic changes associated with recent floods in three western Montana rivers: the Blackfoot, Clark Fork, and Bitterroot Rivers. Funding from the USGS / Montana Water Center seed grant program has supported field data collection and analysis of aerial photography and Lidar of our study systems. Our studies have included:

(1) Data collection along the lower Blackfoot River to document changes associated with 2011 and 2012 floods and how such changes fit into the context of channel adjustment following the removal of Milltown Dam. Data collection included repeat cross sections and longitudinal profiles to assess topographic changes and pebble counts to assess changes in bed-material size.

(2) Data collection along the Bitterroot River to evaluate threshold forces associated with scour of riparian cottonwood seedlings. This work entailed pull tests with a force gauge as well as data collection on other hydrogeomorphic factors influencing seedling scour (topography, texture, plant architecture, groundwater).

(3) Analysis of geomorphic changes along the Clark Fork River between the former Milltown Dam site and the Bitterroot River confluence to assess changes associated with 2011 and 2012 floods and how such changes fit into the context of channel adjustment following the removal of Milltown Dam. In the last year, most of this work has entailed analysis of aerial photographs and USGS sediment transport data.

(4) Acquisition of remote sensing products. Lidar data were collected along the Bitterroot River in fall 2012 by Missoula and Ravalli Counties, and we recently acquired these data. These data will serve as high-resolution topography input data for morphodynamic modeling of the Bitterroot that will determine flood hydraulics and exceedence of thresholds for channel change and sediment transport; this modeling work will commence this summer. We have also acquired NAIP aerial photograph imagery, from summer 2011, for all study systems.

Outreach activities by participants in this project have included volunteering with Missoula's Watershed Education Network, judging the state high-school Science Fair, and teaching about river processes at local elementary schools. The PI also regularly interacts with local groups such as Clark Fork Coalition and Trout Unlimited. Preliminary science outcomes include several presentation on this research (see below), including at the Montana AWRA annual meeting.

Bywater-Reyes, S., A. C. Wilcox, A. Lightbody, K. Skorko and J. C. Stella, 2012, Uprooting force balance for pioneer woody plants: A quantification of the relative contribution of above- and below-ground plant architecture to uprooting susceptibility: American Geophysical Union Annual Meeting 2012, EP41A-0768.

Bywater-Reyes, S., A. Wilcox, J. Stella and W. Woessner, 2012, Scour susceptibility of Black Cottonwood on the Bitterroot River, Montana: Insights for successful restoration of riparian areas: American Water Resource Association Montana Section Annual Meeting, 2012.

Colaiacomo, E. and A.C. Wilcox. 2012. "Downstream spatial and temporal response to dam removal: Reach and bedform scale variations in transport capacity, White Salmon River, Washington." Poster, Montana AWRA Annual Meeting, 10-12 October, Fairmont, MT.

Livesay, R. and A. Wilcox. 2013. Investigating upstream channel response to dam removal, Blackfoot River, MT. GSA Rocky Mountain section meeting. Geological Society of America *Abstracts with Programs*. Vol. 45 (5).

Nutrient dynamics and ecosystem function in coupled aquatic-terrestrial ecosystems during a mountain pine beetle infestation of whitebark pine

Basic Information

Title:	Nutrient dynamics and ecosystem function in coupled aquatic-terrestrial ecosystems during a mountain pine beetle infestation of whitebark pine
Project Number:	2012MT265B
Start Date:	3/1/2012
End Date:	2/28/2013
Funding Source:	104B
Congressional District:	MT01
Research Category:	Biological Sciences
Focus Category:	Ecology, Conservation, Water Quality
Descriptors:	
Principal Investigators:	Laurie Marczak

Publications

There are no publications.

Nutrient dynamics and ecosystem function in coupled aquatic-terrestrial ecosystems during a mountain pine beetle infestation of whitebark pine

Interim and final report – Montana Water Center
MSU Subaward G222-12-W3491

Laurie B. Marczak, The University of Montana

Introduction

Streams are tightly coupled to the terrestrial landscapes through which they flow, particularly in forested headwaters. The forested riparian areas of headwater streams reduce stream primary productivity through shading but simultaneously provide substantial inputs of organic material that fuel stream secondary production (Vannote et al. 1980). These allochthonous inputs of leaf litter, large wood, and dissolved nutrients dominate the resource base of most headwaters (Wallace et al. 1997), drive rates of secondary production (Tank et al. 2010) and determine aquatic food web structure (Marczak et al. 2007). Although often overlooked in management and conservation plans, headwater streams also transform and funnel vast quantities of terrestrial nutrients to downstream, frequently fish-bearing, reaches (Wipfli et al. 2007) aided by the processes of invertebrate and microbial decomposition (Greenwood et al. 2007).

The dependence of headwater stream function and productivity on terrestrial inputs suggests that large-scale basin disturbances have the potential to drive wholesale changes in stream food webs (Nakano et al. 1999, Kominoski et al. 2011). Disturbances that sufficiently alter the quality or quantity of organic matter inputs to streams could alter rates of organic matter processing, food web structure and species composition (Minshall et al. 1989, Minshall et al. 2001). Stream functional changes may ultimately propagate energy regime shifts back to riparian habitats or downstream to mainstem rivers and the communities that depend on them for ecosystem services and economic livelihoods (Wipfli et al. 2007).

This research set out to investigate how the current MPB infestation across Montana, specifically in whitebark pine (WbP) forests in the Greater Yellowstone Ecosystem, is affecting organic matter inputs and subsequent processing rates within headwater streams. The goals of the research were to provide a better understanding of how a loss of forest cover resulting from mountain pine beetle (MPB) infestation alters community dynamics and ecosystem processes in headwater streams and to help to further understand linkages between aquatic and terrestrial systems in alpine environments.

In this project, we combined field observations with experimental manipulations of detrital inputs and subsequent organic matter processing in headwater streams. Our first research question centered on determining the dominant mode of transport and rate of input of MPB-altered WbP litter to high elevation streams. We successfully quantified the rate and mode (vertical or lateral source) of WbP inputs into headwater streams across a beetle induced mortality gradient. Our second research question focused on determining the extent to which MPB-driven changes in stream water and WbP litter chemistry alter rates of microbial and invertebrate decomposition in streams. We conducted this work in streams representing the stages of WbP mortality (green – healthy, red – peak infestation, grey – post infestation).



Figure 1. Location of study sites within the northern portion of the Greater Yellowstone Ecosystem. Branham Lakes basin is in the Tobacco Roots mountains and has some of the highest levels of WbP mortality for the GYE. Sheep Creek basin is in the Absaroka mountains and contains one of the healthiest remaining populations of WbP in the GYE.

Experimental approach

The study was conducted in two watersheds within the Greater Yellowstone Ecosystem (Sheep basin; 42°02' N, 109°58' W, and Branham Lakes basin, 45°31' N, 111°59' W, Figure 1). These two basins characterize two stages of MPB infestation in WbP – early infestation, relatively healthy (Sheep), and peak to post infestation with high mortality (Branham Lakes; Table 1). To determine whether beetle infestation increased the rate, composition, or pathway by which detritus enters stream systems, and to determine how variation in landscape characteristics affects these dynamics, we

quantified vertical and lateral inputs of leaf litter into 10 headwater streams, 5 in each basin. After quantifying the percent of WbP cover and mortality for each basin, as well as each stream catchment, vertical and lateral litter traps (10 of each) were installed along each study stream in early July 2012 and cleared monthly from late July 2012 to mid-October 2012.

Table 1. Whitebark pine cover and mortality in focal streams. WbP in Branham Lakes basin is largely dead due to MPB and WbP in Sheep Creek basin is relatively healthy overall.

Basin	Stream	% WbP cover in catchment	% healthy WbP in catchment	% "red" WbP in catchment	% "grey" WbP in catchment
Branham Lakes (high mortality)	Branham Lakes 1	99%	30%	20%	50%
	Branham Lakes 2	55%	60%	25%	15%
	Branham Lakes 3	95%	10%	30%	60%
	Branham Lakes 4	95%	10%	60%	30%
	Branham Lakes 5	68%	45%	50%	5%
Sheep Creek (low mortality)	Sheep 1	45%	98%	0%	2%
	Sheep 2	40%	97%	0%	3%
	Sheep 3	50%	90%	5%	5%
	Sheep 4	65%	89%	1%	10%
	Sheep 5	55%	97%	1%	2%

Collected litter was sorted by type (coniferous vs deciduous, needle color phase, flower/leaf/branch etc), dried at 50 °C for at 2 days, weighed, combusted at 500 °C for 5 hours and weighed again to determine ash free dry mass (g AFDM). Values from litter traps in each stream were pooled by time period to provide a reach level estimate. In addition, we quantified benthic retention of whitebark litter material by placing a 0.5 x 0.5-m metal quadrat on 10 haphazard benthic locations within the wetted area of each stream and recording the percentage of visual cover of WbP litter. These measurements were repeated three times throughout the study. On the third and final sampling period we collected all of the needles visible within a

quadrat for 3 locations per stream. Collected needles were oven-dried and weighed to obtain dry mass. These data were used to create a linear regression model to determine biomass from the percentage of visual cover and values from each quadrat were pooled and used to extrapolate a reach-level estimate of WbP detrital biomass and cover within each stream.

To determine the extent to which MPB-driven changes in WbP litter chemistry alter rates of microbial and invertebrate decomposition in streams we conducted a common garden style decomposition experiment. Naturally senescing WbP needles were collected from both healthy and beetle-killed trees in each focal catchment (representing healthy and heavily infested conditions) and air-dried. Five grams of needles were placed into litter decomposition chambers that were modified to allow both invertebrate and microbial decomposition or microbial decomposition only.

Decomposition chambers were deployed into streams (1 stream in each focal catchment) in July 2012. We placed 42 of each of the following types of cylinders into each stream: needles from beetle-killed trees (microbes + invertebrates; MPB-I), needles from beetle-killed trees (microbes only; MPB-M), needles from healthy trees (microbes + invertebrates; G-I), needles from healthy trees (microbes only; G-M). Six cylinders of each treatment were removed from the stream after 14, 28, 42, 56, and 84 days of incubation (14, 28, and 42 for the green-stage catchment). Litter from half of the cylinders for each treatment-day was used to determine g AFDM remaining and litter from the other cylinders was used to measure microbial respiration on needles (as a proxy for microbial biomass) and for nutrient (C, N, P) analysis. On each sample day we also collected three replicate water samples and measured stream temperature, dissolved oxygen, and pH. Water samples were later analyzed for nitrate, ammonium, and soluble reactive phosphorus.

Results and discussion

We found that vertical inputs increased significantly with basin level mortality and that vertical inputs were the dominant mode of transport for WbP needles into streams with high levels of catchment mortality. We found that MPB infestation of WbP increases inputs to headwater streams in affected catchments (Figure 2), and that vertical movement is the dominant mode of transport for these inputs. The overall abundance of invertebrates in streams also decreased across a gradient of whitebark pine mortality with this decrease being driven largely by declines in shredder abundance (Figure 3). Benthic retention of needles was comparable between the two basins in this study and it appears that the majority of the needles entering streams are remaining in the benthos. Needles are not leaving the headwater system, regardless of the level of WbP mortality. Thus this litter remains available to detritivores within the headwaters for potentially long periods of time. However, the second portion of this study we found that needles from beetle-killed trees may be a less desirable food source than needles from healthy trees. It is important to note that when assessed at a larger landscape scale (between basins instead by individual stream catchment) organic matter inputs did not differ between basins with different largescale mortality levels of whitebark pine. This emphasizes the importance of streamside mortality when assessing how a MPB outbreak may alter organic matter dynamics in stream systems. An increase in red stage trees within the immediate riparian area will lead to greater needle inputs into headwater streams. However, an increase in red stage trees throughout the basin may not necessarily lead to more litter inputs if streams are not in close proximity and slopes are not steep.

Our results indicate that decomposition rates for MPB-altered needles differ from needles from healthy trees. However, contrary to my hypothesis, needles from healthy trees decomposed faster than needles from beetle-killed trees despite MPB-altered needles being higher in initial quality (Table 2). Overall, pine needles decayed slowly and at similar rates to what has been observed in other studies; in this study k for WBP needles decomposing in a stream already heavily influenced by beetle infestation ranged from 0.006– 0.008 (Figure 4). In comparison, other studies have reported pine needle k values ranging from 0.0030 – 0.0038 (Short et al. 1980) to 0.0054– 0.0093 (Whiles and Wallace 1997). Like other researchers (Morehouse et al. 2008, Keville 2011), I found MPB-altered needles to have a significantly lower C:N ratio than litter from healthy trees. It is possible that the needles from beetle-killed trees decomposed slower because of additional chemical compounds present in these needles. When conifers are attacked by an insect herbivore they employ a number of defenses including chemical responses. For example, researchers have found that monoterpene concentrations in conifers increase following attack by many different species of bark beetles (Raffa and Smalley 1995). More specific to the present study, Erbilgin and Colgan (2012) investigated MPB-induced chemical defenses in jack pine (*Pinus banksiana*) and found that MPB attack led to an increase in monoterpene concentrations in needles. Monoterpenes are a class of chemicals that help plants, particularly conifers, to resist herbivory (White 1994, Litvak and Monson 1998).

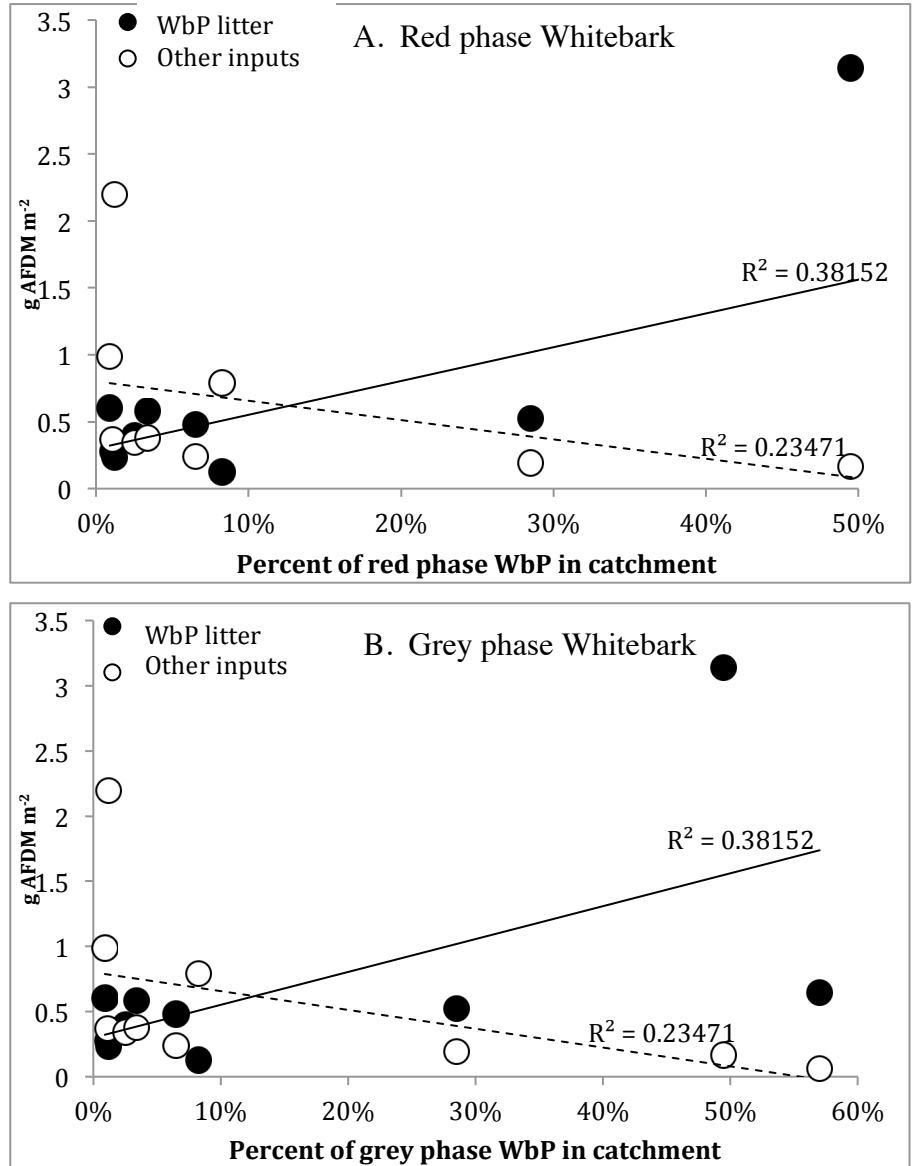


Figure 2. Whitebark Pine litter inputs to high elevation streams increase with tree mortality from mountain pine beetle infestation. Filled circles show the relationship for WbP litter only, open circles show the relationship between all other organic inputs and (A) red phase catchment level mortality and (B) grey phase catchment level mortality.

Table 2. Needle nutrient levels, daily mass loss rates, and *k* values for each treatment. Values are reported as the mean \pm SD.

Stream	Decomposer	Needle Source	Preliminary C:N	Day 14 total P (mg/kg)	Decomposition rate (g/day ⁻¹)	<i>k</i>
Mill	Invertebrate + Microbial	Healthy tree	55.02 \pm 1.09	1102.6 \pm 74.17	0.034 \pm 0.018	0.008 \pm 0.004
Mill	Microbial	Healthy tree	55.02 \pm 1.09	1102.6 \pm 74.17	0.028 \pm 0.009	0.006 \pm 0.002
Mill	Invertebrate + Microbial	MPB-altered	50.51 \pm 0.46	1164.67 \pm 67.99	0.029 \pm 0.010	0.007 \pm 0.002
Mill	Microbial	MPB-altered	50.51 \pm 0.46	1164.67 \pm 67.99	0.026 \pm 0.008	0.006 \pm 0.002
Sheep	Invertebrate + Microbial	Healthy tree	53.27 \pm 3.13	1112.6 \pm 116.17	0.022 \pm 0.014	0.005 \pm 0.003
Sheep	Microbial	Healthy tree	53.27 \pm 3.13	1112.6 \pm 116.17	0.016 \pm 0.007	0.003 \pm 0.002
Sheep	Invertebrate + Microbial	MPB-altered	50.47 \pm 1.29	1223.33 \pm 74.17	0.021 \pm 0.009	0.005 \pm 0.002
Sheep	Microbial	MPB-altered	50.47 \pm 1.29	1223.33 \pm 74.17	0.016 \pm 0.006	0.003 \pm 0.001

At high doses monoterpenes are lethal to insects and can inhibit fungal growth (Langenheim 1994, Raffa and Smalley 1995). These compounds are highly resilient and do not decrease in concentration after needle senescence (White 1991, Wilt et al. 1993). Because of this resilience researchers have proposed that monoterpenes and other secondary chemicals may inhibit decomposer organisms for many years after senescence (Kainulainen and Holopainen 2002). It is likely that needles from MPB-killed trees have higher concentrations of monoterpenes which may in turn slow microbial activity and deter macroinvertebrate consumers. Although we had predicted that invertebrates, particularly shredders, would seek out MPB-altered litter due to its higher quality compared to normally available material and that this would lead to more rapid decomposition of these inputs, it seems that other MPB-induced biochemical changes such as increased defense compounds may have a stronger deterrent effect over the potential attractiveness of the elevated nitrogen profile of those inputs.

This study is the first to document changes in rates of WbP needle decomposition in aquatic systems following landscape scale MPB infestation. Despite an increase in nitrogen-elevated litter entering streams following a MPB outbreak, altered litter is decomposed in streams at a slower rate than available unimpacted WbP inputs and appears less desirable to consumers. Thus, while increasing the nitrogen-content of litter entering streams, MPB infestations may actually decrease the palatability of allochthonous inputs. This change in palatability may explain why invertebrate densities decreased with increasing WbP mortality in catchments, despite the pulsed increase in overall litter quantity. Given that increased resources tend to support greater secondary productivity, we had hypothesized that an increase in total organic matter inputs would lead to increases in invertebrate populations. However, our results indicate that MPB attack likely change needle chemistry in such a way as to inhibit decomposition. Therefore, although more needles are entering streams in MPB-infested stands, this litter is processed more slowly – likely extending the availability of this resource pulse of MPB-influenced needles over longer timeframes than typical nutrient recycling rates in these systems. In turn, it appears that these reduced rates of organic matter processing may be reducing secondary productivity within affected streams. Since the effects of increased monoterpene concentrations in MPB influenced needles are hypothesized (based on work from other taxa) and that their precise interactions with decomposition dynamics are unknown, future research should

quantify MPB-induced monoterpene concentrations in needles and more thoroughly investigate whether these chemicals inhibit detritivore consumption of needles.

This work has formed the basis of an MS thesis in the Wildlife Biology program at The University of Montana (Ms. Hilary Eisen) and is currently in preparation for journal submission in the form of two manuscripts.

Works Cited

- Erbilgin, N. and L. J. Colgan. 2012. Differential effects of plant ontogeny and damage type on phloem and foliage monoterpenes in jack pine (*Pinus banksiana*). *Tree Physiology* **32**:946-957.
- Greenwood, J. L., A. D. Rosemond, J. B. Wallace, W. F. Cross, and H. S. Weyers. 2007. Nutrients stimulate leaf breakdown rates and detritivore biomass: bottom-up effects via heterotrophic pathways. *Oecologia* **151**:637-649.
- Keville, M. 2011. Impacts of mountain pine beetle (*Dendroctonus ponderosae*) outbreak on biogeochemical cycling in a high elevation whitebark pine (*Pinus albicaulis*) ecosystem. University of Montana.
- Kominoski, J. S., L. B. Marczak, and J. S. Richardson. 2011. Riparian forest composition affects stream litter decomposition despite similar microbial and invertebrate communities. *Ecology* **92**:151-159.
- Langenheim, J. H. 1994. Higher plant terpenoids - a phytocentric overview of their ecological roles. *Journal Of Chemical Ecology* **20**:1223-1280.
- Litvak, M. E. and R. K. Monson. 1998. Patterns of induced and constitutive monoterpene production in conifer needles in relation to insect herbivory. *Oecologia* **114**:531-540.
- Marczak, L. B., R. M. Thompson, and J. S. Richardson. 2007. Meta-analysis: Trophic level, habitat, and productivity shape the food web effects of resource subsidies. *Ecology* **88**:140-148.
- Minshall, G. F., J. T. Brock, D. A. Andrews, and C. T. Robinson. 2001. Water quality, substratum and biotic responses of five central Idaho (USA) streams during the first year following the Mortar Creek fire. *International Journal of Wildland Fire* **10**:185-199.
- Minshall, G. W., J. T. Brock, and J. D. Varley. 1989. Wildfires and Yellowstone stream ecosystems. *Bioscience* **39**:707-715.
- Morehouse, K., T. Johns, J. Kaye, and A. Kaye. 2008. Carbon and nitrogen cycling immediately following bark beetle outbreaks in southwestern ponderosa pine forests. *Forest Ecology and Management* **255**:2698-2708.
- Nakano, S., Y. Kawaguchi, Y. Taniguchi, H. Miyasaka, Y. Shibata, H. Urabe, and N. Kuhara. 1999. Selective foraging on terrestrial invertebrates by rainbow trout in a forested headwater stream in northern Japan. *Ecological Research* **14**:351-360.
- Raffa, K. F. and E. B. Smalley. 1995. Interaction of pre-attack and induced monoterpene concentrations in host conifer defense against bark beetle-fungal complexes. *Oecologia* **102**:285-295.
- Short, R. A., S. P. Canton, and J. V. Ward. 1980. Detrital processing and associated macroinvertebrates in a Colorado mountain stream. *Ecology* **61**:728-732.

- Tank, J. L., E. J. Rosi-Marshall, N. A. Griffiths, S. A. Entekin, and M. L. Stephen. 2010. A review of allochthonous organic matter dynamics and metabolism in streams. *Journal of the North American Benthological Society* **29**:118-146.
- Vannote, R. L., G. W. Minshall, K. W. Cummins, J. R. Sedell, and C. E. Cushing. 1980. The river continuum concept. *Canadian Journal Of Fisheries And Aquatic Sciences* **37**:130-137.
- Wallace, J. B., S. L. Eggert, J. L. Meyer, and J. R. Webster. 1997. Multiple trophic levels of a forest stream linked to terrestrial litter inputs. *Science* **277**:102-104.
- Whiles, M. R. and J. B. Wallace. 1997. Leaf litter decomposition and macroinvertebrate communities in headwater streams draining pine and hardwood catchments. *Hydrobiologia* **353**:107-119.
- White, C. S. 1994. Monoterpenes - their effects on ecosystem nutrient cycling. *Journal Of Chemical Ecology* **20**:1381-1406.
- Wilt, F. M., G. C. Miller, R. L. Everett, and M. Hackett. 1993. Monoterpene concentrations in fresh, senescent, and decaying foliage of single-leaf pinyon (*Pinus monophylla* Torr. and Frem.: Pinaceae) from the Western Great Basin. *Journal Of Chemical Ecology* **19**:185-194.
- Wipfli, M. S., J. S. Richardson, and R. J. Naiman. 2007. Ecological linkages between headwaters and downstream ecosystems: transport of organic matter, invertebrates, and wood down headwater channels. *JAWRA Journal of the American Water Resources Association* **43**:72-85.

Student Fellowship Project: Evaluating hydrogeomorphic controls on bull trout spawning habitat in mountain streams, Northwestern Montana

Basic Information

Title:	Student Fellowship Project: Evaluating hydrogeomorphic controls on bull trout spawning habitat in mountain streams, Northwestern Montana
Project Number:	2012MT266B
Start Date:	3/1/2012
End Date:	2/28/2013
Funding Source:	104B
Congressional District:	at large
Research Category:	Biological Sciences
Focus Category:	Ecology, Geomorphological Processes, None
Descriptors:	None
Principal Investigators:	Jared Bean

Publications

There are no publications.

Student Fellowship Project: Evaluating hydrogeomorphic controls on bull trout spawning habitat in mountain streams, Northwestern Montana. Final Report.

PI: Jared Bean, University of Montana

ABSTRACT

I investigated relationships between geomorphology, hydrogeology, and bull trout (*Salvelinus confluentus*) redd occurrence and density at multiple spatial scales in gravel-bed, pool-riffle, snowmelt dominated headwater streams of northwestern Montana. Subreach redd occurrence tended to be associated with the finest available textural facies. In subreach streambed sections hosting bull trout redds, redd density was significantly (at $\alpha=0.05$) positively related to bankfull Shields stress (τ^{*bf} , $p=0.04$) and bankfull Shields stress adjusted for grain stress only (τ^{*bf} , $p=0.02$). In stream reaches hosting bull trout redds, reach-average redd density was significantly positively related to reach-average τ^{*bf} ($p=0.02$) and reach-average streambed grain size (D16, $p=0.01$; D50, $p=0.02$, D84, $p=0.02$). Spawning reaches exhibited high streambed horizontal and vertical hydraulic conductivities, and streambed temperatures were dominated by stream water diurnal cycles to a depth of at least 25 cm. Groundwater provided substantial thermal moderation of stream water for multiple high density spawning reaches. At the valley-scale, redd occurrence tended to be associated with unconfined alluvial valleys. Many previous studies highlight the thermal sensitivity of bull trout. My spawning gravel competence results indicate that a shift in the timing of high flows could increase the likelihood of redd scour during the bull trout egg incubation period.

INTRODUCTION (excerpt from thesis text)

Research at the intersection of fluvial geomorphology, hydrology, and ecology has expanded in recent years (e.g. Poole, 2010), but an improved understanding of physical and associated ecological processes is needed to develop effective conservation and management practices for aquatic ecosystems. Preserving and improving spawning habitat requires defining key physical and ecological processes controlling spawning site selection and successful fry emergence (e.g. Kondolf 2000; Montgomery et al., 1996; Moir et al., 2002; Kondolf et al., 2008; Tonina and Buffington, 2009). Species-specific spawning habitat suitability questions remain, especially for bull trout (*Salvelinus confluentus*) whose native range includes the northern Rocky Mountains and Pacific Northwest.

The purpose of this study was to determine primary micro-, subreach-, reach-, and valley-scale physical factors influencing bull trout spawning occurrence in snowmelt-dominated systems. I hypothesized:

1. At the subreach- and reach-scales, spawning locations are associated with channel sections of
 - a. low spawning sediment mobility at bankfull flows; and
 - b. extensive local streambed hyporheic exchange.
2. At the valley-scale, spawning locations are associated with alluvial valley segments where
 - a. the stream valley narrows; and

- b. hyporheic water and groundwater discharges to the stream.

CONCLUSIONS

My findings indicate that physical processes at multiple-spatial scales influence bull trout redd occurrence in snowmelt dominated systems. At the subreach- and reach-scale, redd occurrence tends to be associated with mobile surface gravels that have high horizontal and vertical hydraulic conductivities. At the valley-scale, redd occurrence tends to be associated with unconfined alluvial valleys where stream temperatures are thermally suitable. Groundwater appears to play a major role in providing favorable conditions for bull trout spawning reaches. In light of the spawning gravel competence results, shifts in timing of high flows associated with climate change (e.g. Isaak et al., 2012) could adversely affect bull trout spawning by increasing the likelihood of redd scour.

The difference between my findings and previous studies related to streambed mobility and salmonid spawning site selection merits further attention. In terms of using and expanding on the findings of this study, basin-wide grain size prediction models (e.g. Buffington et al., 2004) could be used to assess the broader-scale distribution of physically suitable spawning habitat. Basin-wide valley confinement delineations and stream temperature monitoring networks could be used to further assess stream thermal regimes and identify the role of groundwater in modifying the thermal regime of this system. Further clarification of the role of groundwater in patch and subreach-scale bull trout spawning site selection is also merited.

REFERENCES

- Buffington, J.M., D.R. Montgomery, and H.M. Greenberg. 2004. Basin-scale availability of salmonid spawning gravel as influenced by channel type and hydraulic roughness in mountain catchments. *Canadian Journal of Fisheries and Aquatic Sciences* 61 (11): 2085–2096.
- Isaak, D.J., C.C. Muhlfeld, A.S. Todd, R. Al-Chokhachy, J. Roberts, J.L. Kershner, K.D. Fausch, S.W. Hostetler. 2012. The past as prelude to the future for understanding 21st-Century climate effects on Rocky Mountain trout. *Fisheries Management* 37: 542-556.
- Kondolf, G.M., J.G. Williams, T.C. Horner, and D. Milan. 2008. Assessing physical quality of spawning habitat. *American Fisheries Society Symposium* 65.
- Kondolf, G.M. 2000. Assessing salmonid spawning gravel quality. *Transactions of the American Fisheries Society* 129 (1): 262–281.
- Moir, H.J., C. Soulsby, and A.F. Youngson. 2002. Hydraulic and sedimentary controls on the availability and use of Atlantic salmon (*Salmo Salar*) spawning habitat in the River Dee system, northeast Scotland. *Geomorphology* 45 (3): 291–308.
- Montgomery, D.R., J.M. Buffington, N.P. Peterson, D. Schuett-Hames, and T.P. Quinn. 1996. Stream-bed scour, egg burial depths, and the influence of salmonid spawning on bed surface mobility and embryo survival. *Canadian Journal of Fisheries and Aquatic Sciences* 53 (5): 1061–1070.

Poole, G.C. 2010. Stream hydrogeomorphology as a physical science basis for advances in stream ecology. *Journal of the North American Benthological Society* 29 (1): 12–25.

Tonina, D., and J.M. Buffington. 2009. A three-dimensional model for analyzing the effects of salmon redds on hyporheic exchange and egg pocket habitat. *Canadian Journal of Fisheries and Aquatic Sciences* 66 (12): 2157–2173.

Student Research Fellowship: Pool Response to Fine Sediment Loading from Dam Removal, White Salmon River, Washington

Basic Information

Title:	Student Research Fellowship: Pool Response to Fine Sediment Loading from Dam Removal, White Salmon River, Washington
Project Number:	2012MT267B
Start Date:	3/1/2012
End Date:	2/28/2013
Funding Source:	104B
Congressional District:	at-large
Research Category:	Climate and Hydrologic Processes
Focus Category:	Geomorphological Processes, None, None
Descriptors:	None
Principal Investigators:	Erika Colaiacomo

Publications

There are no publications.

Student Research Fellowship: Pool Response to Fine Sediment Loading from Dam Removal, White Salmon River, Washington. Final Report.

PI: Erika Colaiacomo, University of Montana

The removal of Condit Dam from the White Salmon River, Washington has provided me a unique opportunity to study how a bedrock-confined, gravel-bed river responds to the disturbance of a large influx of fine reservoir sediment. In my research, I test a conceptual model of river response to a dam removal on the White Salmon River. I hypothesized that the confined reach below the former Condit Dam will progress back to its pre-breach state while the less confined reach at the mouth of the White Salmon will not. Within the confined reach, I propose that pool-riffle dynamics will play a significant role in sediment storage and local response. I assess these hypotheses through repeat surveys of topography and grain size and calculations of transport capacity. The broader goal of this project is to better understand the forcings, sensitivities, and changes in transport capacity that dictate response to a large pulse of reservoir sediment. As the number and scale of dam removals increases, it becomes essential to better understand and predict the magnitude and duration of geomorphic impacts.

Preliminary results: In the confined reach, median grain size from pre-breach surveys in August 2011 to post-breach surveys in August 2012 decreased from 160 to 50 mm, suggesting an increase in transport capacity that will facilitate sediment evacuation from the confined reach. On average, the post-breach bed elevations in the less confined reach increased more than bed elevations in the confined reach (7.8 m vs. 4.1 m) and bed elevations in pools increased more than bed elevations over riffles (4.7 m vs. 3.6 m). Nine months after the breach, the bed elevations in the confined reach had decreased an average of 2.5 m compared to 1.8 m in the less confined reach. Pools and riffles both decreased by 2.5 m; however, surveys 3 months after the breach show that riffles decreased at a faster rate than pools (2.2 m vs 1.8 m).

The Montana Water Center fellowship allowed me the opportunity to complete additional field surveys at my study site. To date, I have completed all three field surveys and am now working on processing data and writing to complete my research.

Student Research Fellowship: An Investigation of Natural Treatment Systems in Cold Climates

Basic Information

Title:	Student Research Fellowship: An Investigation of Natural Treatment Systems in Cold Climates
Project Number:	2012MT268B
Start Date:	3/1/2012
End Date:	2/28/2013
Funding Source:	104B
Congressional District:	at large
Research Category:	Engineering
Focus Category:	Wastewater, None, None
Descriptors:	None
Principal Investigators:	Katie Davis

Publications

There are no publications.

Student Research Fellowship: An Investigation of Natural Treatment Systems in Cold Climates: Wastewater Treatment at Bridger Bowl Update. Final Report
PI: Katie Davis, Montana State University

Bridger Bowl, Inc. (BBI) is the local Bozeman, Montana ski area located northeast of the town in the Bridger Mountains. The primary operating season extends from approximately December 7 to April 7 with 160,000-180,000 skier visits per year. To manage the wastewater treatment processes for its facilities, BBI utilizes two separate systems. The system observed in this study services the base area. The facilities include 2 ski lodges, offices, and rental and maintenance facilities including several restaurants but no lodging. This system was built in 2001 and uses recirculating sand filter (RSF) technology for wastewater treatment.

MSU students began monitoring the system in 2006 when it became clear that the RSF system was having difficulty consistently meeting the requirements for the DEQ discharge permit. With consistent monitoring, the students were able to make recommendations for improvements in system efficiency. These recommendations included changes in pump timing, piloting heating and aeration components in the RSF, and baffling the recirculation tank.

The BBI system is unique in some of the challenges it faces in nutrient removal for efficient wastewater treatment. First, the system is only seasonally loaded and sees variations in daily loading rates from 1000-8000 gallons per day. The temperatures of the wastewater stream are almost always below optimal temperature for nitrification and denitrification processes and often as low as 2-4°C. Lastly, BBI wastewater streams are 3-4 times as concentrated as typical domestic wastewater due to water saving practices and the lack of generally dilute wastewater sources (e.g. showering and laundry washing, etc.). In 2010-2011, BBI began looking at upgrade or system replacement options to improve the system efficiency to manage the increasing skier visits experienced by the ski area over the last 10 years. After considering many options, BBI decided to build a pilot scale treatment wetland to verify its efficiency for a potential future full-scale system. The wetland system was constructed during the summer of 2012 and treats 1000 gallons per day.

My 2011-2012 research involved monitoring the current RSF system to continue making modifications. The data shows that the system began the ski season working acceptably to meet the DEQ discharge permit requirements. As the season progressed, the system efficiency declined. This could be due to a number of issues. First, the snowfall was late to come in December 2011 and the temperature dropped before there was adequate snowfall to insulate the ground. Thus, the ground temperature may have been cooler than normal therefore cooling the wastewater in the piping between the base area and the RSF site and in the recirculation tank. Second, the system efficiency appeared to decrease as skier numbers and frequency increased suggesting an overload of the system with more highly concentrated influent.

In the spring and summer of 2012, I worked with MSU professors and students, a local engineer, and the Bridger Bowl management to design and build the 1000 gpd pilot treatment wetland system. The system consists of four 16' by 16' media filled cells. Two of the cells contain a gravel media ("pea gravel" sized) (A cells) and two of the cells contain a coarse sand media (B cells). This new pilot system is located next to the old RSF system and discharges to the recirculation tank to be run through the old system. The system is run in series with the water dosed onto the A cells into a transfer tank then dosed onto the B cells. Having 2 parallel trains allows us to vary loading rates on the 2 trains to optimize hydraulic and nutrient loading rates.

In our design process, we incorporated equipment to measure flow rates and allow in-cell sampling. The pump timing and monitoring equipment is run with a LabVIEW program. We are currently constructing an autosampler and temperature and ORV probes to increase our data collection capabilities. Because construction of infrastructure was not completed until late August 2012, planting of the wetlands with native wetland plants was postponed until June of 2013.

During the 2012-2013 ski season, I continued to monitor the old RSF system. In early January we began treating 1000 gpd in the wetland without plants to establish baseline efficiency. Preliminary data analysis showed greater overall RSF system efficiency despite over 10,000 more skier visits as compared to the previous season. This would suggest that the old system simply may not be large enough to handle the flows seen throughout the season. Also, by running the unplanted wetland, we lowered the influent concentrations to the RSF. This may also have contributed to system efficiency. More extensive data analysis will be performed in the next couple of months.

The pilot treatment wetland will be studied for at least 2-3 more seasons to look at system optimization and efficiency under extreme conditions. The goal is to establish hydraulic and nutrient loading rates, recycle ratios, and efficiency rates. If we can optimize this pilot treatment wetland and prove its effective nutrient removal, Bridger Bowl, Inc. would like to install a full-scale system to replace the RSF currently in use. Also, by establishing ideal operational criteria for treatment wetlands, we will be able to provide the Montana DEQ with data to support the use of this technology as an on-site wastewater treatment system statewide.

Student Research Fellowship: Quantifying the Sensitivity of Spring Snowmelt Timing to the Diurnal Snowmelt Cycle

Basic Information

Title:	Student Research Fellowship: Quantifying the Sensitivity of Spring Snowmelt Timing to the Diurnal Snowmelt Cycle
Project Number:	2012MT272B
Start Date:	3/1/2012
End Date:	2/28/2013
Funding Source:	104B
Congressional District:	at large
Research Category:	Climate and Hydrologic Processes
Focus Category:	Hydrology, Climatological Processes, None
Descriptors:	None
Principal Investigators:	Fred Kellner

Publications

There are no publications.

Student Research Fellowship: Quantifying the Sensitivity of Spring Snowmelt Timing to the Diurnal Snowmelt Cycle. Final Report.

PI: Fred Kellner, University of Montana

This report describes the progress on my research which was generously funded by the Montana Water Center. This funding has been valuable in that it has allowed me to spend time in the field collecting data as well as in the office modeling. The following represents a progress report of my research:

Completed Work:

- Two days were spent in Lost Horse Canyon of the Bitterroot Mountain Range of Montana collecting snow water equivalent (SWE), depth data, using ground penetrating radar. These two days provided a testing period to see how effective using a snowmobile and ground penetrating radar was to collect SWE depth data. This method has proven successful and I will be returning to the field to collect more data.
- SNODAS model output from the National Operational Hydrological Remote Sensing Center has been downloaded, and processed for all of the years in which model output is available for the study period.
- A second model that uses ground based temperature observations and potential clear sky solar radiation to determine SWE depth in the study site has been assembled and run for all years of the study period.

Future Work:

- Two more days will be spent in the field in Lost Horse Canyon collecting SWE depth data using ground penetrating radar in late February.
- A third model that uses Weather and Research Forecasting (WRF) model output to model SWE depth in the study area will be assembled and run for all years of the study period. This work is close to being completed and will likely be finished around the time of the New Year.
- An analysis of the differences and similarities between the three different models.
- Comparison of ground penetrating radar SWE depth data with model outputs.
- Combining the three different model results to make an ensemble model output of SWE distribution in the study area.
- Writing and defending of Master's thesis.
- Publication of research results in scientific journal.

Student Research Fellowship: Invisible impacts of changing stream conditions: nongame fish assemblage response to changing stream temperatures

Basic Information

Title:	Student Research Fellowship: Invisible impacts of changing stream conditions: nongame fish assemblage response to changing stream temperatures
Project Number:	2012MT273B
Start Date:	3/1/2012
End Date:	2/28/2013
Funding Source:	104B
Congressional District:	at large
Research Category:	Biological Sciences
Focus Category:	Conservation, Climatological Processes, None
Descriptors:	None
Principal Investigators:	Michael LeMoine

Publications

There are no publications.

Student Research Fellowship: Invisible impacts of changing stream conditions: nongame fish assemblage response to changing stream temperatures. Final Report.

PI: Michael LeMoine, University of Montana

I want to thank the Montana Water Center for the 2012 Graduate Fellowship to support my efforts to investigate “Invisible impacts of changing stream conditions: nongame fish assemblage response to changing stream temperatures”. The application of the funds provided by the Montana Water Center were directed to overall research goal is to understand the composition and changes in cryptic nongame fish species composition associated with increases in temperature. Over 2012, I conducted substantive research in two specific objectives:

- (1) *Define a cryptic species, its distributions, and habitat use by describing currently unknown sculpin species within the Clark Fork River basin.*
- (2) *Assess potential responses of sculpin assemblages to temperature gradients through determining thermal tolerances and temperature-dependent competition. Link these results with current distributions to explore the vulnerability to these species to changing stream temperatures.*

Objective 1. Species Description

In collaboration with U.S. Forest Service Rocky Mountain Research Station and Montana Fish Wildlife & Parks, we used a combination of genetic and morphological methods to delineate and describe *Cottus schitsuumsh*, a potential new species, from Coeur d’Alene River basin, Idaho and tributaries of the lower Clark Fork River, Montana. We used haplotypes of mtDNA cytochrome oxidase c subunit 1 of *C. schitsuumsh* to differentiate this new species from all other members of the genus. We found interspecific genetic distances between this group and other neighbors samples to be typical for congeneric fishes (1.6-2.74% to nearest neighbors) and this group was monophyletic in maximum-likelihood trees. Microsatellite analyses were also used to confirm taxonomic groupings for species potentially sympatric with *C. schitsuumsh* and that fish used in morphological comparisons were unlikely to be introgressed. Although historically confused with the shorthead sculpin (*C. confusus*), the genetic distance between *C. schitsuumsh* and *C. confusus* is 5.00% and the two species can be differentiated morphologically on the basis of differences in second preopercular spine, lateral line pores, head width, and interpelvic width. *Cottus schitsuumsh* is also distinct from all other *Cottus* in this region in having a substantially reduced, skin-covered, preopercular spine.

To date, we have submitted holotype and paratype specimens of the potential new species to the University of Washington’s Burke Museum of Natural History. We are currently drafting a manuscript describing this potential new species and its distribution and plan to submit the manuscript in the summer 2013. *C. schitsuumsh* has an unusual distribution occurring both in the Coeur d’Alene River basin, Idaho and tributaries of the lower Clark Fork River, Montana. We have conduct extensive genetic analysis of specimens found in Montana; however at this time, we have been unable to determine if this new species is exotic to Montana.

Objective 2. Responses of sculpin assemblages to temperature gradients

Over 2012, I attempted controlled laboratory experiments at the University of Montana and field assessments to determine potential responses of slimy sculpin (*Cottus cognatus*) to changes in stream temperatures and competition with longnose dace (*Rhinichthys cataractae*). Laboratory experiments were conducted similarly to recent work comparing trout temperature dependent competition (McMahon et al. 2007); however, slimy sculpin and longnose dace did not survive in confinement. The laboratory experiments were stopped.

Temperature limits of slimy sculpin were observed through 2012 field surveys across 74 sites over 18 streams within tributaries of the Bitterroot River. Using CART analysis, I determined that temperature and barriers to upstream movement associated strongly with slimy sculpin distributions. Slimy sculpin were absent at temperature greater than 19.5° C. In addition, I employed occupancy modeling using present and historical USFS MFWP data to determine that slimy sculpin had a site occupancy rate of 0.478 ± 0.068 (Estimate ± 1 Standard Error) during 1992-1996 and 0.354 ± 0.048 (Estimate ± 1 Standard Error) during 2009-2012, which is a 11.4% reduction in site occupancy over two decades. In addition, longnose dace presence also reduced probability of occupancy of slimy sculpin at sites. These observations suggest that temperature is limiting the ranges of slimy sculpin and that slimy sculpin might be as sensitive to climate change as bull trout, *Salvelinus confluentus*.

My 2012 field information, partially funded by Montana Water Center, will direct my dissertation research over the next two years to investigate temperature related impacts to native fish of Montana. Primarily, I will be investigating how barriers to fish passage and biotic interactions could be influencing the distributions of common nongame fishes (sculpin and dace). It is my hope that further research will illuminate possible dramatic changes in distribution occurring with cryptic nongame fishes that might be negatively affecting stream biodiversity in Western Montana.

Student Research Fellowship: Food web effects of stream invasion by Potamopyrgus antipodarum and interactions with eutrophication

Basic Information

Title:	Student Research Fellowship: Food web effects of stream invasion by Potamopyrgus antipodarum and interactions with eutrophication
Project Number:	2012MT274B
Start Date:	3/1/2012
End Date:	2/28/2013
Funding Source:	104B
Congressional District:	MT at large
Research Category:	Biological Sciences
Focus Category:	Conservation, Ecology, None
Descriptors:	None
Principal Investigators:	Eric Richins

Publications

There are no publications.

Student Research Fellowship: Food web effects of stream invasion by *Potamopyrgus antipodarum* and interactions with eutrophication. Final Report.

PI: Eric Richins, University of Montana

Spatial subsidies are the movement of food items between habitats where a donor habitat bolsters communities of consumers in the recipient habitat. The near ubiquity of these linkages creates the potential for disturbances in one habitat to propagate across ecosystem boundaries to become a disturbance in a spatially disjunct habitat. We are investigating the impacts that the invasive New Zealand mudsnail (NZMS) has on aquatic invertebrates on the Madison and Portneuf rivers and what effects may be subsequently transferred to terrestrial consumers that specialize on the adult emergent stages of those aquatic insects. We know that NZMS have the ability to reduce secondary production in streams and hypothesize that these biomass reductions in benthic invertebrates will translate to reductions in the biomass of emerging adult insects that are dramatic enough to subsequently reduce the abundance of riparian specialist spiders in the family Tetragnathidae.

Together with collaborators at Idaho State University, Colden V. Baxter PhD and Kaleb Heinrich, we are using a paired approach on both the Madison River near W. Yellowstone, MT and on the Portneuf river near Pocatello, ID. Our general approach is to use freestanding insect sticky-traps to quantify aquatic emergence along gradients of NZMS density on both rivers. This will allow us to analyse the potential correlation between NZMS density and aquatic secondary production that reaches terrestrial consumers in present time and to make comparisons to pre-NZMS-invasion data that we have obtained for both rivers. Furthermore we are conducting spider surveys along our study stream reaches to monitor responses in riparian consumers.

Data has been collected on both the Madison and Portneuf rivers during the spring, summer, and fall of 2012. On each river we identified five study reaches with varying NZMS density. Along these reaches we have collected emergent insects using 10 sticky traps at each reach (n=50); this was done in 14-day increments 4 times from June through September. Insects from these samples are currently being assessed for both density and biomass and identified to determine origin (aquatic or terrestrial).

Benthic samples were taken once on both rivers in September, 2012 the season when NZMS densities are known to be highest. This sampling effort was located between sticky traps at each study reach (n=40). NZMS and other snails have been counted from these samples confirming strong gradients in NZMS density among study reaches.

Spider surveys have been conducted three times on each river. These surveys were conducted at night when spider activity is highest. A total of 50 meters of streambank were surveyed from the water (looking onshore within 2m of the water) at each study reach in 10 meter segments (n=5). Our data indicates that spider densities are positively correlated with NZMS densities; we believe that this is due to background productivity in the benthos and we will account for this potential covariate by quantifying stream secondary productivity from our benthic samples (g/m^2).

This summer we are continuing to process samples to quantify adult-stage aquatic insect emergence. Unless we find that we need more field data the analysis should be finished in the fall of 2013 and presented as a Master's thesis for Eric Richins at the University of Montana. We then plan on presenting our findings at the Society for Freshwater Science annual meeting in 2014. We anticipate developing two manuscripts suitable for publication from this work in the next year.

Student Research Fellowship: COLUMBIA RIVER TREATY RENEGOTIATION PROCESS: COLLABORATIVE IN WORD OR DEED?

Basic Information

Title:	Student Research Fellowship: COLUMBIA RIVER TREATY RENEGOTIATION PROCESS: COLLABORATIVE IN WORD OR DEED?
Project Number:	2012MT275B
Start Date:	3/1/2012
End Date:	2/28/2013
Funding Source:	104B
Congressional District:	MT at large
Research Category:	Social Sciences
Focus Category:	Law, Institutions, and Policy, None, None
Descriptors:	None
Principal Investigators:	Anthony Thompson

Publications

There are no publications.

Student Research Fellowship: Columbia River Treaty Renegotiation Process: Collaborative in Word and Deed. Final Report.

PI: Anthony Thompson, University of Montana

The Columbia River Treaty governs the management of the Columbia River system for flood control and hydroelectric power generation benefits in both Canada and the United States. The treaty is administered by BC Hydro in Canada and jointly by the Army Corps of Engineers (USACE) and Bonneville Power Administration in the US. The treaty ensures a certain level of assured flood storage in Canadian reservoirs, in exchange for a yearly compensation for downstream power generation benefits known as the ‘Canadian Entitlement’. Implemented in 1964, the treaty cannot be terminated by either party prior to 2024, and a minimum advance notice of 10 years is required for any proposed alterations to the treaty or termination. Because of this, the earliest possible opportunity for either government to request termination or alterations to the treaty occurs in 2014. In preparation for a recommendation to be made to the US Department of State in September 2013, USACE/Bonneville Power are conducting a thorough review of the treaty including technical analysis and public outreach. This public outreach is critical, as ecological, tribal and other local concerns were not considered during the initial negotiations.

Two teams consisting of officials, technical experts and stakeholders from the region have been formed to carry out this review process. In addition to evaluating the treaty and any future options in terms of flood control and hydropower concerns, the US Entity is also incorporating ecosystem function into the review. The review process has been divided into ‘Iterations’, with each new iteration providing differing levels of analysis. Iteration 1 has been published, and analyzes flood control, hydropower and ecological concerns separately. The purpose of this study is to determine to what degree the Sovereign Review Team (SRT) has succeeded in their stated goal of incorporating collaboration with stakeholders and sovereigns into the review process. From the US Entity’s website:

The Columbia River Treaty 2014/2024 Review will enable the U.S. Entity to make an informed recommendation, **in collaboration with the regional sovereigns and stakeholders**, to the U.S. Department of State by September 2013 as to whether or not it is in the best interest of the U.S. to continue, terminate or seek to amend the Treaty. **The U.S. Entity will ensure an open, collaborative and regionwide engagement process to hear all interests in the Pacific Northwest.**

(<http://www.crt2014-2024review.gov/USEntity.aspx>, emphases mine)

Using qualitative methods to analyze the documents produced and published by the SRT, it has been possible to determine the major concerns expressed by the stakeholders, tribal and governmental representatives and other experts brought in by the SRT in ‘Panel Discussions’. The SRT convened three panel discussions, focussing individually in flood control, hydroelectric power generation, and ecosystem function. By coding the panel summaries, themes emerge that are mentioned more often than others. The following table lists the five most common themes mentioned during each of the three panels and their frequency.

Flood Control		Hydroelectric Power		Ecosystem Function	
Levee Integrity	9	Extra Resources for SRT	11	Ecosystem Health	11
Economic Impacts	6	Collaboration	11	Ecosystem Representation	10

Flood Control		Hydroelectric Power		Ecosystem Function	
Water Quantity	5	Power Production	8	Collaboration	9
Navigation	5	Ecosystem Health	8	SRT Focus	8
Extra Resources for SRT	5	Access to Models/Alternatives	7	Extra Resources for SRT	7

A complete definition of each code, including examples will be included in the final report.

Collaboration itself, indicated by statements in favor of the SRT working closely with stakeholders in the region, appeared in the top five codes (including ties) for all three of the panels. Similar themes, such as the ability for stakeholders to provide additional information or resources to the SRT, also appear near the top of the frequency distributions quite consistently. This indicates a strong desire on the part of stakeholders to ensure the SRT remains true to their stated goal of collaboration. Preliminary results indicate that in terms of stakeholder concerns expressed at official SRT meetings, collaboration itself is one of the most consistently important concerns reported by the SRT. But this does not answer the question of whether the SRT process is being truly collaborative. Expressed concerns mean little if they are not taken seriously or are not incorporated into the recommendation produced by the ‘collaborative’ process. Because the process is ongoing, this question can only be answered as the SRT publishes their iteration results. For example, Iteration 1 results analyze ecological concerns simply in terms of in-stream flows over an average water year, and include no species-level analysis, such as fish migration or even overall ecosystem health, which have been expressed as concerns in the panel discussions.

The second and upcoming part of this analysis is to determine whether the concerns gathered during this process have been incorporated into the technical analysis conducted by the Sovereign Technical Team (STT). As of December 23rd, 2012, the STT has not published Iteration 2, which does include ecosystem function modeling other than general flow levels, including anadromous fish migration concerns and comparing the hydrograph to a ‘normative’ or more natural state. The differences between Iteration 1 and 2 alternatives may indicate the extent to which stakeholder concerns have been incorporated into the review process. Collaborative opinion collection is fine, but if stakeholder concerns have not been incorporated into the alternatives being explored by the STT, they cannot make a real impact, incapacitating the collaborate nature of the process.

In addition to the panel discussions, the SRT has conducted listening sessions (public meetings) which serve to both disseminate information about the treaty review process and to collect regional opinions. Outside the review process, the Universities’ Consortium on Columbia River Governance has convened an annual Symposium to bring regional stakeholders together in an informal discussion of Columbia River issues. I have attended a public listening session and the Symposium in an attempt to document the more informal sides of the process, and a thorough review of these meetings will flesh out the background information in the final paper to be presented at the 2013 UMCUR, an undergraduate research conference this coming spring.

Student Research Fellowship: The Effect of Physiographic Parameters on the Spatial Distribution of Snow Water Equivalent: an Analysis of the Representativeness of the Lone Mountain SNOTEL Site

Basic Information

Title:	Student Research Fellowship: The Effect of Physiographic Parameters on the Spatial Distribution of Snow Water Equivalent: an Analysis of the Representativeness of the Lone Mountain SNOTEL Site
Project Number:	2012MT276B
Start Date:	3/1/2012
End Date:	2/28/2013
Funding Source:	104B
Congressional District:	MT at large
Research Category:	Climate and Hydrologic Processes
Focus Category:	Surface Water, Hydrology, None
Descriptors:	None
Principal Investigators:	Karl Wetlaufer

Publications

There are no publications.

Student Research Fellowship: The Effect of Physiographic Parameters on the Spatial Distribution of Snow Water Equivalent: an Analysis of the Representativeness of the Lone Mountain SNOTEL Site. Final Report.

PI: Karl Wetlaufer, Montana State University

My graduate research, which I received partial funding for from the Montana Water Center has recently been completed. The main focus of this research was to model the spatial distribution of snow water equivalent (SWE) and snow density across a large (as compared to similar previous research) and physiographically diverse basin. The West Fork of the Gallatin River basin was sampled for SWE and snow depth at the time near peak SWE accumulation. This information (along with calculated density) was then correlated to various physiographic parameters (e.g. elevation, radiation, land cover, aspect, etc.) of the locations where samples were taken. This data was then used to model the continuous spatial distribution of SWE and density throughout the basin, also allowing for the estimation of the total basin SWE volume. This modeling was done using one statistical technique that had been commonly used for this type of analysis as well as several that had previously unused providing insight into which may be best for various types of research, among many other original contributions to the field.

The fellowship from the Montana Water Center (MWC) aided me in being able to travel to several professional conferences to present this research. In May 2012 I gave an oral presentation at the Western Snow Conference on my methods and was honored with the best student presentation: runner up award (good considering it was only a methods paper). In December 2012 I presented a poster with much of my results at the American Geophysical Union Fall Meeting and received very positive feedback on the work. Most recently I was able to present my final results at the 2013 Western Snow Conference and received the Dr. J.E. Church Best Student Presentation Award, along with generally lots of good feedback about the work.

Overall the primary academic portion of this research has been completed, with my thesis successfully defended and the final formatting accepted by the graduate school. While the graduation requirements related to this research have been met I still intend to pursue at least one or two peer reviewed publications as much of the analysis does provide many original contributions to the science and operational practice of snow hydrology. The MWC funding of this fellowship enabled me to fully commit to my research and travel to present it.

Student Research Fellowship: Soil temperature and moisture controls on stream recharge from snowmelt events, Lost Horse Canyon, Bitterroot Mountains, MT

Basic Information

Title:	Student Research Fellowship: Soil temperature and moisture controls on stream recharge from snowmelt events, Lost Horse Canyon, Bitterroot Mountains, MT
Project Number:	2012MT277B
Start Date:	3/1/2012
End Date:	2/28/2013
Funding Source:	104B
Congressional District:	MT at large
Research Category:	Climate and Hydrologic Processes
Focus Category:	Hydrology, None, None
Descriptors:	None
Principal Investigators:	Brett Woelber

Publications

There are no publications.

Student Research Fellowship: Soil temperature and moisture controls on stream recharge from snowmelt events, Lost Horse Canyon, Bitterroot Mountains, MT. Final Report.

PI: Brett Woelber, University of Montana

The following is a report on research conducted from the December of 2012 to March 2013. During that time period I made 24 trips to my research site. These research trips were conducted to maintain the University of Montana Watershed Laboratory research station, which continuously monitors a suite of weather conditions as well as groundwater, soil moisture, stream stage, and sap flow rates. This data is part of a legacy dataset that began in 2010 and will be maintained by future graduate students. The funds to support my research travel expenses were not provided by my advisor, but by the grants that I received from these three sources.

In addition to the Montana Water Center Research Fellowship, I received the Montana Geological Society Research Grant, and an American Alpine Club Graduate Research Grant. In October of 2012, I received second place in the student poster presentation awards at the Montana Section of the American Water Resources Association conference in Fairmont Hot Springs, Montana. As a condition of the research grant I received from the Montana Geological Society, I will present my research at a Montana Geological Society luncheon in May of this year.

My research focusses on how diel cycles of radiative forcing drives diurnal fluctuations in groundwater and stream stage. Stream recharge from daily snowmelt events is a complicated process that varies spatially over the watershed scale and temporally over the course of the melt season. To understand this complex relationship, we analyzed net radiation at 15-minute time steps to approximate the energy state of the snowpack and relate it to hillslope hydrologic response and changes in stream stage. By measuring the timing of diurnal peaks in radiation, groundwater response, and stream stage over an entire melt season, we assessed the role of snowpacks and hillslopes as filters that moderate and delay the movement of snowmelt from the top of the snowpack to local stream systems. Contrary to our initial hypotheses, we interpret the seasonal shifts in the timing of diurnal peaks in groundwater and stream stage as an indication that the physical properties of the snowpack control the timing of diurnal melt transmission to local stream systems. Once hillslopes become saturated, they play little role in delaying the movement of meltwater from the base of the snowpack to local stream systems.

With the support of my committee, I plan on submitting my research for publication in Water Resources Research in May of 2013 and defending my research shortly thereafter.

Information Transfer Program Introduction

Supporting students to become water science professionals is a core mission of the Montana Water Center. The center continues to work closely with faculty researchers to engage students in water-related research including producing reports and published papers. The Center encourages students from a wide array of disciplines that are water related to apply for student fellowships. Faculty researchers who received research funding from the Water Center are required to actively mentor students in the research projects. The Water Center also encouraged students engaged in water resource studies to present at regional and national conferences. The presentations and publications of faculty and students reported in their annual reports attest to the support given to students to both take on research and also present it at local and national meetings as well as follow through to publication in national journals.

In addition to working with faculty and students, Water Center programs reached thousands of others interested in water issues in Montana, including water resource professionals, teachers, farmers, ranchers, engineers, drinking water and wastewater system operators.

Specific information transfer activities include the following.

- * Published nine Montana Water e-newsletters (due to budgetary constraints cut back to every other month part way through the year) and distributed them to almost 2,000 professionals, students and decision makers concerned with water resource management. Newsletter archives are posted at <http://water.montana.edu/newsletter/archives/default.asp>.

- * Continued the web information network MONTANA WATER, at <http://water.montana.edu>. Known as Montana's clearinghouse for water information, this website includes an events calendar, news and announcement updates, an online library, water-resource forums and water source links, an expertise directory, water facts and more.

- * The Montana Water Center continues to distribute training CDs funded by the EPA, for small drinking water systems titled Arsenic and Radionuclides: Small Water System Treatment Experiences.

- * Moved the small library of paper documents related to Montana water topics held by the Water Center to the Montana State University library for better exposure to those looking for this material.

- * Helped organize and hold a state water meeting with the Montana Section of the American Water Resources Association in Fairmont Hot Springs, MT on October 11-12, 2012. The theme of this conference was "Montana's Water Resources: Water Management in the Face of Uncertainty". A pre-conference field trip included a stop at the Dry Cottonwood Ranch to observe restoration strategies for the Clark Fork River and tributaries. Other field trip stops included the Silver Bow Creek reconfiguration project, and 2011 Deer Lodge flood sites. Over 140 people attended the conference. Forty speakers and over twenty poster presenters highlighted much of the current water research being conducted throughout Montana by university, federal, state, county and non-profit researchers and resource managers. The conference also had the usual good turnout of student presenters, representing the University of Montana, Montana Tech and Montana State University. The web-based archive of this meeting is found at <http://state.awra.org/montana/conference/2012meeting.htm>.

- * Responded to numerous information requests on water topics ranging from invasive water rights to importance of snowpack to Montanan's, to streamside setbacks to contaminants in Montana's surface and ground water, and ways to better manage these water sources.

Information Transfer Program Introduction

* Sponsored and participated in Montana's 78th Annual Water School October 2012 at Montana State University for 300 staff members of water and wastewater utilities. The school primarily helps prepare new system operators to pass the certification exam, and familiarizes participants with other resources they may find helpful in the future.

* Offered a Wetland Training course supported by an EPA grant through Montana DEQ titled: "Wetland Restoration: Planning for Success". Planning for a 2013 Wetland Training course titled "Monitoring and Assessment of Wetland and Riparian Restoration Sites" is underway.

* The Montana Watercourse (MTWC), which is part of the Montana Water Center, provides hands-on, dynamic, water education through a series of diverse programs that target all levels of water users youth through adults. Using practical, unbiased, legal, and scientific information, MTWC educates Montanans on basic water facts, water problems, and their solutions (mtwatercourse.org). During FY13, these grant funded education programs focused on the following areas: water rights trainings, dam owner workshops, a Water Summit for youth, Project WET curriculum training, river clean-up projects, lake ecology graduate course, and the Montanan Water supply Initiative material. Funding for these programs is provided through eight grants from Montana Department of Natural Resources and Conservation, Montana Department of Environmental Quality and the National Science Foundation.

USGS Summer Intern Program

None.

Student Support					
Category	Section 104 Base Grant	Section 104 NCGP Award	NIWR-USGS Internship	Supplemental Awards	Total
Undergraduate	4	0	0	0	4
Masters	9	0	0	0	9
Ph.D.	2	0	0	0	2
Post-Doc.	0	0	0	0	0
Total	15	0	0	0	15

Notable Awards and Achievements

Publications from Prior Years

1. 2010MT216B ("Ecohydrologic Model Development for the Assessment of Climate Change Impacts on Water Resources in the Bitterroot Valley") - Articles in Refereed Scientific Journals - Maneta, M. and W. Wallender. 2013. Pilot-point based multi-objective calibration in a surface-subsurface distributed hydrologic model. *Hydrological Sciences Journal* 58:1-18.
2. 2010MT216B ("Ecohydrologic Model Development for the Assessment of Climate Change Impacts on Water Resources in the Bitterroot Valley") - Articles in Refereed Scientific Journals - Silverman, N., M. Maneta, S-H. Chen, J. Harper. 2013. Dynamically downscaled winter precipitation over complex terrain of the central Rockies of western Montana, USA. *Water Resources Research* 49:458-470.
3. 2010MT220B ("Assessing hydrologic response to channel reconfiguration: Science to inform the restoration process, Silver Bow Creek, Montana") - Articles in Refereed Scientific Journals - Mason, S.J.K., B.L. McGlynn and G.C. Poole. 2012. Hydrologic response to channel reconfiguration on Silver Bow Creek, Montana. *Journal of Hydrology* 438-439:125-136.